



JOURNAL OF EMERGING INVESTIGATORS

VOLUME 3, ISSUE 2 | FEBRUARY 2020
emerginginvestigators.org

Alarming acidification

How pH drops in Monterey Bay may contribute to proliferation of dangerous algal blooms

Biases in malaise trap investigations

Different attractants can affect the results of insect diversity studies

Are young people more optimistic?

Assessing the correlation between age and outlook

Bubble behavior

The peculiar phenomenon of sinking bubbles

Does Wi-Fi affect insect reproduction?

Looking into the impacts of electromagnetic fields on flies



JOURNAL OF EMERGING INVESTIGATORS

The Journal of Emerging Investigators is an open-access journal that publishes original research in the biological and physical sciences that is written by middle and high school students. JEI provides students, under the guidance of a teacher or advisor, the opportunity to submit and gain feedback on original research and to publish their findings in a peer-reviewed scientific journal. Because grade-school students often lack access to formal research institutions, we expect that the work submitted by students may come from classroom-based projects, science fair projects, or other forms of mentor-supervised research.

JEI is a non-profit group run and operated by graduate students, postdoctoral fellows, and professors across the United States.

EXECUTIVE STAFF

Brandon Sit **EXECUTIVE DIRECTOR**
Michael Mazzola **COO**
Qiyu Zhang **TREASURER**
Caroline Palavacino-Maggio
DIRECTOR OF OUTREACH

BOARD OF DIRECTORS

Sarah Fankhauser, PhD
Katie Maher, PhD
Tom Mueller
Lincoln Pasquina, PhD
Seth Staples

EDITORIAL TEAM

Jamilla Akhund-Zade **EDITOR-IN-CHIEF**
Olivia Ho-Shing **CHIEF LEARNING OFFICER**
Michael Marquis **MANAGING EDITOR**
Laura Doherty **MANAGING EDITOR**
Chris Schwake **MANAGING EDITOR**
Naomi Atkin **HEAD COPY EDITOR**
Eileen Ablondi **HEAD COPY EDITOR**
Lisa Situ **HEAD COPY EDITOR**
Alexandra Was, PhD **PROOFING MANAGER**
Erika J. Davidoff **PUBLICATION MANAGER**

SENIOR EDITORS

Sarah Bier
Kathryn Lee
Nico Wagner
Scott Wieman

**FOUNDING
SPONSORS**



Contents

VOLUME 3, ISSUE 2 | FEBRUARY 2020

- Assessing Attitude Across Different Age Groups in Regard to Global Issues: Are Kids More Optimistic Than Adults?** 5
Adrian Luck (1) and Thomas Keane
Doherty Middle School, Andover, Massachusetts
- Effects of Ocean Acidification on the Photosynthetic Ability of *Chaetoceros gracilis* in the Monterey Bay** 14
Kelly Harvell and Jason Nicholson
Monterey High School, Monterey, California
- Effects of Coolant Temperature on the Characteristics of Soil Cooling Curve** 20
Dawei Wang and Yida Zhang
Boulder High School, Boulder, Colorado
- Efficacy of Mass Spectrometry Versus ¹H Nuclear Magnetic Resonance With Respect to Denaturant Dependent Hydrogen-Deuterium Exchange in Protein Studies** 26
Srish Chenna and Walter Englander
Charter School of Wilmington, Wilmington, Delaware
- Do Attractants Bias the Results of Malaise Trap Research?** 32
Arnauld Martinez, Nick Reeves, Ryan Perry, and Michael Horton
Western Center Academy, Hemet, California
- Effects of Common Pesticides on Population Size, Motor Function, and Learning Capabilities in *Drosophila melanogaster*** 36
Alejandra Abramson and Leya Joykuttu
American Heritage School, Plantation, Florida

Understanding the Relationship Between Perception and Reality Related to Public Safety: A Case Study of Public Opinion on Local Law Enforcement in Andover, MA	41
Alexander Luck and Thomas Keane Doherty Middle School, Andover, Massachusetts	
The Effect of Neem on Common Nosocomial Infection-Causing Organisms	49
Manav Shah, Danielle Ereddia, Jyoti Shah, and Nanette Reese Wheeler High School, Marietta, Georgia	
Threshold Frequency of a Bubble is Positively Correlated to the Density of the Surrounding Fluid	54
Alexander Han and Eric Samson Korea International School, Pangyo, South Korea	
The Effects of Various Plastic Pollutants on the Growth of the Wisconsin Fast Plant	58
Nathan Sobotka and Karissa Baker Saint Paul Academy and Summit School, St. Paul, Minnesota	
Effects of Wi-Fi EMF on <i>Drosophila melanogaster</i>	64
Mary Anand and Herm Anand Anand Homeschool, Pittsburgh, Pennsylvania	

Assessing Attitude Across Different Age Groups in Regard to Global Issues: Are kids more optimistic than adults?

Adrian Luck, Thomas Keane

Doherty Middle School, Andover, Massachusetts

SUMMARY

The world faces many problems. This study attempted to determine to what extent people are aware of the current global issues and whether people believe some of them may be successfully addressed. The main objective of the study was to understand if there is a correlation between the age of a person and their outlook. We hypothesized that a positive outlook, i.e. a general belief that many issues can be resolved, would be common among children, from elementary through high school, whereas adults would have a more negative perspective. This research was conducted using a survey-based study. The results supported the hypothesis and showed that children appear more optimistic than adults and believe that most issues can be addressed in the future. Adults are less optimistic and believe that, even with time, it is impossible to resolve many of these issues. Regardless of age, many respondents commented that technology, improved communication, kindness, and general willingness to change, along with an effective political agenda led by non-corrupt politicians, are essential for successfully resolving major problems. On the other hand, greed, selfishness, and the corrupt political system largely prevent any improvement.

INTRODUCTION

Optimists are people who expect positive outcomes and have positive view of the world around them and pessimists are people who expect negative outcomes and have negative view of the world around them. Anticipating positive versus anticipating negative seems to be linked to different underlining attitudes and behaviors among people. The ways in which optimists and pessimists differ in their view of the world has an impact on their lives and consequently the world they live in. Several psychology studies demonstrate that optimists and pessimists differ in how they confront problems, cope with adversity, and utilize social and socioeconomic resources (1).

Furthermore, research in psychology shows that optimism is observed more frequently in children and less in adults (1, 2). There is "positivity bias" in children as early as three years of age (2). This bias peaks in middle school and weakens later in high school, presumably due to education and experience. Research also indicates that children may remain stubbornly optimistic even when

presented with evidence to the contrary (2). With age, this "stubborn optimism" is tempered and many studies reported a decreasing level of positive future perception with increase in age. Several researchers concluded that adults have a more realistic outlook that is practical and functional than having an overly positive and hence unrealistic perception of their life (3, 4, 5). One study analyzed the results from the Life Orientation Test, evaluating different factors of optimism and pessimism among middle-aged and older adults (5). The results suggested that life stressors may affect disposition and showed a trend toward pessimism over age, especially among caregivers. Interestingly, the research pointed out that it is pessimism, not optimism, that has a stronger influence on outcome and may predict psychological and physical health (5).

Element of time has a definite impact on outlook and the trend of negative view increases over age (7). Exploring optimism and pessimism in terms of age and in the context of current global issues and problems may clarify differences in approach between children and adults. A large body of literature indicates that people who have positive expectations for the future respond to difficulty and adversity in more adaptive ways than people who hold negative expectations (8, 9, 10, 11, 12, 13). Expectations influence how people approach both stressors and opportunities, and they influence the success with which people deal with many challenges and even design solutions. In lieu of the many different global problems described below and as studied in the presented survey, the connection between outlook and age was explored.

The world today faces many serious issues and challenges: global warming, pollution, rapidly declining bee populations, energy crisis, health care crisis, immigration, wars, poverty and hunger, overpopulation, political corruption, and more. The global problems in the survey were selected based on current news and what the major non-profit organizations believe to be of concern (14, 15, 16). The United Nations is a global organization dedicated to safeguarding peace, protecting human rights and international justice, promoting economic and social progress, addressing immigration and climate change. In addition to United Nations, two smaller scale organization, the Borgen Project and GVI, were reviewed to understand what common global issues different types of organizations align on. The Borgen Project is a non-profit organization mainly focusing on addressing poverty and hunger, while the GVI is an organization dedicated to building

worldwide partnerships in order to facilitate global citizenship and teach leadership skills in young adults. Even though there are major differences in size, scale, and membership between UN, Borgen Project and GVI, the three organizations still identify same global concerns which require international recognition, cooperation, and implementation of long-term solutions. Identification of the issues is an important first step to building a better, sustainable, and kinder world (14, 15, 16).

Many scientists agree that global warming is a major problem and the cause of climate change (17, 18). Scientists also agree that humans are at fault. Consequences of increasing temperatures include rise of ocean levels, floods, loss of wildlife habitats, species extinction, reduction of the amount of drinkable water, massive human migrations and potential armed conflicts (17, 18). Air pollution is another serious problem that is not only responsible for global warming, but also results in poor air quality that causes cancer, birth defects, and many other health problems (17, 19, 20, 21). The problem of pollution is not limited just to air. Modern humans contaminate most of the resources they come across, including oceans, freshwater, and soil (22, 23). Oil spills and plastic pollution result in the death of ocean life and eventually have a negative impact on human health (24, 25, 26). Fish eat the poisonous plastic, and consumers eat the poisoned fish (27, 28, 29, 30). Freshwater is affected as well. Drinking water is polluted by sewage, industrial waste, oil spills, heavy metals, and other toxic chemicals. Pollution depletes drinking water drastically and poses many health risks (31, 32).

In addition to air and water pollution, people have polluted the soil which prevents successful farming, and accumulation of insecticides and fungicides has become a major problem, harming productive pollinators like bees (33, 34, 35, 36). Pollution and contaminated flora contribute to bee colony collapse disorder and result in the "bee apocalypse" (36, 37). Many scientists agree that death of bees may cause a major shift in the ecosystem, resulting in extinction of many plants and direct impact on food supply, which in turn may cause hunger, poverty, political conflicts, and maybe even wars.

Another critical problem the world faces is an energy crisis. The production and consumption of fossil fuels have increased dramatically (38). However, natural reserves of fossil fuels are at the verge of depletion and will become more expensive and increasingly scarce (38, 39). Turning to renewable energy like solar or wind power, has been considered as a solution. However, integrating the new sources of energy into mainstream society has yet to be implemented on a global level (38, 39).

Terrorism is a growing issue in the world (40, 41, 42). It is a new problem. Wars, on the other hand, have existed since the rise of human civilization. Terrorism and wars cost life and tremendous suffering (43, 44). It is easy to imagine that food shortage due to the impending bee apocalypse or poor living conditions due to changing climate or limited sources of energy may be the future reasons for tension and potentially

even lead to armed conflicts such as terrorism and wars.

Hunger and poverty are most common in developing nations. However, even in developed countries such as the USA, many children go to bed without dinner (45, 46). More than half of the world's population lives at levels of poverty that deprive them of their basic needs, and more than 1 billion of those people live in hunger (45, 46). Unfair distribution of wealth, poorly utilized land, inefficient agricultural practices, and droughts are the main sources of hunger in the world (46, 47).

In poorer societies, overpopulation results in poverty and hunger. In more developed countries, overpopulation puts a strain on natural resources and impacts issues such as pollution, energy, and health crisis. With increased population and social inequality, migration poses a challenge as less fortunate and oppressed people look for opportunities in more developed regions of the world (48).

Political corruption can make all these problems not only much worse, but also destroy any hope of ever reaching a solution. Corrupt politicians and lobby groups pursue interests of big companies at the expense of their country and citizens (49, 50, 51, 52). The Chapman University Survey of American Fears in 2018 indicated that for the fourth year in a row the top fear of Americans is corrupt government officials (52). The collective fear of political corruption outweighs the fear of losing a loved one, not having enough money for the future, global warming, and pollution. Corruption in the government demoralizes the public and weakens the entire system of policy making and implementing. It diminishes services, undermines trust, and if not checked, will prevent issue resolution and problem solving (52).

All the described issue must be addressed for the successful future of humanity. Many of them require long-term strategies and commitment. However, the first step is agreeing that these issues do exist. Only then can solutions be developed, and actions taken. Each of these problems is multifaceted and interconnected, meaning that many aspects must be considered as part of a solution strategy. Given many debates and challenges associated with addressing some of these global problems, we wondered whether children and adults are aware of them. We also speculated that children, more so than adults, would have an optimistic outlook about solving these problems. This study attempted to determine if people agree that the aforementioned global issues exist and if people feel that those issues can be solved. Our hypothesis is that school-age respondents, from elementary through high school, are more optimistic about solving global problems, while adults are more pessimistic, being influenced by their experiences and understanding of the reality and causes of these problems. We predict that in our study, children will be more optimistic than adults reflecting the conclusions of previous research.

RESULTS

Paintings Demographic Analysis

The demographic results of participants were collected (Table 1). Out of 143 respondents, 56% were female and 44% were male. The ethnicities of the participants were comprised of 66% Caucasian, 15% Asian, 8% African-American, 8% Hispanic, 4% Native American, and 4% other. Among the 143 respondents, 4% were elementary school students, 15% were middle school students, 19% were high school students, 8% were 19-30 years old, 38% were 31-50 years old, 7% were 51-65 years old, and 8% were 65 and above years old. When asked to identify which religion they followed, 49% self-identified as Christians, 12% as atheist, 10% as agnostic, 8% as Buddhist, 6% as Jewish, 5% as Muslim, 3% as Hindu, and 3% as New Age.

The 19-25 years-of-age group was underrepresented at only 4% of the sample size. This meant that the accuracy of data interpretation for that age group was likely low.

Number of Respondents:		143					
Gender	Females	56%					
	Males	44%					
Ethnicity	White	Black	Hispanic	Asian	Native American	Other	
	66%	8%	8%	15%	4%	4%	
	Marital Status						
	Married	Divorced	Widowed	Single			
	40%	5%	6%	43%			
	Political Party						
Democratic	Republican	Independent	Libertarian	Green Party			
22%	13%	36%	3%	2%			
Religion							
Muslim	Jewish	Christian	Buddhist	New Age	Hindu	Atheist	Agnostic
5%	6%	49%	8%	3%	3%	11%	10%
Age							
Elementary	Middle	High	19-30	31-50	50-65	Over 65	
4%	15%	19%	8%	38%	7%	8%	
Age Group							
7-18	19-25	Older than 26					
28%	4%	57%					

Table 1. Distribution of respondents' demographics. Shown are percentages of gender, ethnicity, marital status, political party, religion, age, and age group distributions (n = 143 respondents).

The distribution of selected demographics across the different age groups was also assessed (Table 2). Data from both the summary of demographics, and the distribution of demographics across different age groups indicated that the sample size was relatively diverse.

General Issue Analysis

Based on the survey responses, most people believed that all the listed global issues were indeed a problem (Table 3 and Figures 1-3). The issues that generated more than 90% of "yes" responses were pollution, wars, and poverty and hunger. The issues that generated above 70% but below 90% of "yes" responses were global warming, energy crisis, terrorism, healthcare crisis, and government corruption. Bee apocalypse, immigration from Central America, and overpopulation had the lowest numbers of "yes" responses. The issue of bee apocalypse was the least known, as 34% of respondents were not sure that the bee apocalypse even existed, and 16% did not consider it an issue.

The majority of participants indicated that most of the issues could not be solved in the near future (Table 3 and

Figures 1-3). Instead, more than half of the issues could be addressed sometime in the remote future. The most likely issue to be solved in the next 50 years was energy crisis with 83% agreement from participants. Many respondents believed that pollution and global warming might be resolved with 72% and 58% agreement, respectively. Healthcare crisis, immigration, poverty, and hunger were considered issues of a concern, but less people believed that they could be fixed. Some participants indicated that these problems might be addressed in the short-term future, but more likely would be solved in the remote future.

Wars, terrorism, overpopulation, and political corruption generated the most pessimistic responses, either in the near or in the remote future, with "yes" responses at 50%, 44%, 41%, and 48%, respectively (Table 3 and Figure 1-3). This suggested that most of the people simply did not believe that these four issues could ever be solved.

Age	White	African American	Hispanic	Asian	Other
6-11	80%				20%
12-14	50%	9%	14%	23%	4%
15-18	70%	4%	11%	15%	
19-30	55%	9%	18%	9%	
31-50	50%	30%	10%	10%	
51-65	50%	30%	10%	10%	
65-100	100%				
All	66%	8%	8%	16%	3%

Age	Male	Female
6-11		100%
12-14	64%	36%
15-18	30%	70%
19-30	45%	55%
31-50	47%	53%
51-65	70%	30%
65-100	17%	83%
All	44%	56%

Age	Muslim	Jewish	Christian	Buddhist	Hindu	New Age	Agnostic	Atheist
6-11		40%	40%				20%	
12-14	9%	5%	41%	23%	9%			14%
15-18	4%	7%	59%	7%	4%	4%		7%
19-30	9%		55%				27%	
31-50	4%	4%	45%	7%	2%	4%	15%	15%
51-65	10%		30%	10%		10%	20%	20%
65-100		8%	67%				8%	8%
All	5%	6%	49%	8%	3%	3%	10%	11%

Table 2. Distribution of selected demographics across studied age groups. Shown are different demographics with which the participants self-identified. The data represented as percentages (n = 143 respondents). A) Ethnicity distribution. B) Gender distribution. C) Religious background distribution. Data based on self-identification.

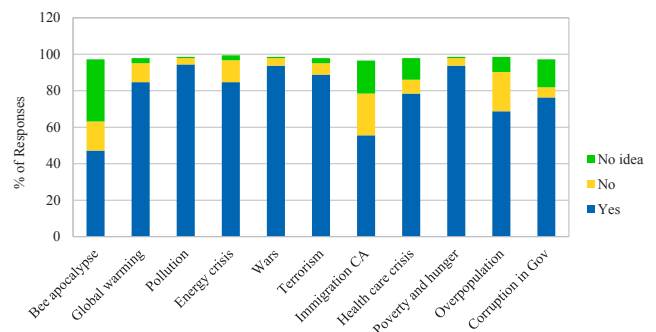


Figure 1. Summary of responses for "Is it an Issue?". Shown is the percentage of "yes", "no" and "no idea" responses to the question of whether each problem is an issue (n=143 respondents).

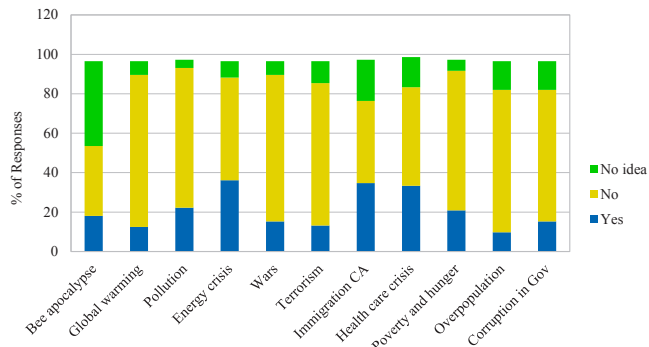


Figure 2. Summary of responses for “Is it possible to solve in near future?”. Shown is the percentage of “yes”, “no” and “no idea” responses to the question of whether it is possible to address each issue in the next 2-10 year (n=143 respondents).

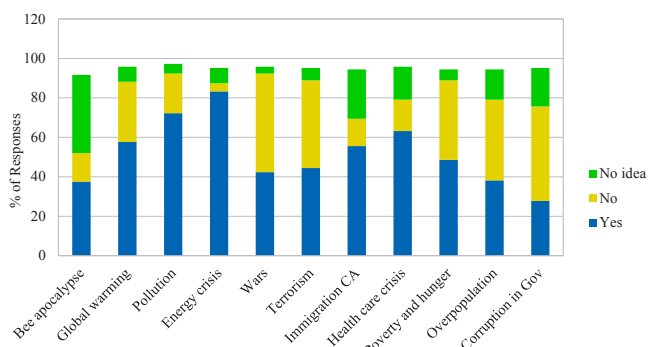


Figure 3. Summary of Responses for “Is it possible to solve in long-term future?”. Shown is the percentage of “yes”, “no” and “no idea” responses to the question of whether it is possible to address each issue in the next 10-50 year (n=143 respondents).

Age Group Analysis

Chi-square analysis of correlation between responses and demographics of the responders revealed several significant correlations (Table 4). While there were correlations with a few demographic characteristics, we focused on the correlation with age groups. Correlation analysis of age groups and the responses demonstrated that global warming, pollution, energy crisis, wars, terrorism, and poverty and hunger were considered real issues by all age groups, with the majority of “yes” responses higher than 80% and for some age groups reaching 100% (Table 4).

Immigration, healthcare crisis, and political corruption were not considered big problems by the elementary and middle school age groups (Table 3 and Figure 1-3). None of the elementary school students believed that immigration was an issue, while only 36% of the middle school participants found it concerning. Only 40% of the elementary students and 55% of the middle school students considered the health care crisis a problem. Interestingly, 20% percent of elementary school children and 42% of middle school children already viewed Congress corruption as an important issue.

Overpopulation was considered a problem by all the age groups, with the exception of the 51-65 age group, of which only 33% considered it a serious issue (Table 3 and

Figure 1-3). Many respondents were not aware of the bee apocalypse, and only the high school aged group recognized it as a problem.

Is it Considered an Issue?		Age						
Issue	Elementary	Middle	High	19-30 years	31-50 years	50-65 years	Above 65	
Bee apocalypse	20%	27%	81%	55%	43%	50%	42%	
Global warming	80%	91%	100%	82%	87%	70%	64%	
Pollution	100%	91%	100%	100%	96%	100%	82%	
Energy crisis	100%	86%	100%	64%	74%	70%	58%	
Wars	100%	95%	96%	91%	96%	80%	0%	
Terrorism	80%	91%	96%	82%	91%	80%	100%	
Immigration CA	0%	36%	70%	45%	66%	50%	70%	
Health care crisis	40%	55%	96%	91%	83%	100%	67%	
Poverty and hunger	100%	95%	100%	100%	91%	90%	100%	
Overpopulation	77%	85%	73%	65%	80%	33%	70%	
Corruption in Gov	20%	42%	93%	82%	87%	90%	91%	

Possible to Solve in 2-10 years?		Age						
Issue	Elementary	Middle	High	19-30 years	31-50 years	50-65 years	Above 65	
Bee apocalypse	20%	9%	11%	36%	18%	30%	33%	
Global warming	40%	27%	11%	27%	0%	10%	27%	
Pollution	100%	91%	100%	100%	96%	100%	81%	
Energy crisis	80%	50%	52%	36%	31%	0%	27%	
Wars	40%	36%	15%	18%	8%	0%	18%	
Terrorism	20%	32%	15%	18%	4%	0%	27%	
Immigration CA	0%	32%	44%	36%	38%	20%	45%	
Health care crisis	40%	23%	30%	55%	35%	30%	42%	
Poverty and hunger	80%	26%	11%	27%	15%	0%	20%	
Overpopulation	40%	23%	7%	9%	4%	0%	15%	
Corruption in Gov	20%	9%	11%	9%	17%	10%	19%	

Possible to Solve in 10-50 years?		Age						
Issue	Elementary	Middle	High	19-30 years	31-50 years	50-65 years	Above 65	
Bee apocalypse	0%	27%	69%	55%	34%	30%	44%	
Global warming	40%	86%	85%	64%	49%	40%	5%	
Pollution	80%	91%	88%	73%	69%	50%	55%	
Energy crisis	60%	91%	96%	91%	96%	70%	40%	
Wars	80%	86%	65%	27%	28%	0%	20%	
Terrorism	40%	82%	77%	36%	28%	20%	33%	
Immigration CA	0%	32%	44%	36%	38%	20%	45%	
Health care crisis	40%	23%	30%	55%	35%	30%	42%	
Poverty and hunger	80%	95%	62%	45%	38%	20%	20%	
Overpopulation	40%	68%	58%	27%	28%	30%	22%	
Corruption in Gov	40%	32%	46%	27%	21%	20%	27%	

Table 3. Summary of yes responses across age groups. Shown are results represented as percentage of “yes” replies across seven different age groups for whether a particular topic is an issue of concern; whether it can be solved in 2-10 years; or whether it can be solved in 10-50 years (n = 143 respondents).

Most participants did not indicate that any of the listed issues could be solved within the next 10 years (Table 3 and Figure 1-3). However, over 60% of respondents across all the age groups believed that the energy crisis, pollution, and global warming could be solved within 50 years. All the age groups agreed that pollution could be solved. As for the energy crisis, all the “yes” responses within the age groups were between 60-90%, except for the above 65 years-of-age group, of which only 40% considered it a challenge.

	Age Group	Educa. Uo.	Gender	Race	Employment	Marital Status	Income	Personality	Faith
Bees	0.004*	0.052	0.157	0.039	0.069	0.031	0.314	0.681	0.313
Warming	0.009*	0.193	0.095	0.216	0.008*	0.006*	0.626	0.987	0.769
Pollution	0.227	0.908	0.666	0.397	0.001*	0.024	0.642	0.334	0.360
Energy Crisis	0.002*	0.120	0.820	0.126	0.000*	0.000*	0.390	0.000*	0.293
Terrorism	0.198	0.326	0.584	0.754	0.582	0.625	0.853	0.547	0.001*
Immigration	0.003*	0.004*	0.781	0.004*	0.009*	0.474	0.359	0.119	0.000*
Health	0.000*	0.000*	0.708	0.459	0.250	0.053	0.029	0.730	0.354
Poverty	0.391	0.014	0.120	0.000*	0.000*	0.600	0.739	0.433	0.001*
Overpopulation	0.064	0.062	0.355	0.120	0.000*	0.003*	0.130	0.535	0.142
Corruption	0.000*	0.000*	0.348	0.029	0.014	0.005*	0.000*	0.124	0.724

Table 4. Correlation of “yes” responses to demographics. Shown are p-values calculated with chi-square; p-values lower than or equal to 0.01 are marked with asterisks.

The issues which were universally believed to be difficult to solve in the long term were immigration and healthcare crisis (Table 3 and Figure 1-3). The percentage of responses for those who believed that those issues could be resolved were low, with about 44% of school-age respondents and only 20% of 19 to 65-year-olds indicating that a solution in the remote future was possible.

Wars, terrorism, poverty and hunger, and overpopulation had unfavorable results for the older age groups (from 19 to 65 and older), but the younger participants (from elementary to high school) stipulated that these issues could be solved (Table 3 and Figure 1-3). For the adult group from 19 to 65, the “yes” response rate ranged from 0% to 45%. For respondents from elementary school to high school, the “yes” response rate ranged from 40-95%. This clearly demonstrated that the younger respondents were more optimistic and hopeful about solving the issues of wars, terrorism, poverty and hunger, and overpopulation than the older participants.

Interestingly, Congress corruption was the only issue that was universally considered the most unlikely ever to get resolved, with only 27% of the older people still thinking that the US Congress could be rectified (Table 3 and Figure 1-3). The younger age groups were not optimistic either, as indicated by a dramatically lower “yes” response rate. This observation was consistent with other research regarding political corruption in the USA (52).

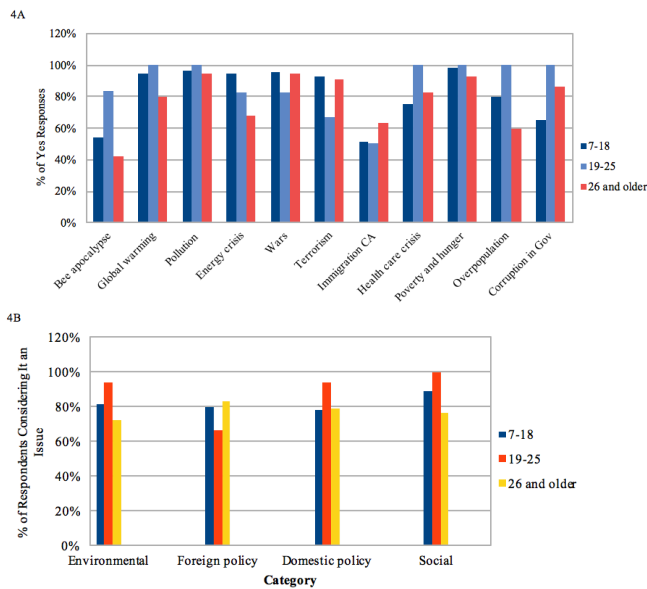


Figure 4. All issues were equally important across all age groups. A) Shown are % of “yes” for each of the issues across three combined age groups. B) Shown are % of respondents for categorized issues across three combined age groups.

To better understand correlation with age, the respondents were grouped into three different age groups (Figures 4-6). The “primary and secondary school” group encompassed the 7-18 year-olds, which included elementary, middle, and high school students. The “very young adults” group consisted of the 19-25 year-olds, which included college students and

working young adults. The third group included the 26 years old and older, in which many people typically finished college, could be employed, and often had their own children and/or grandchildren.

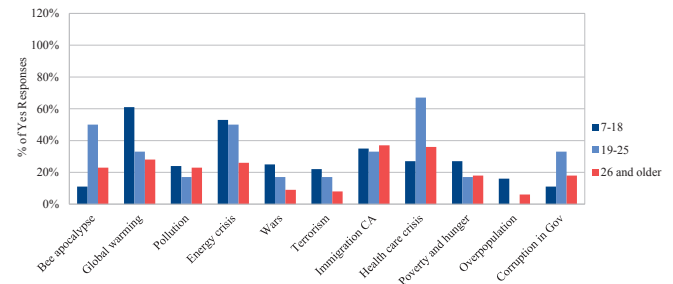


Figure 5. The younger age groups were more optimistic about solving majority of issues in the near future, 2-10 years. Shown are responses for % of “yes” categorized into 3 combined age groups. Younger respondents considered most of the problems to be issues.

The aggregated data clearly showed that children and adults had a different outlook on the presented problems and did not agree whether some issues could or could not be solved (Figures 4-6). Problems such as global warming, wars, terrorism, poverty and hunger, and overpopulation created the most disagreement. It appears that children believed that these challenges could be solved in the remote future, while adults did not think it was ever possible. Based on the written responses, children proposed for people to work together to solve problems. Adults viewed people as greedy, dishonest, and unable to work together to address global concerns.

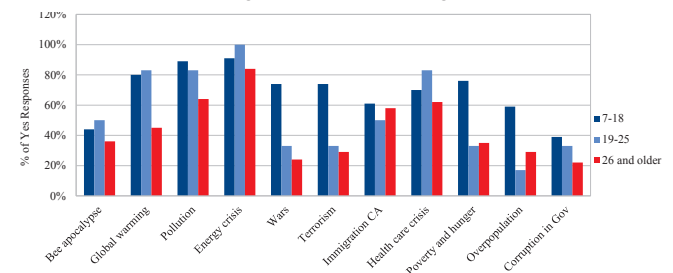


Figure 6. The younger age groups were more optimistic about solving majority of issues in the long term, 10-50 years. Shown are response for % of “yes” categorized into 3 combined age groups. Younger respondents considered most of the problems to be issues.

The 7-18 years-old age group was more confident in solving most of the issues in the long term, while the 26 and older group was significantly less optimistic about resolving the presented topics (Figure 7). These results supported our hypothesis. In contrast to adults, children appeared to be more optimistic and believed that many of the presented issues could be successfully addressed in the future. The level of importance for categorized issues was equally important across all age groups (Figure 4A).

DISCUSSION

The hypothesis of our project was that children are more optimistic than adults in the context of solving world problems.

Overall, the results supported our hypothesis. This survey did not attempt to understand why children are more optimistic than adults, but we clearly saw a correlation with younger age and positive outlook. A possible explanation of why children are more optimistic than adults may center around education, awareness, and understanding of the topics at hand. Perhaps the fact that students do not know in detail about certain issues is the reason why they are optimistic about solving them.

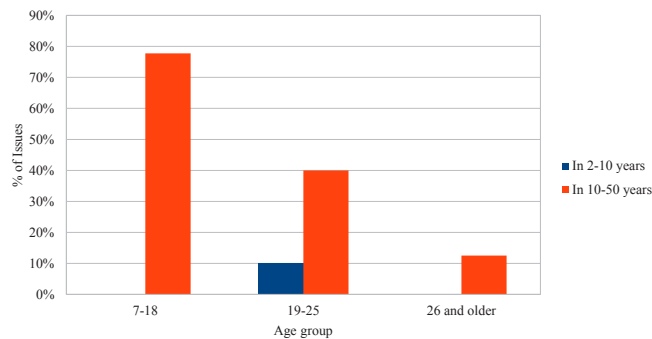


Figure 7. The 7 to 18 age group is the most optimistic. Represented is optimism across combined age groups. Shown are percentages of issues that 65% or more of respondents in the age group believed could be solved in the near or remote future.

An important factor to consider is how often respondents read or watch news. In the USA, children on the average watch more than 20 hours of TV per week, adults watch 35.5 hours per week, and older adults watch around 50 hours per week (53). It is unclear how many hours are spent on news or educational programs versus recreational shows. However, one study found that most broadcasting stations (59%) offered only the minimum of 3 hours per week of educational or informational programming and only 3% of stations offer more than 4 hours (54). Three-quarters of stations confined all their educational and informational programming to weekends, and more than a quarter of programs were rated as high in physical or social aggression (54). Probably, TV contributes very little to children's awareness on topics presented in the survey.

In terms of magazine readership, the age of average reader is increasing. Many magazines report that the average age of their reader is higher than that of the general adult population's (55, 56). Based on research, in the past a newspaper audience has been more educated, affluent, and older than non-newspaper readers, but as digital media has gained in prominence, electronic newspapers attract younger readers (57). Nowadays, younger adults now account for a greater percentage of electronic readers. Readers in the 21 to 34 age group make up 25% of the U.S. population and represent 24% of the total monthly electronic newspaper readership (57). Digital distribution of well-established magazines, journal, newspapers has allowed to reach adults of all ages, but not necessarily school-aged children in elementary through high school level.

Exposure to current news, events, and social media

may influence whether respondents are aware of a certain topic and how they feel about it. Social trends and political pressures may also shape a person's view and influence their perspective.

Other elements that may impact outlook are cultural and family upbringing, urban versus rural setting, or personal character and convictions. None of these were examined in this study. The question whether respondents considered themselves a pessimist, optimist, realist, programmatic, or a whiner is not a sufficient, nor reliable marker of accurate self-reflection and may not fully assesses the person's daily outlook and convictions. A new study would need to be conducted to better understand what influences and drives outlook and perspective on a given topic.

An interesting element of this study was the possibility of tracking at what age people start to learn and be concerned about certain topics. Even though our study did not examine educational background behind each issue, we were still able to show a correlation between age and positive-negative outlook. A longitudinal study may be a more appropriate way to assess topic awareness and may have a better capacity to gauge explanation of a perspective. In addition, such a study may help to identify gaps in the educational system and help to augment what is being taught in schools. It is important for students to be aware of current problems the world faces so that the next generation of leaders are better educated and better equipped to develop proper solutions.

Moreover, it would be interesting to learn if the same adults who are now pessimistic about the issues had a different view when they were younger. People appear to be more optimistic when they are young. Children see endless possibilities and stagnation seems an eternity away. But then the years pass and life proves to be difficult. With age, adults become jaded and gradually lose their sense of optimism. This condition is reflected in our study and it does seem that with age positive outlook slowly degrades. Research indicated that older people process negative information less deeply than they do positive information. Perhaps one explanation is that with age people become desensitized towards negative news. When they are younger, they process negative information deeper (58). In the future, we would like to determine whether adults who are pessimistic were more optimistic when they were children and whether personal experiences acquired with age and broader awareness of how things work result in a more negative impression of the world. We would like to also understand whether the children of today turn into adults with opinions similar to those of adults of today. Again, several limitations were noticed as possible shortcomings in interpreting the presented data and may be better answered via a longitudinal study.

During data analysis, other deficiencies became apparent. Some unintentional bias might have been introduced by using terms such as 'crisis' and 'apocalypse'. These terms might have encouraged participants to pick a more pessimistic response. These questions should be

rephrased in future studies. Another limitation of the study was unclear assessment of whether respondents are optimists or pessimists in their daily lives. A scenario with several potential outcomes to choose from, ranging from optimistic to pessimistic, would assess a person's outlook more accurately than relying on background information or self-description. We did not use Likert Scale since we did not think that it would provide any additional details for the general questions about the future that were used in the survey. However, in another study such a scale may help to better understand variation in outlook and general perspective. Respondents also had an opportunity to express and elaborate on their opinion. Many children noted that most of the issues could be solved with the use of technology, communication, and cooperation. Some children said that if society worked together, it could accomplish anything. One middle school student stated: "With kindness and improved technology, we can solve most problems." Another wrote that "people can talk and solve problems because they are mostly good and reasonable." The belief in the goodness of human spirit was common among children.

There were, however, some noteworthy exceptions among the younger group. Some children were clearly less optimistic about the future. Their opinion was like that of the adults, as they also stated that many people are corrupt and greedy. They believe that our country is setup with greedy and selfish intentions and may be difficult to repair. They noted that 50 years is a lot of time, but still not enough to "fix it". Some children understand that our planet is being destroyed by humans, and it is difficult to control greed and desire for power. It is possible that their opinion might have been influenced by the views of their parents and other adults. It is also equally possible that such a negative opinion might be original and may reflect actual sentiments of those children. Research indicated that half of the GenZers questioned agreed that voting is important and even though most are too young to vote, they are interested in social issues at much younger age than many generations before them (59). Many of them are divided on issues such as healthcare and trustworthiness of government officials, but majority has a hopeful outlook and believes in attaining the "American Dream" (59).

Adults were less optimistic and had a more realistic view of the world and people around them. One response summarized well the general perspective of many adults: "People are greedy and power hungry. Their nature won't change. Problems will persist." Most adults believe that the government is corrupt and greedy. Many stated that people are mostly evil, and wars cannot be prevented because they stem from human nature. Many adults pointed out that political corruption is not only the root cause of so many problems, but also will prevent them from being solved in the future.

However, there were exceptions among adults as well. A few adults believed that problems could be solved due to the extraordinary advancement of human technology,

cooperation, belief in the common good, and reforms in the government which include the elimination of political corruption.

The results of this study clearly demonstrate that children are much more optimistic than adults. Perhaps adults can learn from children to be more hopeful. Perhaps children could learn from adults and from their experiences to be more pragmatic in addressing world issues. Understanding the relationship between optimism, experience, and pragmatic thinking, may be a key to addressing many concerning issues and building strategies to solve them.

MATERIALS AND METHODS

This survey was designed using multiple choice questions to assess demographic characteristics of the participants and their opinions about different world issues. Additionally, there was one open response question giving respondents an opportunity to discuss their opinion in more detail.

The study was approved by Andover public school administration committee. An appropriate Scientific Review Committee (SRC) form was obtained and approved.

Respondents were approached in public places such as the Senior Center, the Youth Center, local stores, streets, and private houses. The survey was anonymous and did not capture respondents' name and contact information.

Results were analyzed using free, open-source PSPSS statistical software. Correlations were evaluated using chi-square method. The data were further analyzed in the free, open-source LibreOffice Calc application.

The number of respondents was 143. Respondents were not limited by residency in a specific town, only to the state of Massachusetts. To determine if the results of the survey matched the population of a typical mid-size town, highest margin of error was calculated for different confidence levels across all of the reported data. The margin of error (MOE) was calculated according to the formula:

This calculation allowed us to determine if the amount of people surveyed was enough to be confident about the accuracy of the data collected. If we assume that a typical mid-size town has a population of around 30,000, the margins of error for the confidence levels of 90%, 95% and 99% are $\pm 6.9\%$, $\pm 8.2\%$, and $\pm 10.7\%$ respectively.

Received: June 10, 2019

Accepted: December 12, 2019

Published:

REFERENCES

1. Carver, Charles S., et al. "Optimism." *Clinical Psychology Review*, vol. 30, no. 7, 2010, pp. 879–889., doi:10.1016/j.cpr.2010.01.006.
2. Boseovski, Janet J. "Children Are Natural Optimists – Which Comes with Psychological Pros and Cons." *The Conversation*, 19 Dec. 2018, theconversation.

- com/children-are-natural-optimists-which-comes-with-psychological-pros-and-cons-93532.
3. Kotter-Grühn, Dana, and Jacqui Smith. "When Time Is Running out: Changes in Positive Future Perception and Their Relationships to Changes in Well-Being in Old Age." *Psychology and Aging*, vol. 26, no. 2, 2011, pp. 381–387., doi:10.1037/a0022223.
 4. Lang, Frieder R., et al. "Forecasting Life Satisfaction across Adulthood: Benefits of Seeing a Dark Future?" *Psychology and Aging*, vol. 28, no. 1, 2013, pp. 249–261., doi:10.1037/a0030797.
 5. Heckhausen, Jutta, et al. "Gains and Losses in Development throughout Adulthood as Perceived by Different Adult Age Groups." *Developmental Psychology*, vol. 25, no. 1, 1989, pp. 109–121., doi:10.1037/0012-1649.25.1.109.
 6. Robinson-Whelen, Susan, et al. "Distinguishing Optimism from Pessimism in Older Adults: Is It More Important to Be Optimistic or Not to Be Pessimistic?" *Journal of Personality and Social Psychology*, vol. 73, no. 6, 1997, pp. 1345–1353., doi:10.1037//0022-3514.73.6.1345.
 7. Carstensen, L. L. "The Influence of a Sense of Time on Human Development." *Science*, vol. 312, no. 5782, 2006, pp. 1913–1915., doi:10.1126/science.1127488.
 8. Brissette, Ian, et al. "The Role of Optimism in Social Network Development, Coping, and Psychological Adjustment during a Life Transition." *Journal of Personality and Social Psychology*, vol. 82, no. 1, 2002, pp. 102–111., doi:10.1037//0022-3514.82.1.102.
 9. Carver, Charles S., et al. "Effects of Good Versus Bad Mood and Optimistic Versus Pessimistic Outlook on Social Acceptance Versus Rejection." *Journal of Social and Clinical Psychology*, vol. 13, no. 2, 1994, pp. 138–151., doi:10.1521/jscp.1994.13.2.138.
 10. Fitzgerald, Terence E., et al. "The Relative Importance of Dispositional Optimism and Control Appraisals in Quality of Life after Coronary Artery Bypass Surgery." *Journal of Behavioral Medicine*, vol. 16, no. 1, 1993, pp. 25–43., doi:10.1007/bf00844753.
 11. Geers, Andrew L., et al. "Dispositional Optimism and Engagement: The Moderating Influence of Goal Prioritization." *Journal of Personality and Social Psychology*, vol. 96, no. 4, 2009, pp. 913–932., doi:10.1037/a0014830.
 12. MacLeod AK, Conway C. Well-being and the anticipation of future positive experiences: The role of income, social networks, and planning ability
 13. Carver, Charles S., et al. "Optimism." *Clinical Psychology Review*, vol. 30, no. 7, 2010, pp. 879–889., doi:10.1016/j.cpr.2010.01.006.
 14. "About the UN." United Nations, *United Nations*, www.un.org/about-un.
 15. "About Us." *The Borgen Project*, www.borgenproject.org/about-us/.
 16. "About GVI - What We Do & How We Got Here." *GVI USA*, www.gviusa.com/about-us/.
 17. Anderegg, W. R. L., et al. "Expert Credibility in Climate Change." *Proceedings of the National Academy of Sciences*, vol. 107, no. 27, 2010, pp. 12107–12109., doi:10.1073/pnas.1003187107.
 18. Essick, Peter. "Air Pollution Causes, Effects, and Solutions." *Air Pollution*, Facts and Information, 25 June 2019, www.nationalgeographic.com/environment/global-warming/pollution/.
 19. Holgate, Stephen. "Every Breath We Take: the Lifelong Impact of Air Pollution – a Call for Action." *Clin Med (Lond)*, vol. 17, no. 1, Feb. 2017, pp. 8–12.
 20. Hong, Chen, and Mark S Goldberg. "The Effects of Outdoor Air Pollution on Chronic Illness." *MJM*, vol. 12, no. 1, Jan. 2019, pp. 38–64., doi:10.1071/NB10026.
 21. Brunnekreef, Bert. "Health Effects of Air Pollution Observed in Cohort Studies in Europe." *J Expo Sci Environ Epidemiol*, no. 17, 2007, pp. 61–65.
 22. Boyd, J.T. "Climate, Air Pollution, and Mortality." *Brit. J. Prev. Soc. Med.*, vol. 14, no. 3, July 1960, pp. 123–135.
 23. Denchak, Melissa. "Water Pollution: Everything You Need to Know." *NRDC*, 23 Oct. 2019, www.nrdc.org/stories/water-pollution-everything-you-need-know.
 24. Owa, F.D. "Water Pollution: Sources, Effects, Control and Management." *Mediterranean Journal of Social Sciences*, vol. 4, no. 8, Sept. 2013, pp. 65–68.
 25. Harse, Grant A. "Plastic, the Great Pacific Garbage Patch, and International Misfires at a Cure." *UCLA Journal of Environmental Law & Policy*, vol. 29, no. 2, 2011, pp. 331–363.
 26. Lebreton, L, et al. "Evidence That the Great Pacific Garbage Patch Is Rapidly Accumulating Plastic." *Scientific Reports*, vol. 8, no. 4666, 22 Mar. 2018.
 27. "Plastic-Choked Seas: Marcella Hansch Wants to Save the Oceans." *Philstar.com*, www.philstar.com/lifestyle/business-life/2018/03/08/1794764/plastic-choked-seas-marcella-hansch-wants-save-oceans.
 28. Andrady, A L. "Microplastics in the Marine Environment." *Mar. Pollut. Bull.*, vol. 62, 2011, pp. 1596–1605.
 29. "Microplastics and Human Health-an Urgent Problem." *The Lancet Planetary Health.*, vol. 1, no. 7, Oct. 2017, p. 254.
 30. Wright, Stephanie L, and Frank J Kelly. "Plastic and Human Health: A Micro Issue?" *Environ. Sci. Technol.*, vol. 51, no. 12, 22 May 2017, pp. 6634–6647.
 31. Cabel, B, et al. "Pollution of Drinking Water with Nitrate." *Osti.Gov.*, vol. 11, no. 111, 1982.
 32. Farwell, John, and Mark J Nieuwenhuijsen. "Contaminants in Drinking Water: Environmental Pollution and Health." *British Medical Bulletin*, vol. 68, no. 1, Dec. 2003, pp. 199–208.
 33. Cachada, Duarte, and Armando C Duarte. "Chapter 1 – Soil and Pollution: An Introduction to Main Issues." *Soil Pollution from Monitoring to Remediation*, edited by Teresa Rocha-Santos, Academic Press, 2017, pp. 1–28.

34. Aktar, Wasim, et al. "Impact of Pesticides Use in Agriculture: Their Benefits and Hazards." *Interdisciplinary Toxicology*, vol. 2, no. 1, 2009, pp. 1–12., doi:10.2478/v10102-009-0001-7.
35. Yeomans, J.c., and J.m. Bremner. "Denitrification in Soil: Effects of Insecticides and Fungicides." *Soil Biology and Biochemistry*, vol. 17, no. 4, 1985, pp. 453–456., doi:10.1016/0038-0717(85)90008-2.
36. Vanengelsdorp, Dennis, et al. "Colony Collapse Disorder (CCD) and Bee Age Impact Honey Bee Pathophysiology." *Plos One*, vol. 12, no. 7, 2017, doi:10.1371/journal.pone.0179535.
37. Oldroyd, Benjamin P. "What's Killing American Honey Bees?" *PLoS Biology*, vol. 5, no. 6, 2007, doi:10.1371/journal.pbio.0050168.
38. Zou, Caineng, et al. "Energy Revolution: From a Fossil Energy Era to a New Energy Era." *Natural Gas Industry B*, vol. 3, no. 1, 2016, pp. 1–11., doi:10.1016/j.ngib.2016.02.001.
39. Miller, Richard G., and Steven R. Sorrell. "The Future of Oil Supply." *Philosophical Transactions of the Royal Society A: Mathematical, Physical and Engineering Sciences*, vol. 372, no. 2006, 2014, p. 20130179., doi:10.1098/rsta.2013.0179.
40. Schuurman, Bart. "Research on Terrorism, 2007–2016: A Review of Data, Methods, and Authorship." *Terrorism and Political Violence*, 2018, pp. 1–16., doi:10.1080/09546553.2018.1439023.
41. Bell, J. Bowyer. "Trends on Terror: The Analysis of Political Violence." *World Politics*, vol. 29, no. 3, 1977, pp. 476–488., doi:10.2307/2010007.
42. Schmid, Alex P. *Political Terrorism: Research Guide to Concepts, Theories, Data Bases and Literature*. North-Holland, 1985.
43. Baalen, Sebastian Van, and Kristine Höglund. "'So, the Killings Continued': Wartime Mobilization and Post-War Violence in KwaZulu-Natal, South Africa." *Terrorism and Political Violence*, vol. 31, no. 6, 2017, pp. 1168–1186., doi:10.1080/09546553.2017.1318126.
44. Craig Briddle. "The Causes of War and Those of Peace." *The Objective Standard*, 17 Oct. 2019, www.theobjectivestandard.com/2014/10/causes-war-peace/.
45. Gundersen, Craig, and James P Ziliak. "Food Insecurity Research in the United States: Where We Have Been and Where We Need to Go." *Applied Economic Perspectives and Policy*, vol. 40, no. 1, 2018, pp. 119–135., doi:10.1093/aep/pxx058.
46. Pollard, Christina M, and Sue Booth. "Food Insecurity and Hunger in Rich Countries—Is Time for Action against Inequality." *International Journal of Environmental Research and Public Health*, vol. 16, no. 10, 2019, p. 1804., doi:10.3390/ijerph16101804.
47. Powledge, Fred. "Food, Hunger, and Insecurity." *BioScience*, vol. 60, no. 4, 2010, pp. 260–265., doi:10.1525/bio.2010.60.4.3.
48. Bavel, Van J. "The World Population Explosion: Causes, Backgrounds and -Projections for the Future." *Facts, Views & Vision in ObGyn.*, vol. 5, no. 4, 2013, pp. 281–291.
49. Wall, Malkie, et al. "Corruption Consultants." *Center for American Progress*, July 2019, www.americanprogress.org/issues/democracy/reports/2019/07/22/472363/corruption-consultants/.
50. Campos, Nauro F., and Francesco Giovannoni. "Political Institutions, Lobbying and Corruption." *Journal of Institutional Economics*, vol. 13, no. 4, 2017, pp. 917–939., doi:10.1017/s1744137417000108.
51. Graycar, Adam. "Corruption: Classification and Analysis." *Policy and Society*, vol. 34, no. 2, 2015, pp. 87–96., doi:10.1016/j.polsoc.2015.04.001.
52. Wilkinson College. "America's Top Fears 2018 - Chapman University Survey of American Fears." *Wilkinson College of Arts, Humanities, and Social Sciences*, 16 Oct. 2018, blogs.chapman.edu/wilkinson/2018/10/16/americas-top-fears-2018.
53. "The Nielsen Total Audience Report: Q2 2016." *Nielsen*, Sept. 2016, www.nielsen.com/us/en/insights/report/2016/the-nielsen-total-audience-report-q2-2016/.
54. Chamberlain, Craig. "Quality, Quantity Lacking in Children's Educational TV, Study Says." *ILLINOIS*, 12 Nov. 2008, news.illinois.edu/view/6367/206121.
55. Ives, Nat. "The Average Newspaper Reader Is Now Older Than Ever." *Business Insider*, 27 May 2009, www.businessinsider.com/the-average-newspaper-reader-is-now-older-than-ever-2009-5.
56. "Median Age of Readership by Magazine." *Pew Research Center's Journalism Project*, 12 Mar. 2007, www.journalism.org/numbers/median-age-of-readership-by-magazine/.
57. "Newspapers Deliver Across the Ages." *Nielsen*, Dec. 2016, www.nielsen.com/us/en/insights/article/2016/newspapers-deliver-across-the-ages/.
58. Mather, M., et al. "Amygdala Responses to Emotionally Valenced Stimuli in Older and Younger Adults." *Psychological Science*, vol. 15, no. 4, 2004, pp. 259–263., doi:10.1111/j.0956-7976.2004.00662.x.
59. Fromm, Jeff. "New Study Finds Social Media Shapes Millennial Political Involvement And Engagement." *Forbes*, Forbes Magazine, 22 June 2016, www.forbes.com/sites/jefffromm/2016/06/22/new-study-finds-social-media-shapes-millennial-political-involvement-and-engagement/#4167deee2618.

Copyright: © 2019 Luck and Keane. All JEI articles are distributed under the attribution non-commercial, no derivative license (<http://creativecommons.org/licenses/by-nc-nd/3.0/>). This means that anyone is free to share, copy and distribute an unaltered article for non-commercial purposes provided the original author and source is credited.

Effects of ocean acidification on the photosynthetic ability of *Chaetoceros gracilis* in the Monterey Bay

Kelly Harvell, Jason Nicholson
Monterey High School, Monterey, California

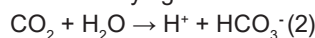
SUMMARY

Ocean pH levels have been dropping since the Industrial Revolution due to increased carbon dioxide gas (CO₂) in the atmosphere. When CO₂ is absorbed by the ocean, hydrogen ions are released, resulting in a decrease in pH. Dangerous levels of carbonic acid in the ocean ecosystem as a result of CO₂ absorption may have an effect on the health of marine algae, such as diatoms. Marine diatoms account for an estimated 20% of oxygen production in the atmosphere and are essential to the aquatic food chain. I hypothesized that increased ocean acidity would decrease the photosynthetic ability of *Chaetoceros gracilis*, a diatom prolific in Monterey Bay, because of the usually corrosive effects of carbonic acid on both seashells and cells' internal structures. I altered pH of algae environments and measured the photosynthetic ability of diatoms over four days by spectrophotometer. Surprisingly, a decrease in pH improved the photosynthetic ability of *C. gracilis*, but only within a specific pH range. The diatoms grown in pH 7.5 medium had the highest average absorbance value; therefore, this pH value is a "sweet spot" that optimizes the growth of this species of diatom. These findings indicate that *C. gracilis* may become more abundant in Monterey Bay as the pH of the ocean continues to drop, potentially contributing to harmful algal blooms.

INTRODUCTION

Climate change is a multifaceted issue that is the result of the burning of fossil fuels (1). Greenhouse gases are released when fossil fuels are used as an energy source; these gases, specifically carbon dioxide (CO₂), absorb heat from solar radiation and reflect it back to Earth's surface. The Industrial Revolution led to the creation of many large-scale factories that emit excess carbon dioxide gas, along with other fossil fuels, to provide energy to their businesses. The potentially detrimental effects carbon dioxide may have on the pH levels of the world's oceans has become a highly contested topic in recent years in conjunction with raising concerns about climate change in general (1). An estimated 30% of CO₂ in the atmosphere is absorbed by the ocean and reacts with water (H₂O) to form carbonic acid (H₂CO₃) (1, 2), which then breaks down into hydrogen and bicarbonate ions. The chemical

formula underlying this ocean acidification phenomenon is:



One way to quantify this phenomenon is by measuring a solution's pH, a value that represents its acidity or basicity. Therefore, as more carbon dioxide gas is absorbed into the ocean, levels of hydrogen ions will increase, leading to decreased oceanic pH levels. The current pH level of the ocean surface has been measured at pH 8.1, which is slightly basic (1). According to the National Oceanic and Atmospheric Administration, "the pH of surface ocean waters has fallen by 0.1 pH units [since the Industrial Revolution]" (3). This may not seem significant but, because the pH scale is logarithmic, a 0.1 pH unit drop is equivalent to a 30% increase in acidity. My experiment explored the behavior of a specific species of diatom when grown in medium of the ocean's original surface pH (pH 8.2), in a more acidic environment with pH 7.5, and at a much more acidic medium at pH 7.0. These pH levels were chosen to represent the steady decline of ocean pH levels following the Industrial Revolution, as our control condition was set to the pH level of the sea before that point in history.

Diatoms are unicellular microalgae that are abundant in freshwater and seawater environments. Increased acidity may contribute to the breakdown of diatoms' internal cellular structures (4). However, other studies have found opposite results with different species of marine diatoms (5). Lower pH levels could be beneficial to the growth of marine diatoms, indicating that these microorganisms could be acidophilic, or able to grow in environments of high acidity (5). Rapid increases in algae populations may lead to algal blooms, which have the capability to decimate entire aquatic ecosystems. When toxin-producing algae multiply rapidly and then die, they starve the water column of oxygen; their remains are decomposed by bacteria, which depletes the dissolved oxygen present in marine environments (6). Fish and other organisms in the water die from anoxia and lack of sunlight. Poisoned seafood can send people to the hospital or even be fatal (7). The effects that increased acidity may have on these microorganisms in the Monterey Bay National Marine Sanctuary (MBNMS) could be catastrophic. The MBNMS, stretching from San Francisco to Cambria on the California coast, is the largest federally protected underwater sanctuary in the United States. It is home to hundreds of diverse and endangered species that are indigenous to this portion of the Pacific Ocean (8). A decrease in the health of the marine diatoms present in the MBNMS could reflect the poor health of diatoms globally which, given that diatoms are responsible

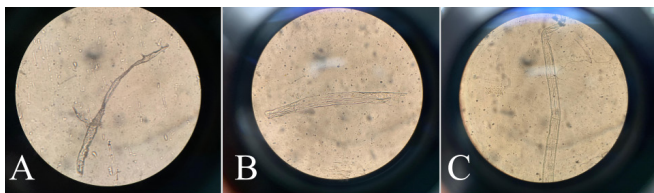


Figure 1. *Chaetoceros gracilis* from sample group cuvettes after 4 days in the pH buffer/seawater mixture. A) *C. gracilis* diatoms in medium of pH 8.2. B) *C. gracilis* diatoms in medium of pH 7.5. C) *C. gracilis* diatoms in medium of pH 7.0. Images taken at 400X.

for generating 20% of the oxygen in Earth’s atmosphere, would catastrophically affect oxygen levels around the world (9).

Limited research has been done specifically on the effects of decreased pH levels on the photosynthetic ability of marine diatoms. The ramifications of ocean acidification on these microorganisms could also vary from species to species because of the differences in individual characteristics across the thousands of species of diatoms in the oceans. The diatom species *Chaetoceros gracilis* was the focus of this experiment because its genus, *Chaetoceros*, is prolific in the Monterey Bay, as observed by an ongoing University of California, Santa Cruz study funded by the California Harmful Algal Bloom Monitoring and Alert Program, or CalHABMAP (10). The sheer diversity of diatom species makes it incredibly difficult for scientists to observe each one’s behavior and characteristics; *C. gracilis*, for example, is only distinguishable by its long, narrow shape and spindles (11). One cannot make an educated assumption about *C. gracilis*’s reaction to a change in the pH of its medium because of the lack of research done on this species.

I hypothesized that a decrease in the pH of media containing *C. gracilis* would cause a decrease in the photosynthetic ability of the diatom. Diatoms exposed to a higher pH (less acidic) will be able to photosynthesize more efficiently than diatoms exposed to a lower pH (more acidic). Using a spectrophotometer, I measured the amount of light the diatoms grown at different pH values absorbed in relation to their photosynthetic ability. The more light the MBNMS samples retained, the more efficiently the assayed diatoms were able to photosynthesize. This data can be used to plot the photosynthetic ability of the samples over time. It was found that, over the experimental timeframe, *C. gracilis* diatoms performed photosynthesis most efficiently at a range from pH 8.2 to pH 7.5. As pH falls past pH 7.5, the photosynthetic ability of the diatoms decreases noticeably.

RESULTS

We used a spectrophotometer to measure the light absorbance of the MBNMS diatom samples, which were kept in three different pH environments and assayed twice daily for four days (Table 1, Figure 1). The spectrophotometer shot light through the specimens and measured absorbance values to quantify the photosynthetic ability of the samples

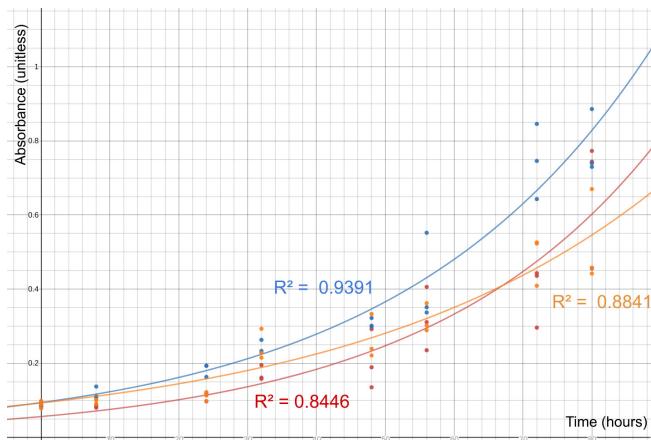


Figure 2. Absorbance Values Over Time. The experiment was performed over the course of 80 hours (four days), and the growth rate of each sample group was quantified by measuring the absorbance rate of each cuvette twice a day. For all sample groups, the absorbance values increased as time increased. Samples grown in medium of pH 8.2 are represented by the red exponential function with the regression equation $y = 0.0560 \cdot 10.3^x$. Samples grown in medium of pH 7.5 are represented by the blue exponential function with the regression equation $y = 0.0937 \cdot 1.03^x$. Samples grown in medium of pH 7.0 are represented by the orange exponential function with the regression equation $y = 0.0928 \cdot 1.02^x$. The coefficient of determination values (R^2) for diatoms in medium of pH 8.2, pH 7.5, and pH 7.0 are 0.8446, 0.9391, and 0.8841, respectively.

(Table 2). The graph of the absorbance values with respect to time clearly displays an upward trend for each sample group (Figure 2). The photosynthetic ability of the diatoms in all samples increases over time, indicating exponential growth of the diatoms’ photosynthetic ability. The regression equations for each pH value are in exponential form: $y = a \cdot b^x$, where “a” is the initial absorbance value, or y-intercept, and “b” is the change factor, or, in this case, the growth rate. This is representative of the growth dynamics of micro-algae. According to Baert’s FAO Fisheries Aquaculture Manual, cultures typically go through different stages of growth: “the lag or induction phase, the exponential phase, phase of declining growth rate, stationary phase, and death or ‘crash’ phase” (12). When our samples were delivered before experimentation, they had already been growing long enough to complete the lag phase. During the timeframe of my experiment, the algae were in the exponential phase, and therefore their growth can be tracked by an exponential regression equation. The diatoms were not cultured long enough to reach the other

pH Level	Experimental Groups			Blanks (B)		
	pH 8.2	pH 7.5	pH 7.0	pH 8.2	pH 7.5	pH 7.0
Distilled Water (mL)	2	2	2	4	4	4
Seawater Medium (mL)	2	2	2	4	4	4
Algae (mL)	4	4	4	0	0	0
Total Volume (mL)	8	8	8	8	8	8
pH Buffer Powder (g)	0.001746	0.001746	0.001746	0.001746	0.001746	0.001746

Table 1. Components in Sample Groups and Blanks. Amounts of each component—distilled water, seawater, pH buffer powder, and *Chaetoceros gracilis* algae—added to the sample group and reference blank test tubes.

	Time (hours)	Cuvette Sample Number	Absorbance of Experimental Groups		
			pH 8.2	pH 7.5	pH 7.0
Day 1; Time 1	0	1	0.097	0.089	0.098
		2	0.081	0.086	0.078
		3	0.083	0.089	0.089
Day 1; Time 2	8	1	0.084	0.108	0.100
		2	0.089	0.110	0.101
		3	0.080	0.137	0.090
Day 2; Time 1	24	1	0.114	0.193	0.098
		2	0.097	0.163	0.122
		3	0.119	0.193	0.113
Day 2; Time 2	32	1	0.158	0.233	0.293
		2	0.161	0.263	0.215
		3	0.195	0.230	0.228
Day 3; Time 1	48	1	0.292	0.299	0.221
		2	0.189	0.301	0.333
		3	0.135	0.322	0.239
Day 3; Time 2	56	1	0.406	0.552	0.362
		2	0.311	0.337	0.302
		3	0.235	0.351	0.289
Day 4; Time 1	72	1	0.436	0.846	0.523
		2	0.443	0.643	0.526
		3	0.296	0.746	0.409
Day 4; Time 2	80	1	0.773	0.886	0.670
		2	0.744	0.730	0.458
		3	0.456	0.740	0.442
Average for all Days			0.253	0.360	0.267

Table 2. Absorbance Values for each Sample Group. Twice a day for four days, the absorbance values for each sample group were measured by spectrophotometer. Reference blanks were used to calibrate the spectrophotometer. Three cuvettes for each sample group were compared with their respective blanks. The table shows the exact absorbance values measured for each sample group on each day, as well as the total average absorbance value for each sample group across all days.

three phases characteristic of algae growth.

At the end of the four-day experiment, absorbance values taken from the two daily time points at each pH value were averaged and used to compare photosynthetic ability across samples (Figure 3). This value represented how the algae grew and increased their surface area to absorb light energy. This simplification was used as a supplement to the exponential functions for data analysis. Diatoms grown at a pH of 7.5 had a 35.13% greater average absorbance value than those at pH 7.0 and a 42.36% greater average than

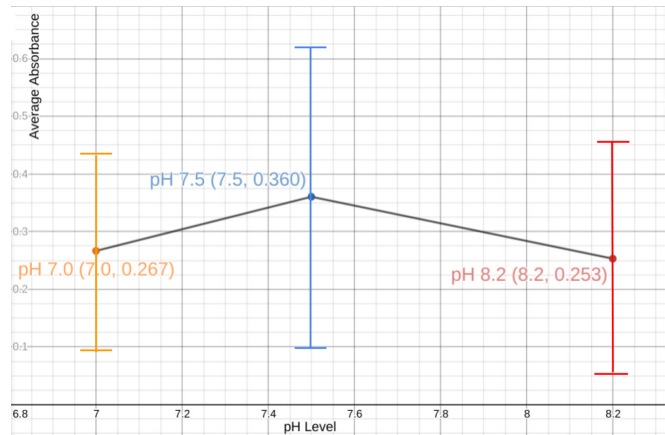


Figure 3. Average Absorbance Values. For each sample group, the absorbance values across all days were averaged to determine the average absorbance value for each of the three different pH levels. The error bars for each pH value represent the standard deviation of the data set.

those at pH 8.2. Samples grown at pH 7.0 had a 5.35% higher absorbance average than those grown at pH 8.2 (Figure 3). However, the average absorbance value for each pH level is not definitive due to the fact that it does not account for the growth rate of the diatoms over time. To further the accuracy of the data, the exponential regression graphs and equations were also taken into account.

The regression equations for each pH level were derived by plotting the absorbance values for each individual cuvette sample at the various pH levels on an absorbance-time graph. The equations represented the relationship between the absorbance values and time; the graph showed an exponential growth trend. A regression equation was fitted to the plotted points using Desmos graphing software for each pH value. The regression equations were very accurate according to their values, or coefficients of determination (Figure 2). A value greater than 0.8 indicates a strong correlation between the independent variable (time) and dependent variable (absorbance values). The coefficients of determination for samples in mediums of pH 8.2, pH 7.5, and pH 7.0 were 0.8446, 0.9391, and 0.8841, respectively. Therefore, the regression equations of the different pH levels fit the data well.

While the average absorbance value for diatoms in medium of pH 7.0 was greater than the overall average for algae grown in medium of pH 8.2, the growth rate (*b*) for those in pH 8.2 was greater than that of those in pH 7.0. This indicates that diatoms in pH 8.2 performed photosynthesis at a faster rate than diatoms at pH 7.0. This is represented by the crossing of the diatom growth rates in pH 8.2 and pH 7.0 cross at approximately hour 67 (Figure 2). At that point, the absorbance values of the samples in pH 8.2 become greater than those of the pH 7.0 samples (Table 2).

The algae samples grown in medium of pH 7.5 were determined to be the best-performing group due to their

high growth rate and high average absorbance; they had a relatively modest initial value (*a*) and a high growth rate (*b*) (Figure 2). Diatoms in pH 8.2 had the same growth rate as those in pH 7.5, indicating that both sample groups performed photosynthesis at roughly the same rate. Nonetheless, samples grown in pH 7.5 had the highest average absorbance of all sample groups.

DISCUSSION

The data observed indicate that a decrease in the pH of media containing *Chaetoceros gracilis* will cause a decrease in the photosynthetic ability of the diatoms. According to my experiment, a decrease in the pH of medium (equivalent to an increase in acidity) can result in *C. gracilis* performing photosynthesis more efficiently. However, there is a specific range within which this species of diatom photosynthesizes most effectively. Diatoms in a medium of pH 7.5 photosynthesized more effectively than those at pH 7.0 (Figure 2). While samples at pH 8.2 and pH 7.5 had the same growth rate, those at pH 7.5 had a greater overall average absorbance (Figure 3).

C. gracilis appeared to perform photosynthesis well at a range from pH 8.2 to pH 7.5. As the pH drops below 7.5, the photosynthetic ability of the diatoms greatly decreases. Current surface ocean water is measured to be at pH 8.1, indicating that *C. gracilis* may not be currently performing photosynthesis at its peak potential (1). As the hydrogen ion concentration in the world's oceans continues to rise, the photosynthetic efficiency of the marine diatom *C. gracilis* may increase, boosting the population of marine algae present in the Monterey Bay National Marine Sanctuary.

The results of this study reveal that ocean acidification is potentially causing rapid algae growth, or "algal blooms." Algal blooms have severe negative impacts on the marine ecosystem, and unanticipated algal blooms could wreak havoc on the Monterey Bay National Marine Sanctuary if measures are not taken to decrease the effects of ocean acidification.

The effects of ocean acidification on the MBNMS are being tracked by the Monterey Bay Aquarium Research Institute (MBARI). They found that oceanic pH, an indicator of acidity, has decreased over the last 20 years in Monterey Bay, which correlates with trends in global ocean pH (13). The results seen in this experiment are an indication that these diatoms may not only prosper in seawater of lower pH in the MBNMS, but also in oceans across the Earth, given the global similarities in acidity change.

Throughout the experiment, some unavoidable potential errors were encountered due to the scope of the study and the materials used. There is the possibility that the ingredients present in the pH buffer powder may have inadvertently acted as a nutrient agent for the diatoms. It is unlikely, however, that the pH buffer had a significant impact, as it was created specifically for marine environments. The algae colonies were ordered from a science supply company, Carolina

Biological Supply, so their initial health was dependent on the company's quality.

Each of the samples' initial absorbance value at hour 0 was slightly different; ideally, they would all be exactly the same. When the samples were received, they likely were not measured out by cell count, but rather by volume. This insignificant difference in cell quantity is likely what determined the initial absorbance value of the diatoms. The average absorbance values of diatoms in mediums of pH 8.2 and pH 7.5 may have been closer if this flaw did not exist in the experiment.

This project can be expanded upon by exploring the effects of pH changes on different species of diatoms in the Monterey Bay National Marine Sanctuary or in different oceanic regions altogether. Additionally, measuring the diatoms' response to increased acidity over a longer period of time could be performed to expand our understanding of the long-term effects of ocean acidification. Studying media containing diatoms with even lower pH levels could provide insight into what may occur if the current trend of increasing carbon dioxide emissions continues. Future studies should focus on long-term effects of pH level changes on different species of diatoms to better understand the phenomenon of ocean acidification and how it may be linked to algal blooms.

MATERIALS AND METHODS

Setup Process

Prior to experimentation, all test tubes were sterilized in an autoclave at 121°C for 15 minutes at 1.157 atm. In order to distinguish between the different pH levels of the samples, three test tube lids were labeled "pH 8.2," "pH 7.5," and "pH 7.0." The other three test tube lids were labeled "pH 8.2 B," "pH 7.5 B," and "pH 7.0 B" with the letter "B" representing the reference blanks. An incubation chamber used for culturing the diatoms was prepared by attaching a 12W LED white light strip to the top of a mylar-walled 46cm • 46cm • 56cm grow box using duct tape. The light was set on a timer for a 12 hours light/dark cycle. The chamber was protected from external light sources to eliminate any effect they could have had on the growth of the diatoms.

Alteration of pH Levels

Before adjusting the acidity of the distilled water for the experiment, an electronic pH meter was calibrated with liquids of known pH (pH 4.01, pH 6.86, and pH 9.18). Buffers are solutions designed to maintain a specific pH value by selectively releasing or absorbing hydrogen ions and are useful when a constant pH is desired in scientific experiments (14). The amount of marine pH buffer in grams needed for 1000 mL of distilled water was calculated for each sample group and reference blank (pH 8.2, pH 7.5, and pH 7.0) to generate solutions that (for the sample groups only), would result in the desired pH. The pH buffer's instructions called for two teaspoons of pH powder to be added to 10 gallons of distilled water; this was converted to milliliters of distilled

water and grams of pH powder (2 teaspoons of pH buffer were measured on a scale to be 8.265 grams).

$$(10 \text{ gallons of distilled water}) \div (2 \text{ teaspoons of pH buffer}) = (37,854.1 \text{ mL of distilled water}) \div (8.265 \text{ g of pH buffer})$$

$$(37,854.1 \text{ mL}) \div (8.265 \text{ g}) = (8.000 \text{ mL of total solution in each test tube}) \div x$$

$$x = 0.001746 \text{ g (of pH buffer for 8 mL of total solution)}$$

Using this information, the amount of pH buffer in grams needed for the sample groups (test tubes with pH 8.2, pH 7.5, and pH 7.0 labels) was calculated.

$$(2.000 \text{ mL of distilled water}) \div (0.001746 \text{ g of pH buffer}) = (1000 \text{ mL of distilled water}) \div (y)$$

$$y = 0.8734 \text{ g (of pH buffer for 1000 mL of distilled water)}$$

Next, the amount of pH buffer in grams needed for the reference blanks (test tubes with pH 8.2 B, pH 7.5 B, and pH 7.0 B labels) was quantified.

$$(4.000 \text{ mL of distilled water}) \div (0.001746 \text{ g of pH buffer}) = (1000 \text{ mL of distilled water}) \div (z)$$

$$z = 0.4367 \text{ g (of pH buffer for 1000 mL of distilled water)}$$

Using the calculations above, the appropriate amount of pH 8.2 buffer was added to a volumetric flask and labeled "pH 8.2." This step was repeated for all test tubes, and the appropriate amount of pH buffer was added to one of the volumetric flasks for each test tube (with respect to the pH level in **Table 1**). The flasks were labeled according to their pH value, just as this information was labeled on the test tubes. A magnetic stir bar was placed inside each volumetric flask, and the flasks were set on stir plates to mix for one hour.

Preparing the Samples and Blanks for Experimentation

Samples were prepared with two mL of saltwater medium and four mL of *Chaetoceros gracilis* marine diatoms in test tubes with pH 8.2, pH 7.5, and pH 7.0 labels. Next, four mL of saltwater medium was transferred into test tubes with pH 8.2 B, pH 7.5 B, and pH 7.0 B labels. For test tube pH 8.2 B, four mL of distilled water with pH buffer was added to the test tube. This process was repeated for all reference blanks (test tubes pH 7.5 B and pH 7.0 B) using the distilled water and pH buffer mixture from volumetric flasks labeled with their respective pH value (pH 7.5 B and pH 7.0 B); this altered the pH of the solution in each test tube. For the sample groups (pH 8.2, pH 7.5, and pH 7.0), two mL of distilled water with pH buffer added was transferred from their respective volumetric flasks to the sample group test tubes. An electronic pH meter was used to measure the pH value of each test tube to ensure that

the solutions were at the desired pH values as indicated in **Table 1**. Finally, rubber stoppers were used to seal each test tube, and the samples were mixed.

Preparing the Cuvettes for Measurement

Exactly 80 μ L of the pH 8.2 mixture was pipetted into three 100 μ L cuvettes, and cuvette lids were labeled "pH 8.2." This process was repeated for sample groups pH 7.5 and pH 7.0, and the lids of their cuvettes were labeled accordingly. For the reference blank pH 8.2 B, 80 μ L of the test tube pH 8.2 B mixture was transferred into one 100 μ L cuvette and the cuvette lid labeled "pH 8.2 B." The process was repeated for reference blanks pH 7.5 B and pH 7.0 B, with their cuvette lids being labeled accordingly.

Measuring Absorbance Values

A spectrophotometer is an instrument used to measure the amount of light absorbed or transmitted through a given sample. Absorbance is quantified by a spectrophotometer when a blank or reference solution is compared against a sample. The output value is a unitless measurement that is the logarithm of the intensity of the light passing through the reference cell divided by the intensity of the light passing through the sample cell, $A = \log_{10}(I_0/I)$ (15). When algae photosynthesize, they absorb light from the sun to begin a chemical reaction that results in the production of glucose ($C_6H_{12}O_6$) and oxygen (O_2), shown in the chemical formula for photosynthesis:



Since absorbance is a measure of how much light is taken in by a given sample, this metric was used to evaluate the photosynthetic ability of *C. gracilis*, similar to methods employed by other studies in the field (17). The solution in each cuvette was mixed by pipetting the solution in and out once. The parameters (the desired 450 nm wavelength and absorbance setting) were inputted into a Genesys 10S UV-Vis Spectrophotometer. The three cuvettes labeled "pH 8.2" for sample group pH 8.2 were inserted into slots 1, 2, and 3 of the 6-position cell holder. The reference blank pH 8.2 B cuvette, labeled "pH 8.2 B," was inserted into slot B (blank) of the 6-position cell holder. The absorbance test was run by the spectrophotometer for sample group pH 8.2 with reference blank pH 8.2 B and the absorbance value for each cuvette was recorded into a scientific notebook (**Table 2**). This process was repeated for sample group pH 7.5 with reference blank pH 7.5 B and then for sample group pH 7.0 with reference blank pH 7.0 B. After the tests were completed, the cuvettes were transferred back into the grow box with their caps slightly ajar to allow airflow. The *C. gracilis* diatoms were left to grow over the course of the next four days (**Figure 1**). These absorbance tests were repeated two times daily for the duration of the growth period at 7:00 AM (time 1) and 3:00 PM (time 2) PST.

Received: Jun 29, 2019

Accepted: December 23, 2019

Published: January 16, 2020

REFERENCES

1. Bindoff, N.L., *et al.* "2007: Observations: Oceanic Climate Change and Sea Level." *Climate Change 2007: The Physical Science Basis. Contribution of Working Group I to the Fourth Assessment Report of the Intergovernmental Panel on Climate Change*. Ed. Solomon, S., D. Qin, M. Manning, Z. Chen, M. Marquis, K.B. Averyt, M. Tignor and H.L. Miller. Cambridge, United Kingdom and New York, NY, USA: Cambridge University Press, 2007. 385-795. Print.
2. Stabenau, Erich K., and Thomas A. Heming. "Determination of The Constants of The Henderson-Hasselbalch Equation, αCO_2 and pK_a , In Sea Turtle Plasma." *Journal of Experimental Biology*, vol. 180, no. 1, 23 Mar. 1993, pp. 311–314.
3. "Ocean Acidification." *Ocean Acidification | National Oceanic and Atmospheric Administration*, U.S. Department of Commerce, Nov. 2013, www.noaa.gov/education/resource-collections/ocean-coasts-education-resources/ocean-acidification.
4. Khairy, Hanan M., *et al.* "Impact of Elevated CO_2 Concentrations on the Growth and Ultrastructure of Non-Calculifying Marine Diatom (*Chaetoceros Gracilis* F.Schütt)." *The Egyptian Journal of Aquatic Research*, vol. 40, no. 3, 2014, pp. 243–250., doi:10.1016/j.ejar.2014.08.002.
5. Kroeker, K. J., Gambi, M. C., & Micheli, F. "Community Dynamics and Ecosystem Simplification in a High- CO_2 Ocean." *Proceedings of the National Academy of Sciences*, vol. 110, no. 31, 2013, pp. 12721–12726., doi:10.1073/pnas.1216464110.
6. Chislock, M. F., *et al.* "Eutrophication: Causes, Consequences, and Controls in Aquatic Ecosystems." *Nature Education Knowledge*, vol. 4, no. 4, 2013.
7. "Harmful Algal Blooms." *National Institute of Environmental Health Sciences*, U.S. Department of Health and Human Services, www.niehs.nih.gov/health/topics/agents/algal-blooms/index.cfm.
8. National Oceanic and Atmospheric Administration. "Monterey Bay National Marine Sanctuary." *Monterey Bay National Marine Sanctuary Home Page*, U.S. Department of Commerce, montereybay.noaa.gov/welcome.html.
9. Alverson, Andrew. "The Air You're Breathing? A Diatom Made That." *LiveScience*, Purch, 10 June 2014, www.livescience.com/46250-teasing-apart-the-diatom-genome.html.
10. Edited by Anna McGaraghan, *Weekly Phytoplankton Sampling - Santa Cruz and Monterey*, University of California, Santa Cruz, 2006, oceandatacenter.ucsc.edu/PhytoBlog/.
11. Wehr, John D., and Robert G. Sheath. *Freshwater Algae of North America: Ecology and Classification*. Academic Press, 2008.
12. Baert, P, *et al.* "Manual on the Production and Use of Live Food for Aquaculture." *FAO Fisheries Technical Paper*, No. 361, 1996, pp. 196–251.
13. Monterey Bay Aquarium Research Institute. "Climate Change." *SIMoN*, Sanctuary Integrated Monitoring Network, <https://sanctuarysimon.org/monterey-bay-nms/climate-change/>.
14. Libretexts. "Buffers." *Chemistry LibreTexts*, Libretexts, 22 May 2019, [chem.libretexts.org/Bookshelves/Physical_and_Theoretical_Chemistry_Textbook_Maps/Supplemental_Modules_\(Physical_and_Theoretical_Chemistry\)/Acids_and_Bases/Buffers](http://chem.libretexts.org/Bookshelves/Physical_and_Theoretical_Chemistry_Textbook_Maps/Supplemental_Modules_(Physical_and_Theoretical_Chemistry)/Acids_and_Bases/Buffers).
15. Hardesty, Jon H., and Bassam Attili. "Spectrophotometry and the Beer-Lambert Law: An Important Analytical Technique in Chemistry." *Collin College*, Department of Chemistry, Collin College, 2010, [www.collin.edu/chemistry/Handouts 2009/Beer's Law.pdf](http://www.collin.edu/chemistry/Handouts%2009/Beer's%20Law.pdf).
16. "Chapter 3: History and Early Development of Photosynthesis." *Molecular Mechanisms of Photosynthesis*, by Robert E. Blankenship, 2nd ed., John Wiley & Sons, 2014, pp. 27–38.
17. Bayat, Leyla, *et al.* "Effects of Growth under Different Light Spectra on the Subsequent High Light Tolerance in Rose Plants." *AoB PLANTS*, vol. 10, no. 5, 12 Sept. 2018, doi:10.1093/aobpla/ply052.

Copyright: © 2019 Harvell and Nicholson. All JEI articles are distributed under the attribution non-commercial, no derivative license (<http://creativecommons.org/licenses/by-nc-nd/3.0/>). This means that anyone is free to share, copy and distribute an unaltered article for non-commercial purposes provided the original author and source is credited.

Effects of coolant temperature on the characteristics of soil cooling curve

Dawei Wang¹, Yida Zhang²

¹ Boulder High School, Boulder, Colorado

² University of Colorado Boulder, Boulder, Colorado

SUMMARY

The cooling curves of soil are graphs that represent the variation of soil temperature with time when it is cooled. Knowledge of soil cooling curves and their characteristic parameters play an important role in most thermal analysis concerning soil freezing and/or thawing. Understanding the effect of environmental temperature on these parameters may help scientists better understand how frost heaves happen and how to predict the occurrence of frost heaves more accurately. For soils with identical type, water content, bulk density, and initial temperature, we believe that the freezing process and associated cooling characteristic parameters would be independent of the variation of external environmental temperature. To test this hypothesis, we carried out a series of freezing process experiments on soils with identical physical properties under different coolant temperature conditions. Here, the coolant temperature represents the magnitude of the environmental temperature. Our results indicate that the coolant temperature affects soil cooling curve profiles by changing the critical parameters of nucleation temperature, super-cooling, and phase-transfer duration of water in soil pores. According to the magnitude of the coolant temperature, soil cooling curves can be categorized into three different types: a “regular” freezing process without or with a little super-cooling, a sudden and small rise in temperature after the super-cooling “dip”, and a permanent super-cooling of non-freezing process. We have shown that the freezing temperature of soils is not influenced by the variation of coolant temperature.

INTRODUCTION

Soil is a three-phase system consisting of solid particles, water, and air. The solid particles are small grains of different minerals and fragments of organic matter, which forms the skeleton of soils (1). The soil voids contain water and air in various proportions. To freeze soil is actually to freeze the water in soil pores. The previous research about water indicates that hot water often freezes faster than cold water (2). This means that the initial temperature will have an influence on water freezing speed. A cooling curve of soil is a temperature-time relationship graph that represents the phase transition of water in soil pores, typically from liquid to solid (1). Accurate cooling curve measurement data can

be used to determine the critical parameters such as super-cooling degree, nucleation temperature, freezing temperature, and phase-equilibrium duration (3-5). All of these parameters are closely related to the existing form of pore water, the driving force for water migration in frozen soils, and the characteristics of cryogenic structure during the soil freezing process (6). The knowledge of soil cooling curves and their characteristic parameters play an important role in all thermal analysis concerning soil freezing and/or thawing.

In general, a typical soil cooling curve shows the sensible heat thermal storage stage, the latent heat release stage, the phase-change stage of free water and soil cooling stage without latent heat effects (**Figure 1**). When wet soil is cooled in an enclosed container, water in soil pores does not freeze at its freezing temperature (T_f) under atmospheric pressure condition. Instead, it is normally cooled below freezing temperature before ice nucleation takes place. At this time, the water in soil pores is called super-cooled water. Super-cooled water herein refers to a state of metastable liquid even though the water temperature is below its freezing temperature. The metastable state will end when ice nucleation occurs at nucleation temperature (T_n). At T_n , embryo nuclei form and grow to the critical sizes, and crystallization begins (7, 8). As a result of the release of the latent heat, temperature of

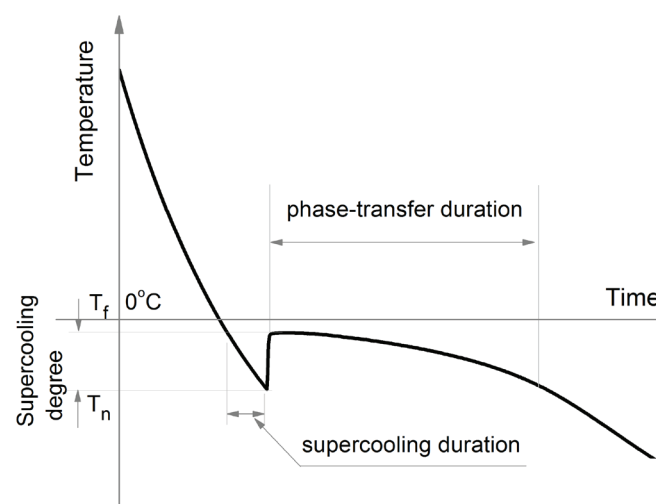


Figure 1. Typical soil cooling curve and its characteristic parameters. T_f represents the freezing temperature, where ice and water coexist inside the soil pores, and T_n represents the nucleation temperature, where embryo nuclei form and grow to the critical sizes, and pore water crystallization begins.

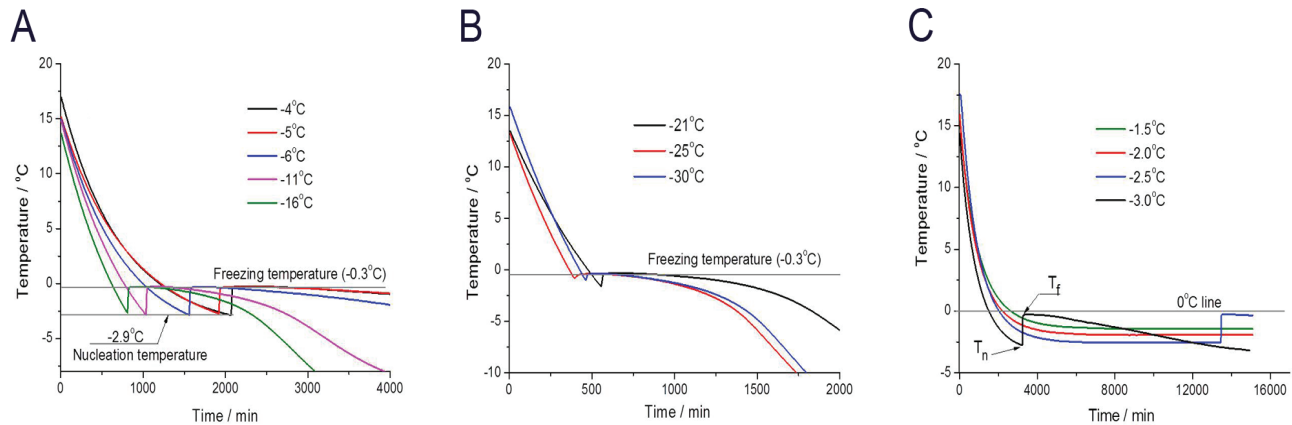


Figure 2: Cooling curves of freezing soil under different coolant temperature. (A) Soil temperature varied over time under the coolant temperature of -4, -5, -6, -11, and -16°C, respectively. (B) Soil temperature varied over time under the coolant temperature of -21, -25, and -30°C, respectively. (C) Soil temperature varied over time under the coolant temperature of -1.5, -2.0, -2.5, and -3.0°C, respectively.

the system rises to the value of T_f , the equilibrium freezing temperature (or freezing temperature), where all free water in soil pores will transfer into pore ice. Further extraction of heat leads to the decrease in temperature and successive freezing of the remaining unfrozen bound water.

In order to determine the threshold value of soil becoming frozen, most studies on properties of soil cooling curve are related to the freezing temperature of soils. For example, by applying the differential scanning calorimetry (DSC) technique, Kozłowski confirmed the strong dependency of the equilibrium freezing temperature (T_f) on the total water content and proved that freezing temperature could be expressed as a power function of the water content and the plastic limit (9). The State Key Lab of Frozen Soil Engineering in China observed that the freezing temperature decreased with increasing salt content and increased with increasing water content independent of the type of soil (10). Konrad and Morgenstern's study showed that the increase of external pressure caused a freezing temperature depression (11). As far as other parameters of soil freezing process are concerned, there is still little information available. If soil samples have an identical soil type, water content, bulk density and initial temperature, we hypothesize that the variation of external environmental temperature has no effect on the soil freezing process and cooling characteristic parameters. To test this hypothesis, we tested the soil cooling process under different coolant temperatures and measured how soil temperature changed over time. In our study, we used the variation of the coolant temperature as the variation of external environmental temperature. Our results may shed light on the understanding of soil cooling processes and may provide information on how the characteristic parameters of soil cooling curves change with the variation of external environmental temperature, which may help to better understand the formation mechanism of cryogenic structure and to predict the frost developing in the cold region's engineering.

RESULTS

We chose the temperature of coolant to match the environmental temperature where the frost-susceptible silty clay soil was frozen. According to the variation of atmospheric temperature in permafrost areas (-1°C to -30°C), the coolant temperature was set in this range with an interval of 4°C or 5°C. However, considering the approximate range of soil freezing temperature and complexity of soil freezing under higher negative temperature between -1 and -4°C, within this temperature range, the coolant temperature was set with an increment of 0.5°C.

Cooling curves of freezing soil under different coolant temperatures

First, we set the coolant temperature to -4, -6, -11, and -16°C, respectively, and measured the temperature-time curves of the tested soil samples (Figure 2A). Generally, the trends of the curves from our data were similar to data that has been previously found (Figure 1). All soil cooling curves have undergone the processes of super-cooling, latent heat release, and free water freezing. Their nucleation temperature and freezing temperature were -0.3°C and -2.9°C respectively, which did not seem to be influenced by the variation of coolant temperature.

Then, we set the coolant temperature to a lower temperature such as -21, -25, and -30°C, respectively. We found that these cooling curve profiles (Figure 2B) differed from the typical soil cooling curve (Figure 1). Some cooling curves did not undergo super-cooling process, while some had a short super-cooling stage before the soil temperatures reached the corresponding coolant temperature (Figure 2B). This phenomenon may be due to the effect of coolant temperature on the soil nucleation temperature. We also noticed that although the freezing temperature for all tested soil samples was -0.3°C, their nucleation temperature was different from each other (Figure 2B). For the soil immersed in the coolant with temperature of -30°C, the nucleation

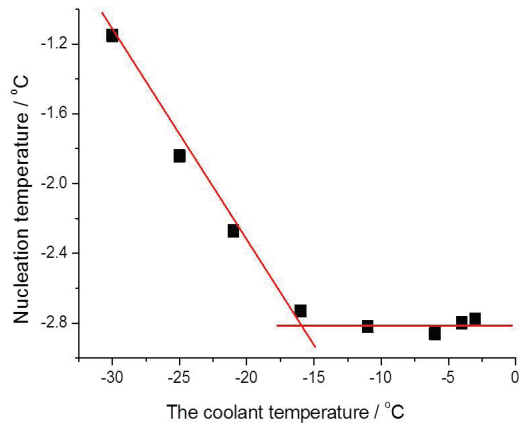


Figure 3: Nucleation temperature of soil at different coolant temperatures. Nucleation temperature (black squares) of soil across coolant temperatures. The red line shows the trend of nucleation temperature when the coolant temperature changes, which is obtained by fitting measured nucleation temperature.

temperature was close to its freezing temperature.

Lastly, we tested the temperature variation of soil in the coolant with a temperature close to or above the nucleation temperature, namely, in the range of -1.5 to -3°C (Figure 2C). We found that compared to the cooling curves obtained at lower coolant temperatures (Figure 2A and 2B), this group of cooling curve profiles were much more complicated (Figure 2C). Some temperature-time curves show the soil temperature had a stage of rapid increase, while some did not. More narrowly, when the coolant temperature was higher than the soil nucleation temperature obtained in Figure 2A, the soil temperature did not have a stage of rapid increase like what happened in the coolant with temperature lower than its nucleation temperature. This indicates that the moisture in soil pores will not be frozen even if the actual temperature of soil is lower than its freezing temperature (Figure 2C). So we cannot determine the freezing temperature of soil from this cooling curve. The moisture in soil pores are in a super-cooled state, namely in a liquid state, forever as long as there is no other external interference.

Effect of coolant temperature on nucleation temperature and super-cooling duration

Generally, the water nucleation temperature is the temperature at which water starts to transfer from liquid to solid, namely, the ice nuclei begin to form at this temperature. On the cooling curves, it is the lowest temperature point in its super-cooling state (Figure 1). Super-cooling duration is the total time water is in the super-cooling state, which can be calculated by the difference between the time when the soil temperature first reaches its freezing temperature and the time when the nucleation occurs (Figure 1). However, for the soils cooled in the coolant temperature above -4°C , the state of the pore moisture will change with the variation of coolant temperature and is in an unstable state (Figure 2C). So, we could neither determine the nucleation temperature,

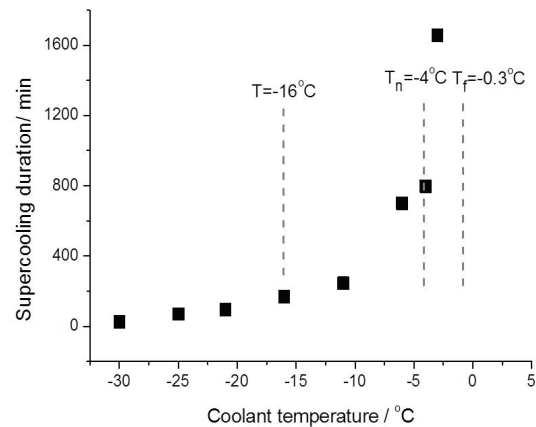


Figure 4: Super-cooling duration vs. coolant temperature. Small black squares represent the super-cooling duration of soil in the coolant with a certain temperature. The freezing temperature (T_f) is -0.3°C , the nucleation temperature (T_n) is -4°C , and the temperature of -16°C , below which the super-cooling duration decreases gradually.

nor the super-cooling duration. The following analysis on the effect of coolant temperature on super-cooling duration will only consider the experimental results obtained with coolant temperatures below -4°C (Figure 3 and 4).

For the soil immersed in the coolant with temperature range from -30°C to -11°C , the super-cooling duration and nucleation temperature depended on the magnitude of coolant temperature. With increasing coolant temperature, the super-cooling duration increased gradually (Figure 4), whereas the temperatures of nucleation decreased sharply (Figure 3). However, for the soil cooled in the coolant with temperatures ranging from -11°C to -4°C , the super-cooling duration of soil pores water increased rapidly along with the increase of the coolant temperature (Figure 4), but there was no obvious variation in the magnitude of nucleation temperature (Figure 3). This means that when the soil was cooled between -11°C to -4°C , the nucleation temperature of the pore water in soil was maintained at a constant value without influence from environmental temperature, and the super-cooling duration increased remarkably with the increase of the environmental temperature.

Effect of coolant temperature on soil freezing temperature and phase-transfer duration

The freezing temperature of soil is defined as the phase transition temperature of water in soil pores, where liquid pore water changes to the pore ice. The relationship between the coolant temperature and the freezing temperature demonstrates that the freezing temperatures of the soil samples immersed in coolant with different negative temperatures were essentially equal; the mean value of the freezing temperature was -0.289°C with a corresponding standard deviation of 0.0309°C (Figure 5). This indicates that for certain types of soil with identical bulk density and water content, the changes of environmental temperature have no

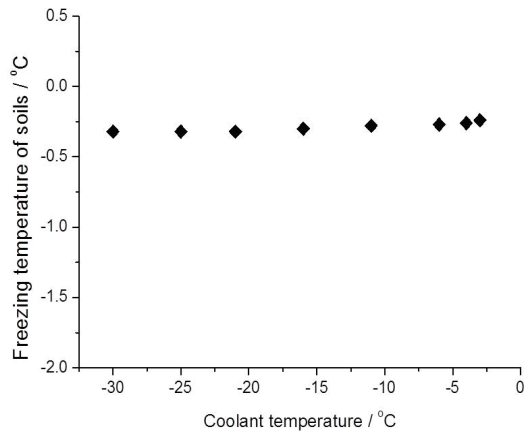


Figure 5: Soil freezing temperature vs. coolant temperature. Small diamond blocks represent the measured soil freezing temperature when soil is freezing in the coolant with different negative temperature. The mean value of freezing temperatures is -0.289°C with a standard deviation of -0.0309°C .

influence on the freezing temperature.

At freezing temperature, ice and water coexist inside the soil pores until the release of latent heat ends. The cooling curves of soil show that the temperatures of soils remain at freezing temperature for a long time and then gradually decrease with time (Figure 2A and 2B). Generally, we define the period from the time that the soil temperature reaches its freezing temperature to the time that the free water is completely frozen as the phase-transfer duration. The relationship between the coolant temperature and the phase-transfer duration suggests that the duration of phase-transfer of water in soil pores increases with the increment of coolant temperature (Figure 6).

DISCUSSION

The purpose of this study is to determine the influence of the environmental temperature on the cooling process of soils with identical physical properties. To do this, we carried out a series of soil cooling process experiments where we obtained the variation of soil temperature with time. Our results show that the environmental temperature influences the profile of soil cooling curves by impacting critical parameters in soil cooling curves such as nucleation temperature, super-cooling duration, and freezing temperature. In order to better understand this effect, we analyzed the response of these parameters to variation in the environmental temperature.

From the analysis of the cooling curves of freezing soil under different coolant temperatures, we conclude that the profile of the soil cooling curve is affected by the magnitude of the environmental temperature even if the initial temperature and the physical properties of the soil are identical. This is different from our hypothesis. According to the magnitude of coolant temperature, the soil will experience three different types of cooling processes: a “regular” cooling process with or without a little super-cooling, a sudden rise in temperature after the super-cooling “dip”, and a permanent super-cooling of non-freezing process.

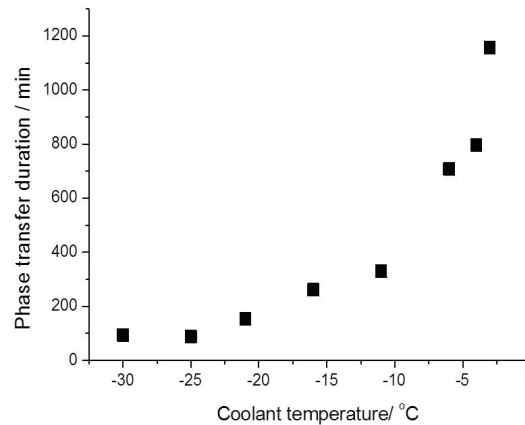


Figure 6: Phase transfer duration of soil across coolant temperatures. The duration of phase-transfer of water in soil pore increases from 100 minutes to 1200 minutes with the increment of coolant temperature from -30°C to -4°C .

Our results indicate that the magnitude of the coolant temperature has no effect on the soil freezing temperature, but it has a significant effect on the phase-transfer duration. With the increase of the coolant temperature, the phase-transfer duration increases gradually. This phenomenon is mainly dependent on the relative magnitude between the release rate of latent heat of soil and the absorption rate of latent heat in the surrounding environment (5, 12). If the latent heat release rate equals the absorption rate, the soil temperature will equal the freezing temperature. If the latent heat release rate is less than the absorption rate, the soil temperature will gradually decrease with time until the end of latent heat release in soil. The end of the latent heat release also means that almost all free water in the soil pores will be frozen into pore ice.

For soil samples with identical physical characteristics and initial temperature, when freezing under different environmental temperatures, their cryogenic structure might be different from each other. This difference will lead to a significant difference in soil frost heave (1). According to our research results about the effect of the coolant temperature on pore water nucleation temperature and super-cooling

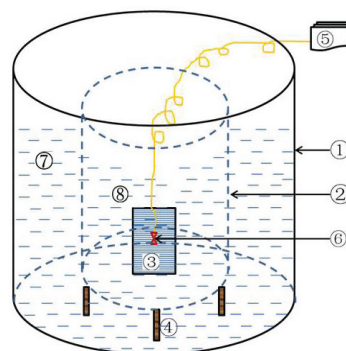


Figure 7: Schematic diagram of the experimental apparatus. The experimental set up included a (1) stainless-steel chamber, (2) isolated cooling tank, (3) aluminum sample cell and tested soil sample, (4) support, (5) data logger, (6) thermistor, (7) circulating coolant, and (8) stationary coolant.

duration, we hypothesize that the cryogenic structure and frost heavy of soils might relate to the pore water nucleation temperature and super-cooling duration. Therefore, in order to better predict the development of soil frost heave, we should investigate the cause of soil frost heave from the perspective of pore water nucleation temperature in future research studies.

METHODS

Soil Samples

The soil used in the freezing experiments was frost-susceptible silty clay taken from the Qinghai-Tibet Plateau. The soil physical parameter of liquid limit and plastic limit was 23.5% and 11.5%, respectively. The water content of the tested samples was 19% and the dry density was 1.78 g/cm³. The grain size distribution is shown in **Table 1**.

Experimental Apparatus

The experimental apparatus was composed of a stainless-steel chamber, an isolated cooling tank, a thermistor, and a data logger. The stainless-steel chamber was a thermostatic chamber filled with circulating coolant (an alcohol-water solution). The temperature of coolant was controlled by a laboratory chiller with a precision of $\pm 0.1^{\circ}\text{C}$. In order to alleviate the interference of vibration caused by coolant cycle on soil water nucleation, a small isolated cooling tank filled with the same kind of coolant was placed into the stainless-steel chamber. The tank was made of aluminum with a wall thickness of 0.5 mm to ensure the coolant temperature inside tank reached the outside tank temperature quickly by heat exchange. At the same time, the temperature of the coolant in tank was monitored in real-time by a thermistor immersed in the liquid coolant. The soil sample cells were placed in the center of the tank (**Figure 7**).

Experimental Approach

As a preliminary preparation for the experiment, a series of saturated soil samples were prepared first. According to the pre-determined results about the tested soils, its saturated water content and dry density were 19% and 1.78g/cm³, respectively. We then calculated the amount of dry soil and distilled water required in our experiments and prepared soil samples in saturated state based on those values. A total amount of 1200 g dry soil was put into a vessel with 240 mL distilled water (a little more water was added because of evaporation loss) to achieve the required uniform water content of 19%. This moist soil was stored in an airtight container for about 24 hours to allow moisture uniformity. Then, we took out 55 g of moist soil and compacted it in three layers into an aluminum sample cell to form a saturated soil specimen (30 mm in diameter by 35 mm in depth). A thermistor with a precision of $\pm 0.05^{\circ}\text{C}$ was inserted into the tested soils before the aluminum sample cell was sealed hermetically. The thermistor was connected to a data logger to record the soil temperature variation during the process of soil cooling.

Table 1. Grain size distribution (%) of studied silty clay

grain size (mm)	sand				clay
	>0.5	0.25-0.5	0.1-0.25	0.074-0.1	<0.074
percentage (%)	1.37	4.49	12.51	7.50	74.13

We prepared 22 samples using this method.

To avoid the effect of different initial temperature on soil cooling process, we made all testing soil samples had an identical initial temperature. Therefore, all sample cells filled with saturated soil were put into a thermostatic chamber for at least 24 hours to make soil sample's temperature equaled with the thermostatic chamber before the cooling process experiment began. The temperature of the thermostatic chamber was 15°C.

In order to measure the influence of environmental temperature on the soil cooling process, different environmental temperatures were applied to different soil samples to collect the soil temperature data during their cooling processes. In our investigation, the variation of coolant temperature represented the variation of environmental temperature for tested soil samples. Two identical soil samples were tested simultaneously for each coolant temperature to avoid contingency factors. Thus, when the coolant temperature in the stainless steel chamber arrived at a desired temperature, two soil samples were taken out from the thermostatic chamber and placed into the cooling tank promptly. The soil samples were cooled under a constant coolant temperature. Temperature variation over time was collected by the data logger simultaneously. Soil temperature data was collected every three seconds during the super-cooling to ice crystal growth stage and every ten minutes from the beginning and ending stage of soil freezing.

ACKNOWLEDGEMENTS

The first author would like to thank Professor Zhi Wen at State Key Laboratory of Frozen Soil Engineering, Chinese Academy of Sciences for his assistance to my experiments in his laboratory.

Received: June 20, 2019

Accepted: January 8, 2020

Published: January 16, 2020

REFERENCES

- Andersland, O. B. and Ladanyi, B. "Frozen Ground Engineering". Second edition John Wiley & Sons, Inc., Hoboken, New Jersey. 2004.
- Takahashi, T. "Is It True that Hot Water Freezes Faster than Cold Water or that Cold Water Boils Faster than Hot Water?" *Scientific American*, 1998.
- Rahman, M. shafiur, *et al.* "Analysis of Cooling Curve to Determine the End Point of Freezing." *Food Hydrocolloids*, vol. 16, no. 6, 2002, pp. 653–659, doi: 10.1016/s0268-

005x(02)00031-0.

4. Zaragotas, D. *et al.* "Supercooling, Ice Nucleation and Crystal Growth: a Systematic Study in Plant Samples." *Cryobiology*, vol. 72, no. 3, 2016, pp. 239-243, doi:10.1016/j.cryobiol.2016.03.012.
5. Hallett, J. "Experimental Studies of the Crystallization of Supercooled Water." *Journal of the Atmospheric Science*, vol. 21, no. 11, 1964, pp. 671-682, doi:10.1175/1520-0469(1964)0212.0.CO;2.
6. Konrad, J.-M. "Freezing-induced Water Migration in Compacted Base-course Materials." *Canadian Geotechnical Journal*, vol. 45, no. 7, 2008, pp. 895-909, doi:10.1139/t08-024.
7. Anderson, D.M. "Undercooling, Freezing Point Depression, and Ice Nucleation of Soil Water." *Israel Journal of Chemistry*, vol. 6, no. 3, 1968, pp. 349-355, doi:10.1002/ijch.196800044.
8. Braga, S.L. & Milón, J.J. "Visualization of Dendritic Ice Growth in Supercooled Water inside Cylindrical Capsules." *International Journal of Heat and Mass Transfer*, vol. 55, no. 6, 2012, pp. 3694-3703, doi:10.1016/j.ijheatmasstransfer.2012.03.006.
9. Kozłowski, T. "Soil Freezing Point as Obtained on Melting." *Cold Regions Science and Technology*, vol. 38, no. 2-3, 2004, pp. 93-101, doi:10.1016/j.coldregions.2003.09.001.
10. Bing, H., *et al.* "Laboratory Investigation of Freezing Point of Saline Soil." *Cold Regions Science and Technology*, vol. 67, no. 1, 2011, pp. 79-88, doi:10.1016/j.coldregions.2011.02.008.
11. Konrad, J.-M. & Morgenstern, N. R. "Effects of Applied Pressure on Freezing Soils." *Canadian Geotechnical Journal*, vol. 19, no. 4, 1982, pp. 494-505, doi:10.1139/t82-053.
12. Gilpin, R. R. "The Effect of Cooling Rate on the Formation of Dendritic Ice in a Pipe with No Main Flow." *Journal of the Atmospheric Science*, vol. 99, no. 8, 1977, pp. 418-424, doi:10.1115/1.3450712.

Copyright: © 2020 Wang and Zhang. All JEI articles are distributed under the attribution non-commercial, no derivative license (<http://creativecommons.org/licenses/by-nc-nd/3.0/>). This means that anyone is free to share, copy and distribute an unaltered article for non-commercial purposes provided the original author and source is credited.

Efficacy of mass spectrometry versus ^1H nuclear magnetic resonance with respect to denaturant dependent hydrogen-deuterium exchange in protein studies

Srish Chenna¹, Walter Englander²

¹ Charter School of Wilmington, Wilmington, Delaware

² University of Pennsylvania Perelman School of Medicine, Philadelphia, Pennsylvania

SUMMARY

Understanding how proteins fold holds the key to many crucial advancements in the medical field, such as the treatment of chronic diseases. Measuring the rate of hydrogen-to-deuterium exchange for labile hydrogens within proteins exposed to deuterium oxide (D_2O) can help elucidate the folding pathway of a protein. Mass spectrometry can be used to determine the extent of deuterium exchange by calculating ΔG_{HX} (mass-to-charge ratio) values. These values were then compared the mass spectrometry results to previous exchange measurements taken by ^1H NMR to investigate if mass spectrometry can be a viable method for measuring hydrogen-deuterium exchange in proteins. Once all of the reactions at different time points (10 seconds to 172,800 seconds) were conducted in the mass spectrometer in a 1.5M guanidine hydrochloride and D_2O solution, the plotted data resulted in sigmoidal curves which showed dissimilar exchange rates to the previously archived ^1H NMR data. After completion of the experiment, we concluded that further studies are necessary to draw a sound conclusion, as the field of study in which we tested solely 1.5M guanidine hydrochloride was too narrow. If reactions at other concentrations of guanidine hydrochloride yield the same exchange rates, denaturant-dependent hydrogen-deuterium exchange techniques can be applied in novel protein studies.

INTRODUCTION

In protein folding research, what is the efficacy of mass spectrometry versus ^1H nuclear magnetic resonance spectroscopy (^1H NMR) in the study of protein folding pathways?

Researching protein folding will lead to a better understanding of degenerative diseases caused by protein misfolding and improper aggregation such as Alzheimer's, Parkinson's, and Type II Diabetes (1). Even after many years of extensive research in protein folding, many laboratories around the world are still striving to find a plausible explanation as to how proteins fold. Linderstrøm-Lang's hydrogen exchange methods now enable us to define the structure of protein folding in various situations (2). In essence, a protein stock is diluted in a solution of deuterium oxide (D_2O). Then, the labile hydrogen atoms can be observed exchanging with deuterium

atoms due to the increase in mass from the extra neutron of the deuterium isotope. The denaturant induces the loss of the quaternary structure, tertiary structure, and secondary structure present in a protein's native state, causing more and more of the labile hydrogens in the amide backbone to be exposed, increasing the ΔG_{HX} (mass-to-charge ratio). ΔG_{HX} helps define the change in mass that a peptide experiences after hydrogen-deuterium exchange has occurred for a set time interval. The longer the protein stays dissolved in the denaturant deuterium oxide solution, the more the protein will unfold, gradually increasing the overall mass of each peptide. Through the results of the hydrogen-deuterium exchange, we can note the degree of protection (P_{struc}) which indicates the degree to which a protein has unfolded at that moment. In viewing the patterns of weight increases, we can observe which areas of the protein exchange faster and which exchange slower compared to other areas to determine the overall hydrogen-deuterium exchange rate.

Hydrogen-deuterium exchange can be monitored either using nuclear magnetic resonance spectroscopy (NMR) or mass spectrometry, two methods widely used to observe proteins (3). Mass spectrometry is an analytical technique that ionizes chemical species and then sorts the respective ions based on their ΔG_{HX} (mass-to-charge ratio); ^1H Nuclear Magnetic Resonance or Proton Nuclear Magnetic Resonance (^1H NMR) is the application of nuclear magnetic resonance to target hydrogen-1 nuclei in the molecules of an organic substance to determine their respective structures (4). One prominent difference between the ^1H NMR and mass spectrometry is that ^1H NMR helps to find the structure of a molecule whereas mass spectrometry helps distinguish the constituents of a molecule. The main area where ^1H NMR is more capable than mass spectrometry is in the observation of denaturant-dependent reactions, when the D_2O solution contains the denaturant guanidine hydrochloride (5). Also, NMR spectroscopy is quantitative and does not require extra steps for sample preparation (6). In this study, deuterium was used instead of tritium, hydrogen-1 hydrogen-4, hydrogen-6, and hydrogen-7 as they are all unstable, making them unfit for hydrogen exchange. However, ^1H NMR is more expensive due to uniform isotopic labelling of ^{13}C and ^{15}N , which enhances the NMR sensitivity but also allows for site-specific interrogation of structures and intermolecular contacts (7);

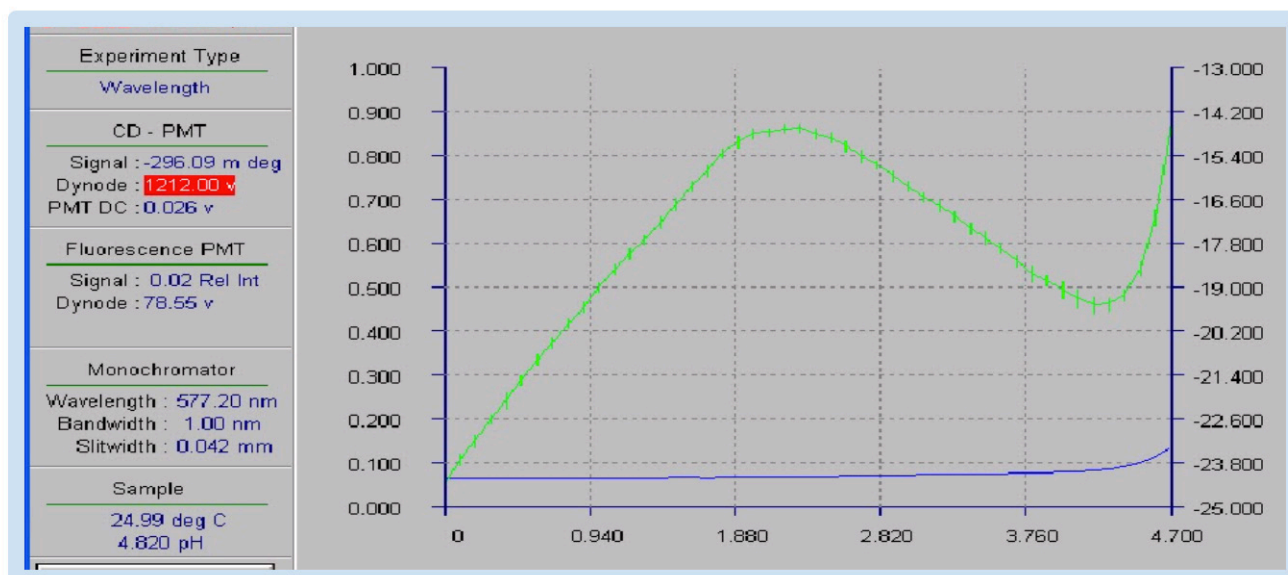


Figure 1: Circular Dichroism Readings. A Circular Dichroism (CD) experiment was performed to deduce the structure of equine Cytochrome c and the concentration of guanidine hydrochloride needed as denaturant in the deuterium oxide solution. The CD uses multiple automated titration mechanisms to induce changes in the concentration of guanidine hydrochloride and equine Cytochrome c to collect fluorescence readings. Green is the CD reading. x-axis numbering represents the concentration of guanidine hydrochloride. The y-axis numbering represents the fluorescence reading.

¹H NMR requires more expertise to operate whereas a mass spectrometer can be used with minimal training; there are limits on the size of the observable protein with ¹H NMR but a mass spectrometer can be used to view almost any protein. Due to their convenience, mass spectrometers are much more commonly used in laboratories around the world than ¹H NMR. Furthermore, measuring hydrogen-deuterium exchange by mass spectrometry can make the EX1 (bimodal isotopic distribution) and EX2 (unimodal isotopic distribution) behavioral difference clear, illustrating a significant advantage of using mass spectrometry (5). In order to draw on the vast benefits of mass spectrometry, we conducted research on denaturant-dependent hydrogen-deuterium exchange reactions via mass spectrometry. Then, we drew a comparison between archived data of cytochrome c denaturant-dependent hydrogen-deuterium exchange via nuclear magnetic resonance and the current collected data of Cytochrome c denaturant dependent hydrogen-deuterium exchange via mass spectrometry.

Cytochrome c was used in this study because of its crucial role in the body; it is vital for oxidative phosphorylation in mitochondria, and it plays an important role in the production of life-sustaining ATP by participating in electron transport (8). Furthermore, due to their structural similarity, both human Cytochrome c and equine Cytochrome c can be studied using the same techniques (9). Also, the ubiquitous nature and sequence of Cytochrome c as a 12 kDa protein with a 104 amino acid peptide chain and a single heme group, allow for it to be used as a model protein for molecular evolution (8).

When all of the hydrogen-deuterium exchange runs at different time points are conducted in the mass spectrometer

in a 1.5 M guanidine hydrochloride deuterium oxide solution, the ΔG_{HX} values will be the same as those obtained from the archived ¹H NMR data prior to this study.

RESULTS

We determined the variables used in this study using information from both background research and pre-study trials. The independent variable was the timepoints for the various mass spectrometry hydrogen-deuterium exchange runs that ranged from 10 seconds to 172,800 seconds, or 48 hours. The rationale for the 10-second time point came from the notion that completing the process of hydrogen-deuterium exchange occurs with increasingly less precision under that time frame. By this point, it becomes necessary to use a stopped-flow kinetics machine, which was not used in this study. The rationale for the 48-hour time frame is derived from the notion that after dissolving Cytochrome c in the D₂O solution, most of the protein's peptides should have fully exchanged after 48 hours, reaching a point of saturated deuterium occupancy. The dependent variable was determined to be deuterium occupancy as a function of time. This value was then used to calculate ΔG_{HX} (mass-to-charge ratio) values. The scientific controls were all-hydrogen runs in a 1.5 M guanidine hydrochloride deionized water solution and all-deuterium runs (48 hours of exchange to reach saturated deuterium occupancy) in a 1.5 M guanidine hydrochloride deuterium oxide solution.

Initially, to determine the structure of the equine Cytochrome c and the concentration of guanidine hydrochloride needed as denaturant in the deuterium oxide solution, a titration plot was produced, which displayed the fluorescence readings from

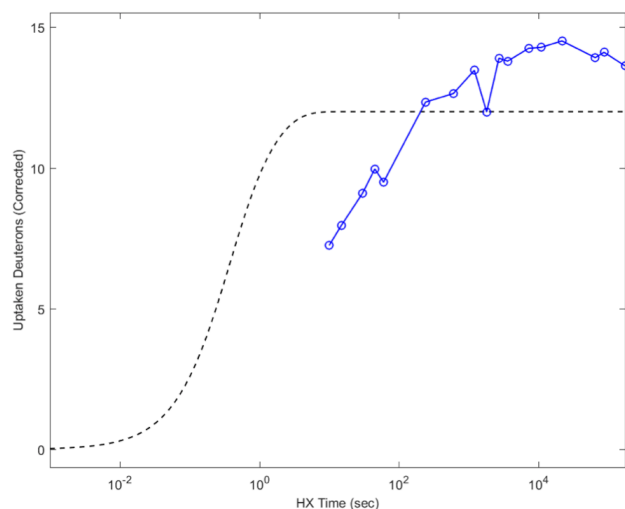


Figure 2: Centroid Average Maps. Example of centroid average map MS-HX data of Peptide 67-82 +2 (+2 is the overall charge) corrected for back-exchange using an all-deuterium run. This means that the protein was in solution for 48 hours for full H-D exchange. The solution was kept in a dry bath at a constant temperature of 45°C. This serves as a control for the all-hydrogen runs and the all-deuterium runs to compare the data. The dotted black line is the estimated amount of deuterium isotopes that were taken up over a given HX time.

the circular dichroism (**Figure 1**). As shown by the low values in the circular dichroism graph which then rise to a peak and then drop off, it is evident that Cytochrome *c* is dominated by alpha-helical secondary structure as opposed to beta-pleated sheet secondary structure. From the CD study, 1.5 M guanidine hydrochloride was selected as the denaturant concentration for the D₂O solution.

As the study was conducted solely at 1.5 M guanidine hydrochloride, there was one main obstacle that prevented us from reaching the objective of the study. There was still not a lot of separation between the exchange rates of different larger scale openings caused by unfolding in the protein, Cytochrome *c*.

The sigmoidal curves are different for the mass spectrometry data and the 1H NMR data suggesting different hydrogen-deuterium exchange rates and disproving the hypothesis. The sigmoidal curves were compared by looking at the slope of the sigmoidal curve and the overall general shape. If the hydrogen-deuterium exchange rates for the 1H NMR and mass spectrometry were the same, then they would reflect the same shape. For the collected data, there are significant differences in the hydrogen-deuterium exchange rates. **Figure 4** shows the comparison between the mass spectrometry data and 1H NMR data for three randomly selected peptides. If the data collected from the MS-HX were similar to the data of the 1H NMR, further protein folding studies could use similar methods. However, as the size of the protein changes, components of the experiment such as the concentration of the denaturant need to be adapted

DISCUSSION

From the results of the circular dichroism, the structure of the studied protein can be identified. As shown by the low values in the circular dichroism graph which rise to a peak and then drop off, it is evident that Cytochrome *c* is dominated by alpha-helical secondary structure as opposed to beta-pleated sheet secondary structure.

The peptide coverage of the MS-HX was highly complete. This was due to the multiple trials done at each time point to ensure a set of data was available for a large number of peptides. Ensuring proper protein coverage was an important step, as collecting data for each peptide would allow for a reasonable comparison between the MS and 1H NMR data.

A wide range of time points were conducted for the MS-HX runs in order to gain an idea of the full spectrum of the protein unfolding pathway. The lower end of the time point range was 10 seconds. This was the smallest time point because at time points lower than 10 seconds, a stopped-flow kinetics is required. The largest time point was 48 hours which was selected because there is almost complete hydrogen to deuterium exchange at that time.

The denaturant dependent hydrogen-deuterium exchange mass spectrometry method was finalized from pre-study trials and background research in order to prevent error in the collected data that was used to calculate the ΔG_{HX} values and to ensure accuracy. From the calculations of the ΔG_{HX} by the lab proprietary software ExMS, the data was shown in hundreds of ΔG_{HX} by time (seconds) graphs. To prevent error, the graphed data was cancelled for back-exchange using an all deuterium run as shown in centroid average maps (**Figure 2**). This data was compared to the NMR data, as the NMR data was previously collected and cross-checked through various other experiments.

From the observations, the folding pathway of the protein can be deduced, including - which segments of the protein fold first, last, and which segments dominate the hydrogen-deuterium exchange rate. For example, the slow rate of hydrogen exchange in a protein, relative to the exchange rate observed with simple peptides under the same experimental conditions is closely related to the conformation of the protein molecule in aqueous solution of denaturant and D₂O(10).

At 1.5 M guanidine hydrochloride, larger scale openings caused by unfolding in Cytochrome *c* dominate the hydrogen-exchange rates of residues included in each opening segment, making it difficult to study smaller local openings in the protein. As the larger scale openings from the unfolding of the protein dominate the exchange rates, the hydrogen-deuterium exchange rate was not similar to that of the 1H NMR. The exchange rate contributed to the EX2 behavior shown by the unimodal isotopic distribution slowly moving over to the right (**Figure 3**).

Through the results of the denaturant-dependent hydrogen-exchange reaction in the mass spectrometer, the degree of protection (P_{struc}) was noted, which helped draw conclusions regarding the folding pathway of the equine Cytochrome *c* (5). The results also showed that in EX2 exchange (**Figure**

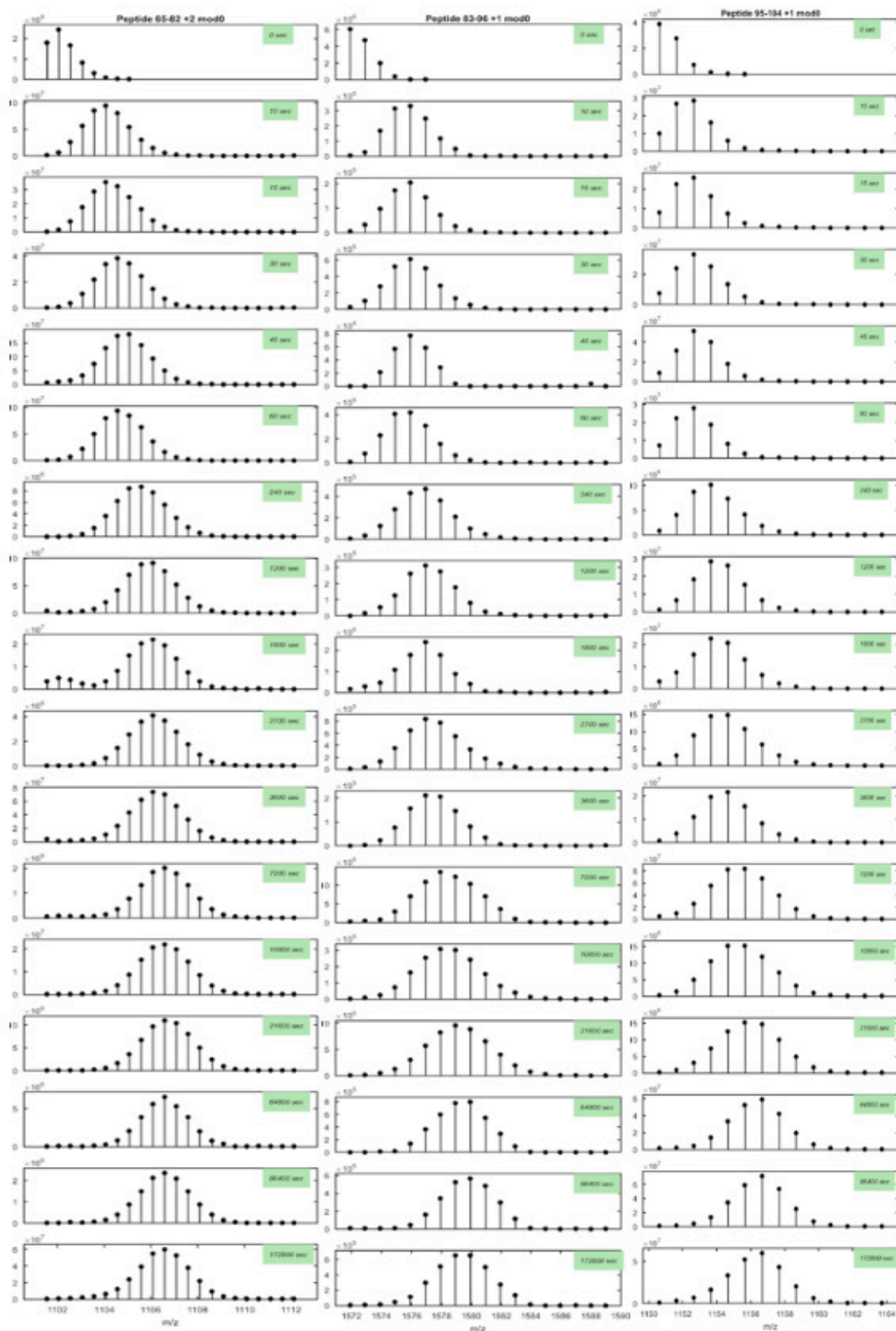


Figure 3: MS-HX data. These samples of mass spectrometry hydrogen-deuterium exchange (MS-HX) data were collected from the time point runs done with Peptide 83-96 +1, Peptide 65-82 +2, and Peptide 95-104 +1 (+1 and +2 are the overall charges). The unimodal isotopic distributions represented at each timepoint for each peptide are shifting due to a positive increase in the ΔG_{HX} (mass-to-charge ratio) as the time points also increase in duration, representing EX2 behavior. Y-axis numbering represents the mass-to-charge ratio.

3), individual amino acids are not correlated. Thus, they will always show a unimodal isotopic distribution that moves from starting to ending conditions (hydrogen to deuterium or deuterium to hydrogen) with longer exchange times.

The data collected using the mass spectrometer during the time point runs indicated that the hydrogen-to-deuterium exchange rates were not similar at 1.5 M guanidine hydrochloride when compared to the archived 1H NMR data disproving the hypothesis. Further testing with the same hypothesis but at a different guanidine hydrochloride concentration may provide more promising results.

In order to elucidate further conclusions regarding the efficacy of hydrogen-deuterium exchange mass spectrometry in conjunction with denaturant-dependent reactions, further experiments are necessary. The spectrum of the study can be increased by gathering data at more time points to check for a better concentration of guanidine where the denaturant-dependent hydrogen exchange can occur with similar exchange rates as 1H NMR. This can be done by simply changing the concentration of guanidine hydrochloride in the deuterium oxide solution and keeping the rest of the procedure the same. If further experimentation in denaturant-dependent hydrogen-deuterium exchange mass spectrometry methods yields the same ΔG_{HX} values, this novel mass spectrometry technique can then be applied to other protein folding studies aiding in the research on chronic diseases.

METHODS

An AVIV Circular Dichroism Spectrometer Model 202 was used to deduce the structure of equine Cytochrome *c*. The CD used multiple automated titration mechanisms to induce changes in the concentration of guanidine hydrochloride and Cytochrome *c* to collect fluorescence readings (Figure 1). The protein stock sample in the cuvette was placed in the CD and 1.5 M guanidine hydrochloride solution was titrated in by the CD. This data enabled the visualization of the protein's secondary structure, which allowed us to determine the approximate order in which each segment of the protein unfolds.

The variables were determined using information from both background research and pre-runs. The independent variables consisted of the various guanidine hydrochloride concentrations in the pre-runs and timepoints for the various actual runs ranging from 10 seconds to 172,800 seconds, or 48 hours.

The mass spectrometer used was a Mass Spectrometer OrbiTrap XL. 1H nuclear magnetic resonance ΔG_{HX} values were previously calculated from prior lab study data and the data from the mass spectrometry hydrogen-deuterium exchange were both calculated using the lab proprietary ExMS software. Then, the 1H NMR ΔG_{HX} values and the mass spectrometry ΔG_{HX} values were graphed on the same plot to compare the resulting approximate sigmoidal curves (Figure 4). Using the protection factor (P_{struc}) derived from the deuterium occupancy, the ExMS program calculates ΔG_{HX}

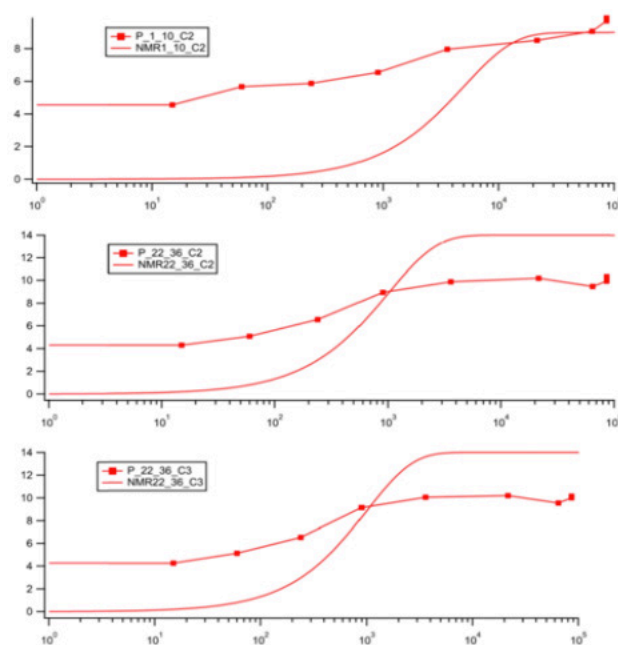


Figure 4: 1H NMR and MS-HX data comparison. A sample of the data from the mass spectrometer and the 1H NMR on the same graph for each peptide. The x-axis shows the time in seconds and the y-axis shows the mass/charge values. While the curves for the MS-HX data are relatively smooth, they do not align with the perfectly sigmoidal 1H NMR-HX data. The x-axis shows the time in seconds. The y-axis shows the mass-to-charge ratio. Legend: MS-HX data is shown by 'P' and the charge is shown by 'C'; 1H NMR data is shown by 'NMR' and the charge is shown by 'C'. (Peptide 1-10 +2, Peptide 22-36 +2, Peptide 22-36 +3).

which is also often reported in free energy units as $\Delta G_{HX} = -RT \ln(K_{op})$: Where T is the temperature, R is the gas constant, and $1/K_{op}$ is the protection factor of the protein segment, with K_{op} as the structural opening rate that exposes the amide.

For the mass spectrometer hydrogen-deuterium exchange (MS-HX) runs, two main 10 mL solutions were made. One consisted of Cytochrome *c* (pH 7) and the other was a D₂O solution (pH 7) prepared with 1.5 M guanidine hydrochloride as a denaturant. The concentration of guanidine hydrochloride deuterium oxide solution was checked with a refractometer. Before the actual run in the mass spectrometer, the protein solution samples consisting of 10 μ L protein stock and 90 μ L D₂O solution were mixed, and the hydrogen-deuterium exchange was allowed to occur for time intervals of 0 (all hydrogen run), 10, 15, 30, 45, 60, 240, 1200, 1800, 2700, 3600, 7200, 10800, 21600, 64800, 86400, and 172800 seconds. Multiple trials were conducted for each time interval in order to ensure full peptide coverage. The reaction was then quenched using 25 μ L of diluted phosphoric acid, which lowered the pH to 2.5 in order to slow the hydrogen-deuterium exchange reaction. The solution was injected into the lab-proprietary HPLC (High-Performance Liquid Chromatography) apparatus, wherein proteins were cut into peptides by a pepsin trap column and then sprayed into the mass spectrometer. The experiment was replicated three

times for each time point.

The resulting data from the mass spectrometer, which was collected in ExMS, was then cancelled for back-exchange (error) to ensure accuracy. If the reacting sample solution is kept at room temperature too long after mixing the deuterium solution with the protein solution or if the ambient temperature is below 0°C, there may be back exchange of deuterium atoms to hydrogen atoms.

ACKNOWLEDGEMENTS

Enormous gratitude is extended to Dr. Walter Englander, Dr. Leland Mayne and all the other members of the Englander Laboratory in the Department of Biochemistry and Biophysics at the Perelman School of Medicine, University of Pennsylvania, Philadelphia, PA.

Received: December 10, 2018

Accepted: October 14, 2019

Published: January 22, 2019

REFERENCES

1. Chaudhuri, Tapan K., and Subhankar Paul. "Protein-Misfolding Diseases and Chaperone-Based Therapeutic Approaches." *FEBS Journal*, vol. 273, no. 7, 2006, pp. 1331–1349., doi:10.1111/j.1742-4658.2006.05181.x.
2. Englander, S. W., *et al.* "Hydrogen Exchange: The Modern Legacy of Linderstrøm-Lang." *Protein Science*, vol. 6, no. 5, 1997, pp. 1101–1109., doi:10.1002/pro.5560060517.
3. Chung, E. W., *et al.* (1997). "Hydrogen exchange properties of proteins in native and denatured states monitored by mass spectrometry and NMR." *Protein Science*, 6(6), 1316-1324. doi:10.1002/pro.5560060620
4. "Nuclear Magnetic Resonance | NMR | Spectroscopy | Solutions." Bruker.com, 22 Nov. 2018, www.bruker.com/products/mr/nmr.html.
5. Mayne, Leland. "Hydrogen Exchange Mass Spectrometry." *Methods in Enzymology Isotope Labeling of Biomolecules - Applications*, 2016, pp. 335–356., doi:10.1016/bs.mie.2015.06.035.
6. Emwas, Abdul-Hamid M. "The Strengths and Weaknesses of NMR Spectroscopy and Mass Spectrometry with Particular Focus on Metabolomics Research." *Methods in Molecular Biology Metabolomics*, 2015, pp. 161–193., doi:10.1007/978-1-4939-2377-9_13.
7. "Isotopic Labeling for NMR Spectroscopy of Biological Solids." Sigma, <https://www.sigmaaldrich.com/technical-documents/articles/stable-isotopes/isotopic-labeling-for-nmr-spectroscopy.html>.
8. "Cytochrome c - A Model Protein for Molecular Evolution." H2NC6H4CO2C2H5, Drugs, www.sigmaaldrich.com/life-science/metabolomics/enzyme-explorer/learning-center/cytochrome-c.html.
9. European Bioinformatics Institute Protein Information Resource SIB Swiss Institute of Bioinformatics. (2019, January 16). Cytochrome c. Retrieved from <https://www.uniprot.org/uniprot/P00004>
10. Hvidt, Aase, and Sigurd O. Nielsen. "Hydrogen Exchange in Proteins." *Advances in Protein Chemistry*, 1966, vol. 21, pp. 287–386., doi:10.1016/s0065-3233(08)60129-1.

Copyright: © 2019 Chenna and Englander. All JEI articles are distributed under the attribution non-commercial, no derivative license (<http://creativecommons.org/licenses/by-nc-nd/3.0/>). This means that anyone is free to share, copy and distribute an unaltered article for non-commercial purposes provided the original author and source is credited.

Do attractants bias the results of malaise trap research?

Arnauld Martinez¹, Nick Reeves², Ryan Perry³, Michael Horton¹

¹Western Center Academy, Hemet, California

²Mount San Jacinto College, San Jacinto, California

³University of California, Riverside, Riverside, California

SUMMARY

The study of biodiversity is crucial to the stability of the planet as it assists scientists with the knowledge and tools necessary to maintain a functional and sustainable environment. Previous research has utilized malaise traps to collect insects in order to study trends in biodiversity. However, malaise traps may have a potential for bias, depending on the type of attractant used, given that flies are attracted to rotting, fermented fruit. This study aims to test whether inadequate sampling occurs during the collection of flying insects. We hypothesized that attractants do bias the results of malaise trap research. The project was designed to test this hypothesis. We placed two identical traps in similar areas of the Southwestern Riverside County Multi-Species Reserve near Western Center Academy. All variables were maintained across these traps, except for the type of attractant used (independent variable). Traps were placed three feet apart, both parallel to the prevailing wind in a homogeneously vegetated field. After one week, we counted and identified the insects down to order manually under a microscope and their genomes were sequenced. This process was repeated the following week. The data from the two traps were compared to each other and to a concurrent Mount San Jacinto Junior College study to test our hypothesis. Based on analysis of our data, we found our hypothesis to be supported by the data and there was indeed a bias when using denatured alcohol.

INTRODUCTION

As the most abundant taxon in the animal kingdom, insects play a critical role in their communities, while both positively and negatively impacting our ecosystem. To illustrate, insects are pollinators, decomposers of organic matter, and significant sources of energy in the food chain. However, insects can also carry disease, harm crops and livestock, and damage landscapes (1). To investigate these impacts, researchers commonly use malaise traps to collect flying insects. Swedish entomologist, Rene Malaise, discovered in the 1930s that more flying insects were captured by using his tent than by using traditional netting. Malaise traps, resembling tents, are now the most effective and ubiquitous flying insect trap in the world (2). However, bias resulting from attractants used in malaise traps could create inadequate sampling in studies,

ultimately leading to a misunderstanding of the relative diversity and ecology of insects and perhaps cause scientists to overlook potential patterns and inaccurate trends.

The state of California contains over 14,000 protected areas, administered by various public and non-profit organizations, in addition to various private conservation areas and easements. Although it is difficult to estimate the exact area of all protected land in California, the California Protected Area Database estimates protected land to comprise almost 47% of the state's total area (3). State law protects these lands in order to preserve the biodiversity and maintain the landscape ecology of flora and fauna populations. As a result, these protected lands are ideal for conducting various types of research. In our study, we used malaise traps just inside and just outside one of these protected lands to collect flying insects that we then sorted, identified by order, and counted. Collaborators at Mount San Jacinto College (MSJC) used the same type of traps to collect and identify insects from a location approximately 11 miles southwest of our study location. In total, we identified nearly a thousand insects and to verify our identifications, we extracted, purified, and amplified the DNA of 150 insect specimens. We sent all specimens for this portion of the study to the University of Guelph to be barcoded for inclusion into the International Barcode of Life Database, as part of the 2016 international School Malaise Trap project. This database, maintained by the University of Guelph, is used worldwide to study the biodiversity genomics and identification of insects (10).

Informed by previous literature, we hypothesized that the townes-style malaise trap is preferred for unbiased insect collection, as this trap involves a passive form of collection with minimal required maintenance (4, 5). Scientists commonly use townes-style malaise traps to assess the relative abundance and diversity of flying insects that are active in shrublands where there is a reasonable amount of shelter. This was most consistent with the specific protected reserve area chosen. Some research, however, suggests the shape, model, and size of the trap may contribute to varying data sets (6). Still, others question the very materials the trap is made of (7). We utilized the townes-style malaise traps to test our hypothesis that attractants bias the results of malaise trap research. Denatured ethanol was used as one of the independent variables, not only because ethanol anesthetizes and preserves the insects over the course of a week, but it minimizes the Lepidopteran from damage and sticking to

other insects. At the same time, the Vapona insecticide strips were used as the other independent variable in the dry trap. We decided to check on the traps daily since dry attractants do not preserve the specimens as well as the ethanol.

RESULTS

In order to test our hypothesis that attractants bias the results of malaise trap research we collected insects in two identical malaise traps at a predetermined location inside the nature reserve, near the Western Center Academy (WCA) using a wet and dry attractant (**Figure 1A**). A similar collection was made during the same time period near the MSJC campus approximately 11 miles southwest of our location by an MSJC Honors Biology students research team (**Figure 1B**). The collections made at the Western Center Academy were specifically designed to test the hypothesis and to simultaneously participate in the School Malaise Trap program. The insects collected at MSJC verified that our traps worked properly and the expected number and variety of insects we anticipated were caught. We caught and counted mostly Diptera, which we believed would be the most abundant. We also caught Hymenoptera, Lepidoptera, Hemiptera, Coleoptera, Orthoptera, and Trichoptera. The DNA of 150 insects collected from the WCA site were sequenced the first week. The results of the DNA sequences helped us to realize that an insect of the order Lepidoptera was misidentified as belonging to the order Trichoptera; we went back and corrected the data to reflect this. Our findings concluded a much greater population of insects (625%) had been caught with the wet denatured ethanol traps when compared to the dry Vapona traps. The greatest increase of insects, however, were those in the order Diptera. When compared to a dry anesthetic trap, insects of the order Diptera were caught an average of 1,024% more in both weeks one and two (**Figure 2 & 3**). The results appeared to show a clear bias in the population of insects caught when using either the denatured ethanol or Vapona. This data supports that there may be a bias based on the type of attractant used. Specifically, denatured ethanol traps may enrich for Diptera, as these insects normally feed on rotting fruits which produce alcohol. After a quantitative comparison of the findings, we concluded that our malaise traps research revealed that attractants do bias the results of malaise trap research.

DISCUSSION

We aimed to investigate whether attractants may bias the results of malaise trap research. Because no previous work in the field has addressed our hypothesis, we decided to make this question the focus of our research. We set up two malaise traps, with all variables identical, except for the type of attractant used (denatured ethanol or Vapona). We quantitatively measured and identified all the insects by morphology in order to place each of the insects into the appropriate Order. We verified our insect identifications via DNA barcodes. When we initially submitted our data, the



Figure 1: Experimental set up and location. (A) Photo of town-style malaise trap used and its location near Western Center Academy in the northeastern part of the Southwestern Riverside County Multi-Species (SWRCMS) Reserve located west of Diamond Valley Lake. **(B)** Aerial map of northern portion of Southwest Riverside County Multi-Species Preserve located in Southern California. The locations are 11 miles from where the MSJC and WCA research teams placed their malaise traps. WCA set up their traps in an uninterrupted area of the reserve, while MSJC set their traps in a high-traffic area of the campus.

barcode data revealed that we had misidentified one species of insects by hand, so we went back and corrected our mistake in order to ensure the data was correct. We clearly found a much larger number of Diptera caught in the denatured alcohol trap than in the Vapona trap, as well as many more insects overall. We compared our research data with that performed by Dr. Reeves and his MSJC team. In their project, they studied how human impact affects the genetics of specimens in high traffic areas as evidenced by gene flow, genetic drift, and other biodiversity trends. However, their study only used traps with denatured ethanol so it is conceivable that bias may have occurred in their collection. We used their data as additional verification to confirm that we collected very similar insects when using the same attractant.

The most difficult decision we made when setting up the malaise traps was finding their best placement for collection (8). We considered a diverse range of variables, including the insects' flight line, outside day and night temperatures, wind direction and speed, and hours of direct sunlight (9). We also had to consider that the reserve management board did not want the trap visible from any roads. We were able to set up both our wet and dry traps in the identical spot for two weeks in September 2016 during a time and at a location where we felt there would be minimal negative environmental influences and we would get the best, most consistent collection.

In addition, insects we collected had their DNA extracted, sequenced, and barcoded for possible inclusion in the

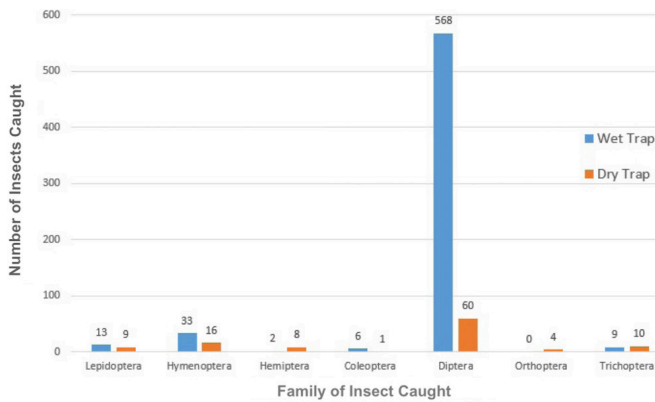


Figure 2: Distribution of insects caught week 1. Bars indicate type and number of insects caught in traps during week 1 of collections. Blue bars indicate insects caught by wet traps while orange bars indicate dry traps.

International Barcode of Life Project database maintained by the University of Guelph in Ontario, Canada. This DNA barcode-based reference library is used worldwide by scientists to study the diversity and identification of insects internationally (10). This research made an important contribution to the International Barcode of Life project, as new and rare species were added to their DNA barcode library database. We sent 820 specimens to the University of Guelph. A summary of our data was compiled, and our sample ranked 35th in biodiversity out of 67 other research groups who contributed to the program (11).

The purpose of this study was to determine if attractants influence and bias collected data when looking at malaise traps and the type of attractant used. Based on our data analysis, we concluded that the denatured alcohol trap proved to entice far more insects, particularly those in the order Diptera. Thus, Diptera may be especially attracted to the trap for they are naturally attracted to fermented fruits. Our data suggests that the denatured alcohol trap tends to bias the results of malaise trap diversity research. This could call into question any diversity studies done with malaise traps. Our data supports our hypothesis that there is a bias when using denatured ethanol in malaise traps.

METHODS

Malaise traps are made to resemble tents using the polyester fiber Terylene. This design allows insects to fly into the tent and get funneled into a collection jar which is located at the highest point. The collection jar uses a killing agent. We used both a wet (ethanol) and dry killing agent (Vapona) as the independent variables to test our hypothesis. We found that the agent ethanol tends to damage Lepidopteran but at the same time preserves them long enough for the purpose of our study. It is used during research primarily for the collection and preservation of flies (Diptera) and wasps (Hymenoptera). However, they can also be used to catch many other flying insects. Such traps are normally placed in predetermined locations for long periods of time, but they need to be checked

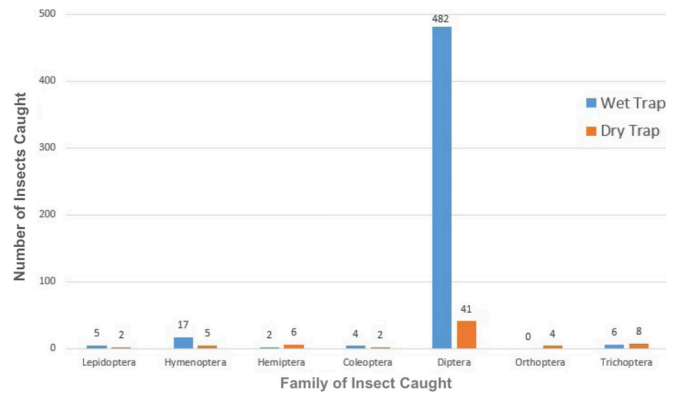


Figure 3: Distribution of insects caught week 2. Bars indicate type and number of insects caught in traps during week 2 of collections. Blue bars indicate insects caught with wet traps while orange bars indicate dry traps.

daily or weekly depending on the type of killing agent used. Our malaise traps had two short walls, one middle wall, and a roof peaked on one end. The walls can vary in color and the roof is usually white. Poles are used to support the trap at each corner like a tent, and at the peak in front. Poles can be adjustable so that the sample jar may be raised or lowered to fit the specific circumference (8).

We set up two identical townes-style malaise traps for our research. Both traps were 5-feet high at the highest peak in the front, 4-feet high in the back, 6-feet in length, and 3-feet in width. Our traps were placed three feet apart from each other to ensure that variables such as outside temperature, wind direction and speed, hours of direct sunlight, and path of insect flight line remained constant. The traps were placed parallel to the wind direction to make certain that one trap was not up-wind from the other. The capture principle of the wet and dry traps given the natural features of the environment were based on positioning the traps for maximum interception of the insects' flight by means of a fabric barrier and subsequent positive phototropism by the flying insects. Since the intercepted insects are attracted by the sunlight at the top of the trap, they would subsequently hit the fabric barrier, be funneled upwards, and fall inside a collection jar with either attractant. The jar was removed while the malaise trap was left in place after the first week. During the first week, we checked the traps every day to confirm that the traps were all intact and not damaged or altered in any way by wind, birds, or animals that inhabit the preserve. We put new collection bottles for the second week, at which time we switched the independent variables just in case there was a difference in location. We noted that collections were similar for both weeks, so the external variable which could affect the results remained constant.

We found that denatured ethanol works best as it kills and preserves insects caught during the week. In addition, it keeps Lepidopteran scales that cover the wings, head, and parts of the abdomen from getting damaged or clinging to other insects in the collection bottle. Alternatively, a dry killing

agent Vapona, was used in the collection jar of the second trap.

We hand sorted the collected insects in each jar using fine point precision forceps (Fisherbrand) and identified each one down to their order by using a dichotomous key provided by Dr. Reeves. Samples of each order of insects were mounted and labelled for display. This method was conducted by inserting the pin into a top hole on the 3-stair block making sure the tear drop paper is aligned with the hole. After this, a smudge of silicone gel (shellac) is pasted on the tear drop paper. Finally, a pair of tweezers was used to place the insect on its left side with its wings and antennae facing up. The pin was stabbed through the small blank paper and the identity was labeled.

In the first week, we collected 484 insects in total. We counted the number of insects belonging to each order. The following week, we returned to the same spot, inserted a new collection bottle, and collected an additional 336 insects.

ACKNOWLEDGMENTS

I thank Dr. Nick Reeves for his mentorship throughout this research project, in addition to his technical guidance regarding malaise traps and DNA extraction from insect specimens. Another thank you goes to Dr. Ryan Perry who taught us Entomology and assisted us in determining how to pin the insects we caught and to identify the specimens. Finally, I would like to personally thank Vice Principal Michael Horton for his unwavering support and the way he effectively motivates students and encourages hands-on education through science.

Received: January 14, 2019

Accepted: June 9, 2019

Published: January 21, 2020

REFERENCES

1. Harwood, Jessica, *et al.* "Importance of Insects." CK, CK-12 Foundation, 4 July 2019, www.ck12.org/biology/importance-of-insects/lesson/Importance-of-Insects-MS-LS/.
2. Vårdal, Hege, and Andreas Taeger. "The Life of René Malaise: from the Wild East to a Sunken Island." *Zootaxa*, vol. 3127, no. 1, 2011, p. 38., doi:10.11646/zootaxa.3127.1.2.
3. "What's CPAD?" *California Protected Areas Database*, www.calands.org/.
4. Aguiar AP, Sharkov A. Blue pan traps as a potential method for collecting Stephanidae (Hymenoptera). *Journal of Hymenoptera Research*, 1997, k422-423.
5. Campos, W.G. , Pereia D.B.S. and Schoereder, J. Comparison of the efficiency of flight interception traps models for sampling Hymenoptera and other insects. *Anais d Sociedade Entomologica do Brasil*, vol. 29, 2000, 3381-389.
6. Hutcheson, J.A. Malaise trap collection jar: a cheap simple modification. *New Zealand Entomologist*. Vol.14, 1991, pp 48-49.
7. Darling, D.C. and Packer, L. Effectiveness of Malaise traps in collecting Hymenoptera: The influence of the design, mesh, size and location. *The Canadian Entomologist*, 1988, pp.787-796.
8. "Malaise Traps." *Malaise Traps- Collecting Methods Mississippi Entomological Museum Home*, mississippientomologicalmuseum.org.msstate.edu/collecting.preparation.methods/Malaise.traps.htm.
9. Evans, F.C. and Owen, D.F. Measuring insect flight activity with a Malaise trap. *Papers of the Michigan Academy of Science, Arts, and Letters*, Vol. L, 1965, pp. 89–94.
10. "International Barcode of Life", ibol.org.
11. "Species List." *School Malaise Trap Program*, malaiseprogram.com/site/wp-content/uploads/2016/12/FSMTP_2016_Individual_Species_List_Western-Center-Academy.pdf.

Copyright: © 2019 Martinez, Reeves, Perry, and Horton. All JEI articles are distributed under the attribution non-commercial, no derivative license (<http://creativecommons.org/licenses/by-nc-nd/3.0/>). This means that anyone is free to share, copy and distribute an unaltered article for non-commercial purposes provided the original author and source is credited.

Effects of common pesticides on population size, motor function, and learning capabilities in *Drosophila melanogaster*

Alejandra Abramson, Leya Joykuty

American Heritage School, Plantation, Florida

SUMMARY

In this study, we aim to examine the effects of commonly used pesticides on population size, motor function, and learning in *Drosophila melanogaster*. Specifically, we examined the effects of metolachlor, glyphosate, chlorpyrifos, and atrazine on *Drosophila*. Pesticides are toxins used to control pests and weeds in crops and in the past, have been connected to multiple health issues in those exposed. Overall, the results were collected using a negative geotaxis assay, aversive phototaxis assay, and a larval learning assay whose data was averaged. This project can be applied to the 1.8 billion people who are exposed to pesticides and assist in defining the connections in between pesticides and the tested diseases.

INTRODUCTION

Pesticides are products intended to kill or repel unwanted plants or animals. They can be categorized by their intended target; herbicides (weed killers), insecticides (bug killers), and fungicides (fungus killers) are all types of pesticides. While they are commonly used in many settings around the world, farmers rely particularly heavily on pesticides to protect their crops from weeds and insects. However, a consequence of using pesticides is the fact that some of it is washed off the farm to surface water. This contaminated water may be toxic to animals that live in it, as well as to humans. Since the 1940s, farmers have been forced to increase the strength of pesticide treatments in order to effectively kill their targets. This occurs because of “pesticide treadmill,” a phenomenon in which plants or insects evolve immunity to a particular pesticide treatment conditions and farmers must employ more and more extreme measures to overcome this resistance. Ultimately, this results in higher concentrations of pesticides in surface water and more exposure by humans and other animals.

Pesticide exposure has been linked to cancer, reproductive harm, and health issues in children (2). Other recent studies have concluded that organophosphorus and organochlorine pesticides are linked to a variety of human diseases and disorders, including ADHD, Alzheimer’s disease, Parkinson’s disease, and birth defects (5). Neurodegenerative diseases affect the brain; many are fatal and have no cure. These illnesses complicate daily tasks, using medicine or surgery can help slow the progression, eventually causing

severe disability (7). About one in six children in the U.S. has a developmental disorder, some more than one. Scientists hypothesize that toxic chemicals in the environment can be taken in by the mother and may cause the child to have developmental or neurological issues ranging from learning problems to intense behavioral or emotional disorders. (6). Birth defects are physical derangements that occur before a baby is born. The cause of these diseases have been credited to infections, genetics, and certain environmental factors, like pesticides. Connections between these disease and pesticides have presented themselves in the past with people who would have constant exposure to pesticides. The best example that encompasses the three conditions being tested took place in 2005. Three women and their husbands lived and worked at a large farm that would have allowed constant exposure to pesticides. The women each had kids, and all of them developed some sort of health deficits within 5 years of birth. As they grew older, the adults all began to experience symptoms of neurodegenerative diseases, and it lead scientists to connect it back to their work life at the farm. Since then, research over pesticides has been much more concentrated on its affect towards humans then before.

This study aims to examine the short-term and long-term effects of pesticides on population size, motor function, and learning capabilities in *Drosophila melanogaster*. *Drosophila* are a species of fruit flies commonly used for scientific research. The genome of this species is 75% identical to the genome of humans, making *Drosophila* an effective model system for biological studies. In addition, this species is a viable model organism for transgenerational experiments, as a single pair of flies can produce hundreds of offspring in a short period of time and both females and males become sexually mature within a week of becoming adults or ten days of life.

The pesticides used within the parameters of this project are atrazine, metolachlor, glyphosate, and chlorpyrifos. Atrazine and glyphosate are herbicides used primarily to manage corn crops, yet the risks induced by these chemicals caused them to be banned from use in certain parts of the world. Both of these, as well as the insecticide chlorpyrifos, are based off of phosphorous compounds, making them organic phosphorous compounds (organophosphates). Metolachlor, another common herbicides, is an organochlorine (based off of a chlorine compound). Each pesticide has been shown to cause a broad range of adverse effects. Short-term exposure

is generally associated with nausea and vomiting, while long-term impacts may vary by pesticide. Organophosphates have been known to cause memory problems, while organochlorines target motor functions. We hypothesize that exposure to atrazine, metolachlor, glyphosate, and chlorpyrifos will have a negative effect on viability, motor function, and learning capabilities in *Drosophila melanogaster*. In this study, we will assess the effects of these pesticides on viability by measuring population size, motor function using the negative geotaxis assay, and learning with the aversive phototaxis suppression assay and the larval learning assay. The *Drosophila* will be tested and given the pesticides through means of ingestion and the control group will be the flies given normal food without any pesticides.

RESULTS

The *Drosophila* were fed their designated pesticide food for 14 days before the data was collected. The treatment groups were chlorpyrifos, atrazine, metolachlor, glyphosate, and the control group that was left untouched by pesticides. Ten *Drosophila* were assigned to each trial and ten trials of each assay and pesticides were conducted. Population size was monitored by counting the amount of *Drosophila* each day using carbon dioxide to anesthetize them.

Population size

Population size was monitored by counting the amount of adult *Drosophila* everyday during the 14-day span of testing. The population of *Drosophila* greatly decreased in both the metolachlor and glyphosate settings. On the final day, the amount of *Drosophila* remaining was compared to the starting population on the first day of testing, imposing the inference that these two pesticides had a greater effect towards the longevity of the *Drosophila*.

Motor function

We performed the negative geotaxis assay to measure the effect of pesticides on motor function in *Drosophila*. This test relies on the flies' natural geotaxis instincts, which is to move upward without need for stimulation. After 10 seconds, the amount of flies passed in the 8 cm line on the vial were counted to produce the results for each pesticide for decreased motor function. In the negative geotaxis assay, we found that flies treated with all of the tested pesticides demonstrated impaired motor function compared to untreated flies (see **Figure 1**). The flies that were exposed to metolachlor significantly showed less motor functions than the ones introduced atrazine. Unexpectedly, the flies exposed to the pesticides that were not previously researched had a lesser capability to climb the designated height, allowing the possibility to conclude that metolachlor, being the most unstudied and the one having the most effect, had a greater impact towards the flies' motor functions.

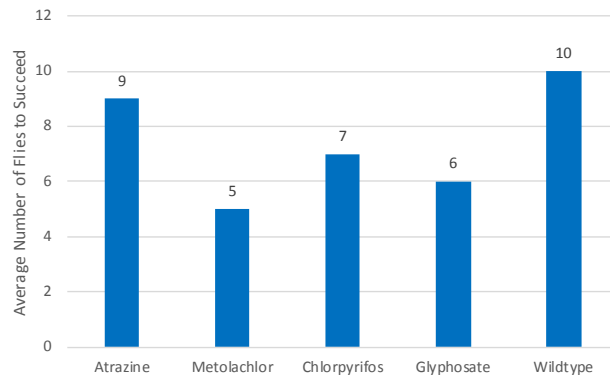


Figure 1: Effect of pesticide exposure on motor function. The negative geotaxis assay tested the motor function of adult *Drosophila*, measuring the effect on the neural synapse bridge by measuring motor function speed. This figure depicts metolachlor having a slower response time to the control variable, indicating a specific effect towards the nervous system of the *Drosophila*.

Learning

The most important assay was the aversive phototaxis suppression assay, which tested whether the adult flies ability to retain information shortly learned before. This test watched for the flies not being able to hold information from the sugar reward test and using that information for a stimulant test. The results showed that their incapacity to retain information that was learned a short while before seemed to be very prevalent within the metolachlor variable assays described in **Figure 2** (p -value < .00001, calculated by a t -test). Without a doubt, the metolachlor had the heaviest impact on the adult *Drosophila*'s capability to remember information compared to the control.

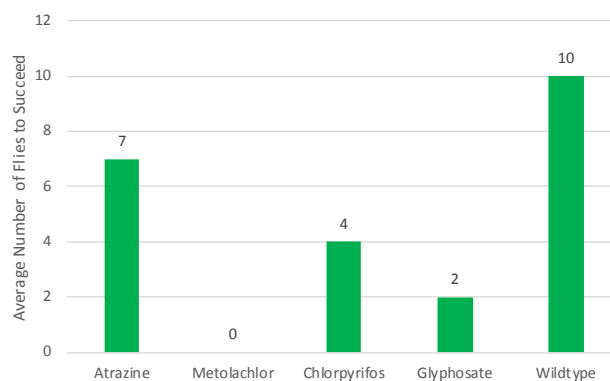


Figure 2: Effect of pesticide exposure on ability to retain information. Age-synchronized *Drosophila* adults were put in a 3D T-maze ($n = 10$) and were trained using a rewards system to gear away from their normal stimuli. After the time passed, the number of flies in the correct stimuli were counted and the ones that "failed" were averaged. *Drosophila* exposed showed a significant drop into the successful results of chlorpyrifos and metolachlor (p -value < .00001).

Transgenerational effect

Lastly, the larval learning assay using a baiting technique in order to test flies in their larvae stage. This test measured for the larvae's capacity to follow olfactory stimulants that would

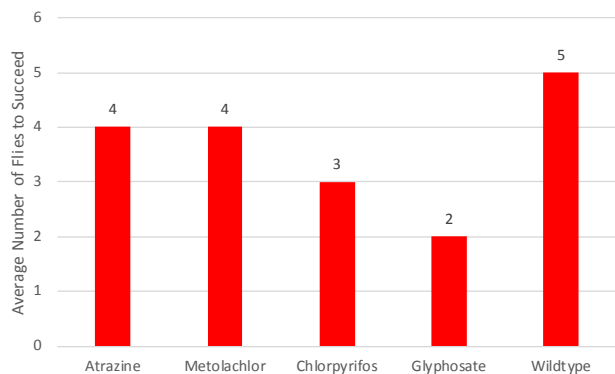


Figure 3: Effect of pesticide exposure on larval learning assay performance. Age-synchronized *Drosophila* larvae ($n = 10$) were placed on a plate and allowed to move towards aversive and positive olfactory stimuli. At the end of the assay, the number of flies that had moved towards each stimulus was counted, with flies that had moved toward the positive stimulus considered “successful.” Flies exposed to metolachlor and chlorpyrifos showed decreased assay performance, although this was not statistically significant ($p > 0.05$).

normally be easily distinguished. After testing, it was found that the ones exposed to both metolachlor and chlorpyrifos both were greatly unable to follow the simple stimuli and go to the sugar reward (Figure 3), so it can be concluded that the metolachlor, which had a greater impact, showed the most harm towards the flies exposed (non-significant results for a $p > 0.05$). These results could suggest that atrazine caused the least effect towards the proceeding generations.

DISCUSSION

This project came to very unexpected results. Instead of being the most harmful as expected, the atrazine had the least impact compared to all the other pesticides while metolachlor had the most. The reason behind this could have been attributed to multiple factors, but the main one would have been the most crucial: while atrazine is the most deadly known, there are many other pesticides that haven't been studied yet because of the amount in pesticides. But the biggest factor could be attributed that the toxicity of the other pesticides, such as metolachlor and glyphosate, in smaller amount has a greater toxicity than the large amount of the most common ones. Another potential factor could be the higher concentration of chlorine in the base of metolachlor than atrazine, glyphosate, chlorpyrifos lack, strengthening its toxicity. Most organophosphates ended up having a strong affect towards the memory assay of the aversive, yet in most assays, metolachlor surpassed the other variables. Lastly, glyphosate had an aversive effect towards the *Drosophila* out of any of the other organophates tested, another reason for the strength could have been the fact that it is based off of glycine instead of ester, giving it a stronger based.

We encountered several limitations during experimentation. Although the flies were maintained in a controlled environment, their consumption of pesticide-treated medium could not be controlled. Another limitation in

this study is that the anesthesia used on the flies could have had an effect on motor function and learning capabilities of the flies in addition to the effect of the pesticide treatment. The potential effects of anesthesia on flies' movement and learning were controlled as much as possible by allowing a minimum five minute acclimation period following exposure to anesthetic. Additionally, by comparing the treated flies to the untreated, it highlights the negative factors of the pesticides in any aspect, because the toxin will most definitely have an effect. In addition, carbon dioxide (CO₂) was used as the anesthetic in these experiments instead of Flynap™, because CO₂ has a shorter anesthetic period. Another limitation in these experiments is the potential toxicity of the pesticides; for example, if the pesticide treatments are severely toxic to *Drosophila*, the doses used may have impacted their ability to perform on the assays due to reasons other than impairment of motor function or learning capabilities. However, we accounted for this limitation by calculating an appropriate dosage for *Drosophila*. Finally, designing and 3D-printing the prototype for the aversive phototaxis suppression took longer than expected.

Future research could be conducted to show the effects of other common pesticides, or to further investigate the specific neural pathway that the toxins affect. Some toxins, such as organophosphates and organochlorines, are already known to target specific synapses and destroy connections between transmission neurons. Also, it could be researched whether there is a different effect between genders, and the specific way that it affects both. Different medium types and model organisms could also be tested, along with time of exposure and mode of exposure (not just by consumption).

New studies have shown that 1.8 billion people globally per year are exposed to pesticide, both in household products for gardening or weed killers used on farms. Individuals who live in areas surrounding farms or agriculture may inhale aerosolized pesticides, and farmers may come into contact with pesticides when harvesting crops or pulling out weeds. This is also a concern for the next generation, as individuals who have come into with toxins through skin absorption or inhalation, may carry the poison in their system, and when they have children, they may pass on the built-up toxins, which can affect the child's health. In general, the health and methods of the agricultural system could be completely revolutionized with continuation of such research in efforts to better the way that farms are run along with the population's health.

MATERIALS AND METHODS

Safety

First, these pesticide toxin extracts may be harmful to humans if the liquid form comes to contact with the skin or is inhaled. Multiple measures were taken for security including goggles, gloves, lab coat, and a filter face mask. The pesticide powders were handled under the fume hood to further provide protections. At the end of the experiment, the

diluted pesticides were disposed of in the South Household Hazardous Waste Drop-off.

Animals

The flies were kept at room temperature in a monitored 12 hour light/12 hour dark cycle. Transfer between vials with new medium was done every three to four days to assure no risk of bacterial infiltration of the food. They were all supplied by Carolina Biological and were listed under the wildtype strain named Oregon-R. Before they were trialed, they lived in the vials with different media for about 14 days in a correspondent light/dark cycle, each group using about 10 flies in the vial. *Drosophila* were fed with 15 mL of distilled water and blue medium from Carolina Biological in shatterproof vials.

Experimental setup

The experiment was set up over a 15-day period to test short-term exposure. On the first day, the medium powder was separated into five different vials that would be changed throughout the testing period every three days. Aside from the medium, the distilled water poured into each had the designated pesticides incorporated: atrazine, metolachlor, glyphosate, and chlorpyrifos (Sigma Aldrich). Each toxin was diluted in water through serial dilutions to 0.0002 micrograms/milliliter from 100% (1 g of toxin powder in 1 mL of dH₂O) concentration to represent the dilution of what a normal human would be exposed to per square acre of land.

Aversive phototaxis suppression assay

After transferring the flies from the medium vials into the aluminum-covered side of the 3D printed T-maze (designed by the researcher) by using carbon dioxide anesthesia, flies were allowed to wake up and acclimate for five minutes. The movable trapdoor in the middle was left closed so they were unable to pass to the light side. To train the *Drosophila*, the flies were left in the dark side which was covered by aluminum and a gooseneck lamp was attached to the opposing side (which the flies could not enter) with no olfactory stimuli. The flies were counted based on how many made it to the light side once the trap door opened, reflecting their ability to detect visible stimuli of the light, which they should normally be attracted to. The ones that moved towards the light stimulation are viable for further testing and can be transferred back into the dark side. This will occur until there are ten testable flies in the dark side all coming from the same variable setting. The rest of the flies were returned back to the medium vial for longevity and transgenerational studies. For the flies that are in the T-maze, filter paper with 20 uL of aversive stimuli (quinine hydrochloride) was added to the light side. The lamp was turned on again with the open trapdoor. After one minute, the number of flies that have diverted away from the light side because of the aversive stimuli were counted as passes and the flies that remained there were counted as fails. Retest 10 different flies from each variable each trial.

Negative geotaxis assay

Ten flies were separated into five different vials with no medium and were labeled according to the pesticide treatment: metolachlor, glyphosate, atrazine, chlorpyrifos, and non-treated. After being transferred using carbon dioxide to a 50 mL conical tube, the 8 cm line was marked (calculated based off of standard height per second) and then the flies were allowed to acclimate for five minutes in the tubes. After the five minutes passed, the flies were woken up using sugar bait. The vials were tapped lightly on the counter to let all the flies fall to the bottom. A timer was set for ten seconds and the number of flies that surpassed the 8 cm mark line were counted.

Larval learning assay

The flies to sleep in each variable vial using carbon dioxide and 10 age-synchronized larvae were collected and transferred to a half fructose agar / half agarose plate with set stimuli. The aversive stimuli, concentrated octanol (Sigma Aldrich), was placed in Teflon containers with pre-poked fragrance releasers. One octanol container was located in the agarose side of the plate. On the opposing fructose agar side, a positive stimuli of amyl acetate (made with paraffin oil) was placed in the Teflon containers. After insertion of the containers, larvae were placed in the middle of the plate. Once the timer was started, the plates with larvae were left in a lighted area for five minutes. Then, the number of larvae on each side of the plate was counted.

Analysis

The results of the assays were analyzed for mortality and decreased function in comparison to the non-treated or non-altered flies. The information was input into an Excel sheet and the total mortality rate was calculated based on number of deceased flies and total fly population along with each assay's individual results.

Received: March 10, 2019

Accepted: July 30, 2019

Published: January 25, 2020

REFERENCES

1. Miller, Conrad. "*Drosophila Melanogaster*." *Animal Diversity Web*, animaldiversity.org/accounts/Drosophila_melanogaster/.
2. "Pesticides 101." *MSD Manual*, www.panna.org/pesticides-big-picture/pesticides-101.
3. Powell-Hamilton, Nina N. "Overview of Birth Defects." *MSD Manual*, www.merckmanuals.com/home/children-s-health-issues/overview-of-birthdefects/overview-of-birth-defects.
4. Ganzel, Bill. "How Insecticides Work." *Living History Farm*, The Ganzel Group, 2009, livinghistoryfarm.org/farminginthe70s/pests_06.html.
5. "Attention-deficit Hyperactivity Disorder (ADD,

- ADHD)." *MSD Manual*, [www.msmanuals.com/home/SearchResults?query=Attention-Deficit%2fHyperactivity+Disorder+\(ADD%2c+ADHD\)&icd9=314.0%3bMM667](http://www.msmanuals.com/home/SearchResults?query=Attention-Deficit%2fHyperactivity+Disorder+(ADD%2c+ADHD)&icd9=314.0%3bMM667).
6. Sulkes, Stephen Brian. "Learning Disorders." *MSD Manual*, www.msmanuals.com/home/children-s-health-issues/learning-and-developmentaldisorders/learning-disorders.
 7. Huang, Juebin. "Alzheimer's Disease." *MSD Manual*, www.merckmanuals.com/home/brain,-spinal-cord,-and-nerve-disorders/deliriumand-dementia/alzheimer-disease
 8. "What Is Farm Runoff Doing to the Water? Scientists Wade in." Produced by Abbie Fentress Swanson, 5 July 2013. www.npr.org/sections/thesalt/2013/07/09/199095108/Whats-In-The-Water-Searching-Midwest-Streams-For-Crop-Runoff. Transcript
 9. "ISEF Rules Wizard." *Society For Science and The Public*, ruleswizard.societyforscience.org.

Copyright: © 2020 Abramson and Joykuty. All JEI articles are distributed under the attribution non-commercial, no derivative license (<http://creativecommons.org/licenses/by-nc-nd/3.0/>). This means that anyone is free to share, copy and distribute an unaltered article for non-commercial purposes provided the original author and source is credited.

Understanding the relationship between perception and reality related to public safety: A case study of public opinion on local law enforcement in Andover, MA

Alexander Luck, Thomas Keane

Doherty Middle School, Andover, Massachusetts

SUMMARY

Living in a small town with low crime rates and relatively high education levels usually gives the perception of a safe and comfortable community. In many, but not in all ways, that perception reflects reality. The following study tries to understand the connection between the perception, as defined by the collected public opinion, and the reality, as defined by the crime data reported by the US census and FBI data. The public opinion on property crime, violent crime, drug related crime, general feeling of safety, and on assessment of local law enforcement was collected from the Massachusetts community of Andover. The study tested the hypothesis that the opinion of the participants reflects the crime data and that citizens of Andover feel safe and are confident that local law enforcement works well. According to the results of the survey, people in Andover indeed have a positive view of the police department. The majority believe that the crime rates to be relatively low and, in general, most participants feel safe in the town. The findings also indicate that there are a few areas where public opinion does not match the FBI data, with the issues of property crime and drug usage possibly being of concern.

INTRODUCTION

Andover is a town located in Essex County, in the northeastern part of Massachusetts (MA). It occupies 32.1 sq. miles, of which 31 sq. miles are land and 1.1 sq. miles are water (1). According to the 2018 census, the estimated population of Andover is 35,898 (1). Of that population, 52% are female and 48% are male (1). Andover's population consists of 79.4% Caucasians, 12.3% Asians, 2.5% Black or African-Americans, 3.7% Hispanics, and 2.1% other (1). Thus, Andover is a predominantly white community with less than 20% of minorities.

According to the US Census Bureau, in 2017 the average income per capita in Andover in the past 12 months was \$63,468 (1). This is 25% higher than the average in MA and 59% higher than the national average (2). The median household income in Andover was \$143,292, which is higher than the average in MA and higher than the national average (3). The poverty level is also low, at about 4% (3). This makes Andover a relatively wealthy town.

Andover's education system consists of 11 public

schools, 5 private schools, and 4 post-secondary schools (4). The Andover school system is rated above average. The Andover public school test scores are around 80%, which is 24% higher than the Massachusetts average and 62% higher than the national average (4). Between 2013 and 2017, 98% of people successfully graduated high school, and 74% of people received a bachelor's degree or higher (5). Based on these statistics, Andover has an educated population, most of which went to college.

Preventing and fighting crime is an important aspect of any town, city, or village. Andover has a low crime rate. The rate of violent crimes in Andover is 83% lower than the MA average and is 84% lower than the national average (6). The rate of property crime in Andover is 61% lower than the MA average and 75% lower than the national average (6). According to public records, Andover appears to be a safe and low-crime community.

Even though Andover appears to be a well-to-do, educated, and safe town, it still has problems, which are often reported in the local media and vocalized by the townspeople. Property crime and drug-related incidents are reported by local newspapers frequently. For example, robberies of unlocked vehicles and a spate of house break-ins occurred in 2007 (7-10). More recently, at the end of 2018, police were asking for the public's help in identifying a burglar who broke into Andover Country Club Lane homes (11). In February of 2019, police reported 14 car thefts (12).

In addition, Andover, as in many other places across the United States, faces a drug problem. In 2014, there were over 1,000 opioid-related deaths across MA (13). Essex County had the second largest number of fatalities, totaling 146 deaths (14). In 2015, 21 heroin overdoses, 5 resulting in deaths, were reported in Andover (15). In October 2018, a man was arrested for trafficking fentanyl drugs (16). At the end of 2018, a couple in Andover was arrested for dealing cocaine (17). At Andover High School, drug usage is prevalent. Between September 2017 and June 2018, the police department has responded to 10 incidents involving drugs at the high school (18). Drug-sniffing dogs were brought to Andover High School to investigate drug dealing and usage in the school (19). One Andover student, Keagan Casey, has made a documentary about the drug use in Andover titled "The Other Side of Andover" (20, 21). The movie describes how teenagers are taking strong painkillers and heroin to cope with stress and emotional problems or simply to experiment. In it, students

recall horrid memories of their addiction and how it affected their families and life. This evidence demonstrates that despite the lower than average crime rate, Andover still has its fair share of criminal problems.

At the center of any community's general safety is the local police enforcement. Policing is a service industry with the main objective of serving the community (22, 23). Understanding the community's opinion may be important for understanding the relationship between citizens and the local law enforcement. It may also provide a way to assess the level of safety in the community. Once this relationship is well understood, police will work more efficiently and will be able to identify areas of improvement.

In this study, we designed a survey based on some of Mastrofski's conceptualizations of police service quality. Mastrofski developed 6 aspects of survey quality in policing, including attentiveness, reliability, responsiveness, competence, manners, and fairness (23, 24). According to Mastrofski's research, citizens want the police to be available and accessible, as indicated by police officers' attentiveness. Citizens also want the police to be predictable and consistent, as indicated by officers' reliability, and client-centered, as indicated by officers' responsiveness. Citizens also want police officers to be effective in their jobs, as indicated by their competence. And lastly, people want the police to treat them with respect and use fair practices, as indicated by officers' manners and fairness.

In designing the survey, we used Mastrofski's concepts to help us understand the public opinion. We collected, analyzed, and compared responses to the crime rates reported by the FBI to understand the relationship between perception and reality. We hypothesized that most respondents would consider Andover a safe town with an effective police force and that public opinion would align with the FBI data.

RESULTS

The study consisted of analyzing 142 surveys. Detailed demographic information was collected (**Table 1**). Most of the participants lived in Andover (88%), while some worked but did not live in Andover (12%). The participants consisted of 44% males and 55% females. The following ethnic groups were represented: White (70%), Asian (11%), African American (8%), Latino (8%), Native American (1.5%), and other (1.5%). Age groups were categorized in the following way: under 13 (8%), 13-17 (7%), 18-24 (6%), 25-34 (16%), 35-44 (17%), 45-55 (21%), 64-60 (10%), and over 60 (15%). The majority of participants had a college degree and were either employed or retired. The income ranged from \$10,000 to over \$200,000. Additionally, 50% of participants were married, 24% were single, 1% were in a domestic partnership, 4% were divorced, 8% were widowed, and 1% were "too young for a relationship." In terms of political parties, 25% identified as Democrats, 30% as Republicans, 28% as Independent, 0.7% as Libertarian, 1.4% as Green Party, and 7.0% as "Other" (**Table 1**). The demographic breakdown by gender, ethnic group, and income

was representative of the Andover community as documented by public records. Overall, the participants spanned a broad range of demographic attributes.

Based on the responses to the survey, residents of Andover had a positive impression of the local police force

Demographic variable	% of participants
Age group	
Under 13	7.75%
13-17	7.04%
18-24	5.63%
25-34	16.20%
35-44	17.61%
45-54	21.13%
55-60	9.86%
Over 60	14.79%
Gender	
Female	54.93%
Male	44.37%
Other	0.70%
Ethnicity	
White	69.72%
Black	8.45%
Latino	7.75%
Native American	1.41%
Asian	10.56%
Other	1.41%
Household Income	
Below \$10k	0.70%
\$10k-\$50k	11.27%
\$50k-\$100k	21.83%
\$100k-\$150k	15.49%
\$150k-\$200k	19.72%
Over \$200k	11.97%
Other	14.79%
Marital Status	
Single	23.94%
Married	50.70%
Partnership	0.70%
Divorced	4.23%
Widowed	8.45%
Other	6.34%
Political Party	
Democrat	25.35%
Republican	30.28%
Independent	28.17%
Libertarian	0.70%
Green party	1.41%
Other	7.04%

Table 1: Participant demographics. Shown is a summary of percentages for different demographic variables analyzed ($n = 142$).

(Table 2). They believed that the police force was well-mannered, attentive, responsive, and fair. Our data revealed that 79% of the participants agreed that the Andover police arrived quickly when called. Based on the 85% agreement rate, the participants believed that the Andover police was friendly, respectful, and professional. A large majority of people (80%) stated that the police department was not corrupt. Additionally, 71% of participants confirmed that the Andover police was not intimidating, and 56% of people thought that the Andover police did not use excessive force. Many people (63%) believed that the Andover police was well trained. Most importantly, 71% of people were confident that the Andover police cared about its town and the town's people.

We also assessed public opinion on violent crime, property crime, and drug usage (Table 2). Many participants (69%) did not think that the rate of violent crimes in Andover was high. Most people (64%) agreed that Andover police was doing a good job of preventing violent crimes. This indicated that the Andover police was considered competent, reliable, and responsive.

Property crimes appeared to be of some concern (Table

2). About 30% of participants stated that the rate of property crimes was high. Approximately half of the participants (46%) agreed that Andover police was doing a good job of preventing property crimes. These results suggested that a significant portion of the Andover public felt somewhat apprehensive about property crimes and their prevention.

A little more than half (55%) of the participants believed that drug usage in Andover was high, and 51% believed that the rate of drug dealing in the town was high (Table 2). About 32% believed that the police were making good progress in reducing drug problems in Andover, while 20% did not believe progress was being made, and 46% of people were not sure. Drug dealing and drug use were a concern. The large percentage of unsure responses reflected people's lack of confidence in police effectiveness in drug crime prevention.

Despite some concerns about property crime and a larger concern about drugs, overall, people in Andover felt safe (85%). Almost the same number of people felt safe walking at night (86%). Yet 63% percent of participants preferred to keep their door locked.

In general, race is an important element of how people are treated by the police. Concerns about the interaction between

Question	Mastrofski's concept assessed	Grouped response (percent of participants)			
		Disagree	Not sure	Agree	Missing
Arrives quickly when called	Attentiveness, Responsiveness	8%	11%	79%	3%
Friendly and respectful	Manners	8%	6%	85%	1%
Professional	Manners, Competence	8%	6%	85%	1%
Intimidating to deal with	Manners, Fairness	71%	15%	13%	1%
Cares about the town and its people	Attentiveness, Responsiveness	5%	24%	71%	0%
Corrupt	Fairness	80%	15%	4%	1%
Too much presence in public places	Responsiveness, Reliability	49%	43%	7%	1%
Too little presence in public places	Responsiveness, Reliability	19%	44%	36%	1%
Well trained	Competence	8%	28%	63%	0%
Uses too much force	Manners, Fairness	56%	39%	4%	1%
Is successful in preventing property crimes	Competence, Reliability	25%	28%	46%	0%
Rate of property crimes in the town is high	Competence, Reliability	42%	27%	30%	1%
Is successful in preventing violent crimes	Competence, Reliability	11%	23%	64%	2%
Rate of violent crimes in the town is high	Competence, Reliability	69%	20%	9%	1%
Rate of drug use in the town is high	Competence, Reliability	20%	24%	55%	1%
Rate of drug dealing in the town is high	Competence, Reliability	18%	32%	51%	0%
Police is making a good progress in reducing drug use in the town	Competence, Reliability	20%	46%	32%	1%
I feel safe in the town	Competence, Reliability, Responsiveness	4%	10%	85%	1%
I feel safe walking in the town at night	Competence, Reliability, Responsiveness	8%	8%	84%	1%
I can leave the door unlocked	Competence, Reliability, Responsiveness	63%	13%	23%	1%

Table 2: Summary of survey responses. Shown is summary of participants' ($n = 142$) opinions regarding Andover police. Responses are grouped into 4 categories: disagree, not sure, agree, and missing. Results are shown as percentages. For each question, Mastrofski's concept is identified.

race and the disposition of the police towards citizens are not new (25-28). Many police officers treat everyone fairly, but some may display racial prejudice in their interactions with the public. This could affect how people of different races perceive the police. Therefore, we examined survey responses based on race and asked a subset of questions to assess racial bias. The data indicated that there was no correlation between race and how people view the Andover Police (Table 3). However, there were slight variations in the degree of responses for some questions. For example, Latino participants only “somewhat agreed” that the police were friendly and respectful, while White, Black, and Asian participants “strongly agreed” (Table 3). There were also differences for assessing whether police were intimidating and if they used excessive force. Black and Latino participants “somewhat disagreed,” while White and Asian participants “strongly disagreed” (Table 3). Our survey did not identify the origin of these variations. Given the low crime rates in Andover, it is unlikely that many participants had personal interactions with the police. It is possible that participants’ opinions were influenced by secondhand stories, media, and potential stereotypes of the police.

To further evaluate the hypothesis, we compared public opinion to the public FBI crime rate data from 2017 (detailed 2018 rates are not yet available) (29). Based on public records, crime rates in Andover were low in comparison to the state of MA and the rest of the country (Table 4, Figures 1 and 2). Violent crime and aggravated assault incidents per 100,000 inhabitants in Andover were only 0.006% of that of the US. Robbery, burglary, and property crime incidents were 0.003% in comparison to the US. The numbers of violent crime and aggravated assault incidents per 100,000 inhabitants in Andover were 0.3% compared to MA. The property crime, burglary, and robbery incidents were 0.2% compared to MA.

Selected Questions	Native				
	White	Black	Latino	American	Asian
Corrupt	1	1	1	4	1
Friendly and respectful	5	5	4	3	5
Uses too much force	2	3	2	2	2
Intimidating to deal with	1	2	2	2	1
Is successful in preventing violent crimes	4	5	5	4	5
Rate of drug use in town is high	4	4	4	2	4
I feel safe in the town	5	5	5	3	5
I feel safe walking in the town at night	5	5	5	3	5
Number of respondents	98	12	11	2	15

Table 3: Summary of median responses to selected questions. Shown above is a subset of selected questions and their distribution across racial groups to better understand impact of race on views about the police. Participants self-identified as White, Black, Latino, Native American, and Asian. Participants responded using a scale from 1 to 5: 1 = “strongly disagree”; 2 = “somewhat disagree”; 3 = “neutral/not sure”; 4 = “somewhat agree”; 5 = “strongly agree.”

Place	Violent crime	Aggravated assault	Burglary	Robbery	Property crime
FBI UCR statistics: total number of incidents					
USA	1,283,220	870,825	1,401,840	319,356	7,794,086
MA	24,560	17,319	17,089	4,871	198,575
Andover	72	64	25	3	287
FBI UCR statistics per 100,000 inhabitants					
USA	394	267	430	98	2,393
MA	358	252	249	71	2,895
Andover	201	178	70	8	799
FBI UCR statistics per 100,000 inhabitants (% difference)					
MA/USA	91%	94%	58%	72%	121%
Andover/USA	51%	67%	16%	9%	33%
Andover/MA	56%	71%	28%	12%	28%

Note. Total population for USA = 325,719,178; MA = 6,859,819; Andover = 35,898.

Table 4: FBI Uniform Crime Reporting (UCR) statistics for USA, MA and Andover from 2017. FBI crime data showcasing USA vs. MA vs. Andover (29).

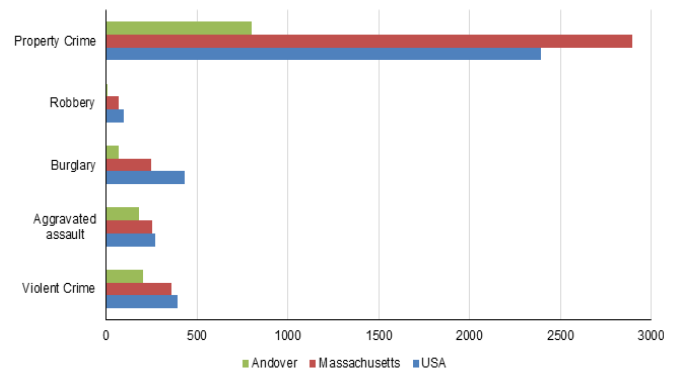


Figure 1: 2017 FBI UCR crime rates. Andover has lower crime rates compared to the rest of MA and the USA. Data are normalized per 100,000 inhabitants.

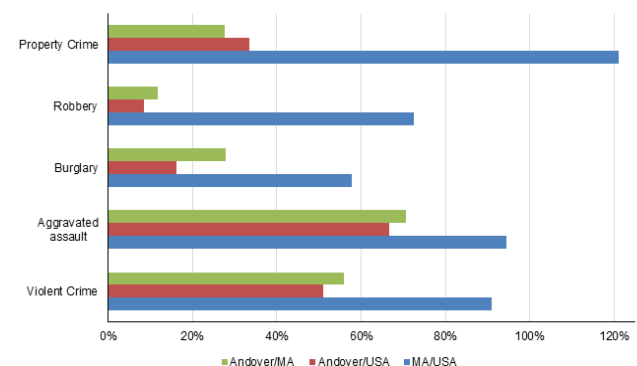


Figure 2: 2017 FBI UCR crime rates % comparison. Andover has lower crimes in comparison to MA and USA. Data are normalized per 100,000 inhabitants.

The public data shows that Andover was a safe town with crime rates below the national and MA averages.

The FBI data aligned well with the survey data in terms of violent crimes. The survey showed that over 60% participants believed that the rate of violent crime rates in town was low and that police were doing a good job at preventing violent crimes. The positive public opinion matched the very low violent crime rates reported by the FBI. In contrast, the survey indicated that people in Andover were somewhat concerned about property crimes. These concerns were not supported by the FBI data. In fact, 30% of participants believed that the rate of property crimes was high, while the FBI data showed that the reality was just the opposite. The cause of such a divergence was not clear. An interesting observation was that, according to the FBI data, violent crimes and aggravated assaults in Andover were higher than property crimes. However, people thought that property crime was more of a concern.

A significant number of participants agreed that Andover faces a drug problem. As compared to the entire US, MA has a lower rate of drug incidents (Tables 5 and 6). Among 10,000 people from MA, about 6 people possessed heroin, cocaine, and their derivatives, and 1 person had some type of synthetic drug. In the US, about 8 people in 10,000 possessed heroin, cocaine, and their derivatives, and 2 people possessed synthetic drugs. In 2017, Andover had 2 deaths caused by drug overdoses and 44 overdoses which lead to calls to EMS.

Furthermore, we attempted to assess what the participants believed were areas for improvement (Table 7). Twenty-three participants believed that the Andover police ought to improve drug crime prevention. Eleven participants stated that an increased number of officers was needed. Seven participants declared that property crime prevention

Drug type	MA	USA	MA/10,000 inhabitants	USA/10,000 inhabitants
Arrests for sales or manufacturing of drugs in 2017, not counting marijuana				
Heroin, cocaine and their derivatives	2,690	66,811	3.9	2.1
Synthetic drugs	419	20,513	0.6	0.6
Other dangerous non-narcotic drugs	287	51,488	0.4	1.6
Total	3,396	138,812	5.0	4.3
Arrests for drug possession in 2017, not counting marijuana				
Heroin, cocaine and their derivatives	4,370	263,744	6.4	8.1
Synthetic drugs	652	62,019	1.0	1.9
Other dangerous non-narcotic drugs	654	303,845	1.0	9.3
Total	5,676	629,608	8.3	19.3

Note. Total population for USA = 325,719,178; MA = 6,859,819.

Table 5: Drug-related crime rates in MA and USA (total and normalized by 10,000 inhabitants) (29).

Incident	Andover	MA	Andover/10,000 inhabitants	MA/10,000 inhabitants
Overdose with a call to EMS	44	22,213	12.3	32.4
Overdose resulting in death	2	1,945	0.6	2.8

Note. Total population for MA = 6,859,819; Andover = 35,898.

Table 6: Drug-related incidents in Andover and MA (total and normalized by 10,000 inhabitants) (29).

Area for improvement	Number of respondents
Politeness	7
Drug crime prevention	23
Violent crime prevention	1
Property crime prevention	7
Increase number of police officers	11
Decrease the number of police officers	1
Increase police budget	1
Decrease police budget	0
Increased training of the officers	2

Table 7: Areas for improvement as identified by the respondents. Shown are the categories that the participants believed Andover Police would need to improve upon.

and politeness were to be improved. The areas of least concern were decreasing the number of police officers, increasing and decreasing police budgets, and increasing training of the officers.

DISCUSSION

We designed a survey to test the hypothesis that Andover citizens believe that Andover is a safe town with an effective police force. We evaluated whether the public opinion aligns with the FBI census data. Demographics of the participants reflected the general population of Andover (Table 1).

Overall, most people feel safe in the town of Andover (Table 2). Many participants feel safe living in town and are comfortable walking alone at night (Table 2). In addition, most participants have a positive opinion about the local law enforcement and believe that the police are doing a good job in crime prevention and keeping Andover safe.

The survey results both agreed and disagreed with the FBI census data. Public opinion on violent and aggravated crime occurrences and prevention aligned well with the FBI data. The rates of violent crime and aggravated assaults in Andover are relatively low in comparison to MA and USA. However, many people reported alarm regarding drug-related crime and property crime. This perception does not align with the low FBI statistics regarding drug and property crime as compared to state and national level. To further reiterate these concerns, a large group of participants suggested that drug and property crime prevention were areas for improvement and require further attention (Table 7). Some people also

indicated that the town may benefit from an increased number of officers and, potentially, more training.

According to the FBI census data, Andover does not have a drug problem (**Table 6**). However, over 50% of respondents think that drug dealing and use are problems in Andover. Consequently, people do not believe that the Andover police, similar to police in most other localities across the United States, are doing a good job in preventing drug dealing and use. We speculate that drug dealing and use in Andover may be underreported to police and EMS but may be well known on the personal level.

There are many factors that influence crime rates in a community, such as geographical location, climate, population density, urbanization, and youth concentration (30). Cultural, recreational, religious, and educational characteristics play a role in shaping crime levels. Economic conditions, employment rates and opportunities, and poverty levels will influence crime. Moreover, local police departments and criminal systems, such as prosecution, judicial, correctional, and probational, may affect crime. Other important considerations are citizens' desire to report crime and to work with the police and public attitude towards crime and police. Although all these factors may contribute to crime, they have not been evaluated directly in our survey. Additional studies will need to be conducted to assess the impact of these issues and their contribution to the public opinion.

In this study, we did not analyze crime rates or their dependencies. Instead, we analyzed perceptions of crime, safety, and police efficiency and compared them with the reality as reflected by crime rates. We also speculated about the causes of divergence of such perceptions from the reality.

It is interesting to explore the relationship between reality and perception. In this study, we compared public opinion with FBI and census data and noted some discrepancies between perception and reality. If people perceive that they live in a safe community with a dependable and efficient police force who cares about the residents they serve, then a favorable impression about the police will form (31). This may be the case for Andover. At the same time, if the police perceive that the residents appreciate their work effort and trust in their abilities, then, most likely, the law enforcement will be more eager to serve and to care. In fact, confidence in police was influenced by impressions that crime has decreased in the community and by having positive encounters with the police (31). This was not evaluated in our study, but in the future, it may be of interest to determine how the Andover police views the public they serve.

However, if some incidents or negative media messages speak of police unfavorably or sensationalize incidents, negative reactions and opinions may appear. This can lead to an unmotivated police force and distrustful public in a negative feedback loop. This was not evaluated in this study but may be yet another explanation of the unfavorable responses regarding drug and property crime prevention

In an NPR analysis, Americans are now more afraid

of crime, even though the crime rates are down. The more people consume bad news in the world, the more they believe it is more dangerous than it really is (32, 33). Is this true for Andover? Some studies found differences between newspapers which were classified as "sensational" and which carried proportionally more crime reports and reported crimes in a relatively sensational style than the newspaper that were classified as "non-sensational." Some findings indicated that sensational newspapers (compared to non-sensational newspapers) tended to negatively influence the public's perceptions of fear of crime and attitudes towards police (23, 33). Again, it would be worthwhile to understand if that is the case for Andover, MA.

There is still work to be done to better understand what influences public's perception of safety and police in Andover. It seems that both direct and indirect measures need to be used. Direct measures of police performance include crime rates, as reported in this study, as well as number of arrests, clearance rates, and calls for service response times. Indirect measures of police performance include questionnaires, like the one used in this study, as well as direct observations of social behavior, situational studies, and independent testing. Together, they will give a more accurate picture of the police force and may better assess perception versus reality.

MATERIALS AND METHODS

The survey was designed to analyze public opinion regarding public safety and Andover Police. All the questions in the survey were multiple choice. We developed survey questions that directly and indirectly assessed six aspects, based on Mastrofski's conceptualization of police service quality, including attentiveness, reliability, responsiveness, competence, manners, and fairness (24). The last three questions of the survey were designed to indirectly measure the police force's overall competence, reliability, and attentiveness by asking the respondents about their general "feeling of safety" in the community. We also compared participants' opinions to the FBI reported crime rates to understand the relationship between perception and reality.

The survey was approved by the Andover Public School superintendent and administration panel. The appropriate Scientific Review Committee form was acquired and approved. The survey was distributed randomly in public places such as the Senior Center, the Youth Center, public library, local shops and businesses, private houses, and streets. The participants were approached on a volunteer basis. Participants' consent was obtained, and their identity was kept anonymous.

The responses were recorded and analyzed using PSPSS software, which is a free, open source statistical software application used widely for statistical analyses of various complexity. LibreOffice Calc was also used.

There were 142 surveys that were analyzed. To determine whether the results of the survey matched the population of Andover, the margin of error was calculated for different confidence levels. This calculation allowed us to

understand if the amount of people surveyed was enough to obtain confidence about the accuracy of the data collected. The highest percentage margin of error was calculated based on Andover's population size of 35,937, the sample size of 142 respondents, and several different confidence levels. Instead of calculating a margin of error for responses to

$$MOE = z * \sqrt{\frac{p * (p - 1)}{(N - 1)} * \frac{n}{N - n}}$$

each question, a proportion of 50% ($p = 0.5$) was used as the highest possible predicted margin of error for any given question. The margin of error (MOE) is calculated according to the formula:

where z is 1.645, 1.96, or 2.576 for confidence levels of 90%, 95%, and 99%, respectively; p is proportion; N is population size; and n is sample size. For a confidence level of 90%, the highest margin of error is 6.9%. For a confidence level of 95%, the highest margin of error is 8.2%. And for a 99% confidence level, the highest margin of error is 10.8%.

Received: June 6, 2019

Accepted: September 10, 2019

Published: January 25, 2020

REFERENCES

1. "U.S. Census Bureau QuickFacts: Andover Town, Essex County, Massachusetts." *Census Bureau QuickFacts*, U.S. Department of Commerce, www.census.gov/quickfacts/fact/table/andovertownessexcountymassachusetts/PST045218.
2. "Andover, MA Employment." *Areavibes*, www.areavibes.com/andover-ma/employment.
3. "U.S. Census Bureau QuickFacts: Andover Town, Essex County, Massachusetts." *Census Bureau QuickFacts*, U.S. Department of Commerce, www.census.gov/quickfacts/fact/table/andovertownessexcountymassachusetts/PST045218.
4. "Andover, MA Schools." *Areavibes*, www.areavibes.com/andover-ma/schools/.
5. "Andover Town-MA Massachusetts Education Attainment Charts." *TownCharts*, www.towncharts.com/Massachusetts/Education/Andover-town-MA-Education-data.html.
6. "Andover Crime Rate Report (Massachusetts)." *CityRating*, www.cityrating.com/crime-statistics/massachusetts/andover.html.
7. "Spate of Housebreaks Hits Andover." *Eagle Tribune*, 14 June 2007, p. 1.
8. "No Leads at All as Break-Ins Continue in Andover Homes." *Eagle Tribune*, 21 June 2007.
9. "Local Indian Families Targeted by Thieves." *Eagle Tribune*, 21 April 2007, p. 1.
10. "Thieves Striking It Rich in Unlocked Andover Vehicles." *Eagle Tribune*, 18 September 2008, p. 1.
11. "Andover Police Seek Burglary Suspects." *Eagle Tribune*, 14 October, 2018, p. 1.
12. "Police Report 14 Car Burglaries in Less than One Week." *Eagle Tribune*, 11 February, 2018, p. 1.
13. Lima, Tim. "Other Side of Andover: Student's Documentary Brings Heroin Epidemic Home Andover Townsman." *Andover Townsman*, 9 June 2015.
14. Kirk, Bill "Heroin OD Deaths Spike in Andover: Drug Claims 5 Lives This Year: 'Potent' Form Suspected." *Andover Townsman*, 21 May 2015.
15. Tennant, Paul. "Two Suspects Charged with Possession of Marijuana with Intent to Distribute." *Andover Townsman*, 30 August 2018.
16. LaBella, Mike. "Andover Man Faces Drug and Weapons Charges." *Andover Townsman*, 11 October 2018.
17. Tennant, Paul. "Couple from Tewksbury Charged in Cocaine Bust." *Andover Townsman*, 27 November 2018.
18. Bode, Kelsey. "Police Respond to Drug Incidents at Andover High, Greater Lawrence Tech." *Andover Townsman*, 7 June 2018.
19. Bode, Kelsey. "Drug-sniffing Dogs Roam the Halls of Andover High School." *Andover Townsman*, 19 October 2017.
20. Lima, Tim. "Other Side of Andover." *Eagle Tribune*, 7 June 2015.
21. Keagan, Casey, director. "The Other Side of Andover Massachusetts." *YouTube*, uploaded by 3AD, www.youtube.com/watch?v=Lrq2S7qbZ-o.
22. Mastrofski, Stephen. "Surveying Clients to Assess Police Performance." *Evaluation Review*, vol. 5, no. 3, 1981, pp. 397–408. doi:10.1177/0193841x8100500308.
23. Maguire, Edward R., and Devon Johnson. "Measuring Public Perceptions of the Police." *Policing: An International Journal of Police Strategies & Management*, vol. 33, no. 4, 2010, pp. 703–730. doi:10.1108/13639511011085097.
24. Mastrofski, Stephen. "Policing for People." Police Foundation, Third Ideas in American Policing Lecture, November 1998, Washington, D.C.
25. Sampson, Robert J., and Janet L. Lauritsen. "Racial and Ethnic Disparities in Crime and Criminal Justice in the United States." *Crime and Justice*, vol. 21, 1997, pp. 311–374. doi:10.1086/449253.
26. Boyd, Lorenzo M., et al. "Race and Policing in America: Conflict and Reform." *Policing: An International Journal of Police Strategies & Management*, vol. 30, no. 4, 2007, pp. 698–700. doi:10.1108/13639510710833947.
27. Sim, Jessica J., et al. "Understanding Police and Expert Performance." *Personality and Social Psychology Bulletin*, vol. 39, no. 3, 2013, pp. 291–304. doi:10.1177/0146167212473157.
28. Gelman, A., et al. "An Analysis of the New York City Police Department's 'Stop-and-Frisk' Policy in the Context of Claims of Racial Bias." *Journal of the American Statistical Association*, vol. 102, no. 479, 2007, pp. 813–823.
29. "Massachusetts Offenses Known to Law Enforcement

by City 2017.” FBI: UCR Crime Justice Information Services Division, ucr.fbi.gov/crime-in-the-u.s/2017/crime-in-the-u.s.-2017/tables/table-8/table-8-state-cuts/massachusetts.xls.

30. “Variables Affecting Crime.” FBI, 5 Nov. 2012, ucr.fbi.gov/hate-crime/2011/resources/variables-affecting-crime.
31. Nofziger, Stacey, and Susan Williams. “Perceptions of Police and Safety in a Small Town.” *Police Quarterly*, vol. 8, no. 2, June 2005, pp. 248–270.
32. “Why the Public Perception of Crime Exceeds the Reality.” *NPR All Things Considered*, NPR, 26 July 2016.
33. Chan, Angela, and Venessa Chan. “Public Perception of Crime and Attitudes Toward Police: Examining the Effects of Media News.” *Discovery – SS Student E-Journal*, vol. 1, 2012, pp. 215–237.

Copyright: © 2020 Luck and Keane. All JEI articles are distributed under the attribution non-commercial, no derivative license (<http://creativecommons.org/licenses/by-nc-nd/3.0/>). This means that anyone is free to share, copy and distribute an unaltered article for non-commercial purposes provided the original author and source is credited.

The effect of neem on common nosocomial infection-causing organisms

Manav Shah¹, Danielle Ereddia¹, Jyoti Shah¹, Nanette Reese²

¹Wheeler High School, Marietta, Georgia

²Kennesaw State University, Kennesaw, Georgia

SUMMARY

Nosocomial infections are a major source of morbidity and mortality, affecting more than 2 million patients annually in the United States. Furthermore, the hospital environment supporting the acquisition of resistance to antibiotic agents by pathogens, complicates the treatment of infections due to drug-resistance of these pathogens. Ethnopharmacological reports support the use of neem (*Azadirachta indica*) against bacterial and fungal infections such as typhoid, yeast infection, and periodontitis. However, there is a lack of research about the effect of neem specifically on nosocomial organisms. We conducted this study to evaluate the effect of aqueous and ethanolic extracts from neem leaves and neem oil on the growth of several human pathogens which are known to cause hospital-acquired, or nosocomial, infections, including *Saccharomyces cerevisiae*, *Micrococcus luteus*, *Staphylococcus aureus*, *Escherichia coli*, and *Pseudomonas aeruginosa*. Neem extract in distilled water showed the strongest average inhibition across all microorganisms except *S. aureus*. Activity of neem extract in 95% ethanol was comparable to that of 10% bleach. Under the conditions of this study, we concluded that neem leaf extract has a significant antimicrobial effect against nosocomial organisms, supporting its use as an alternative or combination treatment for hospital-acquired infections.

INTRODUCTION

Bioactive compounds obtained from certain plants have been recognized worldwide for their medicinal uses (1). For the past few years, there has been increasing interest in using these properties in therapeutic fields to fight against harmful pathogenic microorganisms (1). The resilience of these microorganisms to widely used drugs has furthered this focus. One such plant that has been researched to solve this problem is neem. Neem, or *Azadirachta indica*, is a member of the *Meliaceae* family, subfamily *Meloidae*, and tribe *Melieae* mainly cultivated on the Indian subcontinent (1). The versatile multifarious tropical tree has been widely renowned for its various biomedical properties due to its many bioactive components. As a result, neem has been indigenously cultivated for at least 4,000 years. (2). Neem's properties include being antiallergenic, antidermatitic, antiviral, antifungal, anti-inflammatory, anti-pyorrhoeic, insecticidal, larvicidal, and nematicidal (2).

Neem is effective against many bacteria, protozoa, fungi, and viruses, and is traditionally consumed through dietary sources after being grown naturally (1, 2). However, while there are extensive studies on the effectiveness of neem on these microorganisms, there is a gap in knowledge of neem's potential effectiveness against nosocomial infections, defined as hospital-acquired infections of microorganism origin. The aim of this work is to study the effectiveness of neem against common nosocomial organisms.

Escherichia coli, *Staphylococcus aureus*, *Pseudomonas aeruginosa*, *Saccharomyces cerevisiae*, and *Micrococcus luteus* are the primary microorganisms that cause nosocomial infections (3). These microorganisms colonize a patient's skin, mucous membrane, anterior urethra, or other soft tissues (3). These microorganisms mainly cause nosocomial infections by forming biofilms on colonized surfaces, which are difficult to eliminate and are highly correlated with nosocomial infections (3). *E. coli* is known to cause diarrhea, urinary tract infections, respiratory illness, and pneumonia (4). Most *E. coli* are harmless and serve an important role in a healthy human intestinal tract (4). However, some *E. coli* are pathogenic, meaning they can cause illness outside of the intestinal tract (4). *S. aureus* is a bacteria that causes infections such as bacteremia, pneumonia, endocarditis, and osteomyelitis (5). Strains of bacteria found widely in the environment cause *Pseudomonas* infections, of which the most common type causing infections in humans is called *Pseudomonas aeruginosa* (6). *S. cerevisiae*, or brewer's yeast, is a one-celled fungus which is rich in minerals and nutrients and causes fungemia, endocarditis, pneumonia, and skin infections in people with weakened immune systems (7). *M. luteus* is a common gram-positive bacteria that causes endocarditis after surgery of patients, as it colonizes the surface of heart valves (8).

Neem most likely inhibits the microorganisms listed above because of its strong antibacterial and antifungal properties. Neem is composed mainly of quercetin and a number of limonoids, the main substances in neem that are active against bacteria and fungi (9). Quercetin, a polyphenolic flavonoid, accounts for many antifungal and antibacterial properties in neem (9). Limonoids found in neem oil are oxygenated modified triterpenes that have many antifungal properties (9). It can be assumed that neem has these properties because of this distinctive chemical structure such as hydroxyl groups at sites on the aromatic rings. This results in inhibition of

energy metabolism, inhibition of the attachment and biofilm formation, alteration of the membrane permeability, and attenuation of the pathogenicity.

Previous studies have found neem to be an effective antibacterial and antifungal against organisms such as *S. aureus* and *P. aeruginosa* (2, 11, 12). For example, Mahmoud et al. showed that all concentrations of the aqueous extract effectively suppressed the mycelial growth of *Aspergillus* species (*A. niger*, *A. flavus*, *A. terreus* and *A. fumigatus*), *Microsporium gypseum* and *Candida albicans* and that this effect was found to increase with concentration where a maximum activity was reached using the last one (20%) (12). The authors also reported that complete inhibition in the growth of *A. niger* was obtained in the assay with 20% concentration of aqueous leaf extract of neem (12). It was concluded that all concentrations of organic extracts effectively suppressed the mycelial growth and the recorded values were increasing gradually with concentration, reaching the highest values with 20% (12). Similarly, Sultana et al. showed that the minimum inhibitory concentration of neem was 1.4 g/mL to kill *S. aureus* and *P. aeruginosa* (11). Mondali et al. studied the efficacy of different extracts of neem leaf on *Aspergillus*, and *Rhizopus* (2). The growth of both fungal species was inhibited significantly and controlled with both alcoholic and water extracts of all tested concentrations (2). The alcoholic extracts of neem leaf were most effective in comparison to aqueous extract for retarding the growth of these species (2).

Nosocomial infections are a large, growing problem because as multiple bacteria and fungi are becoming resistant to drugs, the number of people fatally succumbing to these infections is growing at an alarming pace (3). The purpose of our experiment is to analyze the effectiveness of neem against these common nosocomial organisms so that hospitals will be able to properly combat these infections. In this experiment, the process of finding the zone of inhibition and the minimum inhibitory concentration will be replicated with five different microorganisms. We propose that neem extract, if applied to the common nosocomial organisms *E. coli*, *S. aureus*, *P. aeruginosa*, *S. cerevisiae*, and *M. luteus*, will inhibit microorganism growth. This experiment fits into the existing body because it continues to compare and study neem's effectiveness against certain infections. However, our approach is unique because we investigate neem's effectiveness purely on nosocomial infection-causing organisms and analyze how neem plays a role in growth inhibition. Previous studies have only looked at the infections themselves, but not clearly at the microorganisms causing the infections; this experiment aims to address that gap.

RESULTS

To investigate the effectiveness of neem we cultured each of the five microorganisms on agarose with varying concentrations of neem. Evaluations of zone of inhibitions showed that neem oil had the clearest agar surrounding it

in contrast to the bacterial and fungal growth on the plate and produced the least erosion of the agar-drilled wells it was in (Figure 1). In this context, the zone of inhibition is the radius surrounding a well filled with solution in which bacterial colonies do not grow. As a control, 10% bleach had the most erosion of the agar-drilled wells in comparison to the other wells. Neem powder resuspended in 95% ethanol had the most opaque agar, indicating a smaller zone of inhibition surrounding it compared to the other solutions.

The antibacterial effectiveness of negative control (distilled water), positive controls (95% ethanol and 10% bleach) and test materials (neem powder in distilled water, neem powder in 95% ethanol, and neem oil) against *E. coli*, *M. luteus*, *P. aeruginosa*, and *S. aureus* are shown in Figure 1. *S. cerevisiae* was also studied, however, due to contamination the data were eliminated.

P. aeruginosa was found to be the most susceptible to neem extract in distilled water, followed by *E. coli*. Neem extract in distilled water showed significantly higher inhibitory activity than positive control 95% ethanol for *E. coli* and *M. luteus*. Neem extract in 95% ethanol produced comparable zones of inhibition for all organisms, with significantly higher inhibition than 95% ethanol alone for all organisms except *P. aeruginosa*. The test solution neem oil was most effective against *P. aeruginosa* with a 2.1 mm zone of inhibition, followed by a 1.4 mm zone of inhibition for *S. aureus*. However, neem oil was not comparable in effectiveness to either positive control and was shown to be least effective of all test solutions. The positive controls demonstrated a similar pattern to neem oil with both being most effective against *P. aeruginosa*, followed by *S. aureus*. *P. aeruginosa* cleared a 4.5 mm zone of inhibition for the 10% bleach solution and a 4.3 mm zone of inhibition with 95% ethanol, while *S. aureus* produced a 2.9 mm zone of inhibition for the 10% bleach solution and a 1.1 mm zone of inhibition for 95% ethanol. *M. luteus* was least susceptible, with the smallest zones of inhibition in all tested solutions except neem powder in distilled water. *S. aureus* was least affected by neem powder in distilled water.

Figure 1 shows a graphical representation of the mean zone of inhibition of all solutions. Figure 1 demonstrates the differences in the zones of inhibition between the experimental solutions, neem in distilled water, neem in 95% ethanol, and neem oil, and the control solutions, distilled water, 95% ethanol, and 10% bleach. The high variance is due to several outliers in the data, including a 2 mm zone of inhibition in 10% bleach for *S. aureus*, a 2 mm zone of inhibition in neem in distilled water for *E. coli*, a 1.5 mm zone of inhibition in 95% ethanol for *P. aeruginosa*, and a 1.5 mm zone of inhibition in neem powder in distilled water for *P. aeruginosa*. It is interesting to note that the zones of inhibitions measured for neem powder in 95% ethanol and neem oil have smaller standard deviations in comparison to the other solutions. It is also interesting to note that 95% ethanol and 10% bleach inhibited *P. aeruginosa* to similar levels.

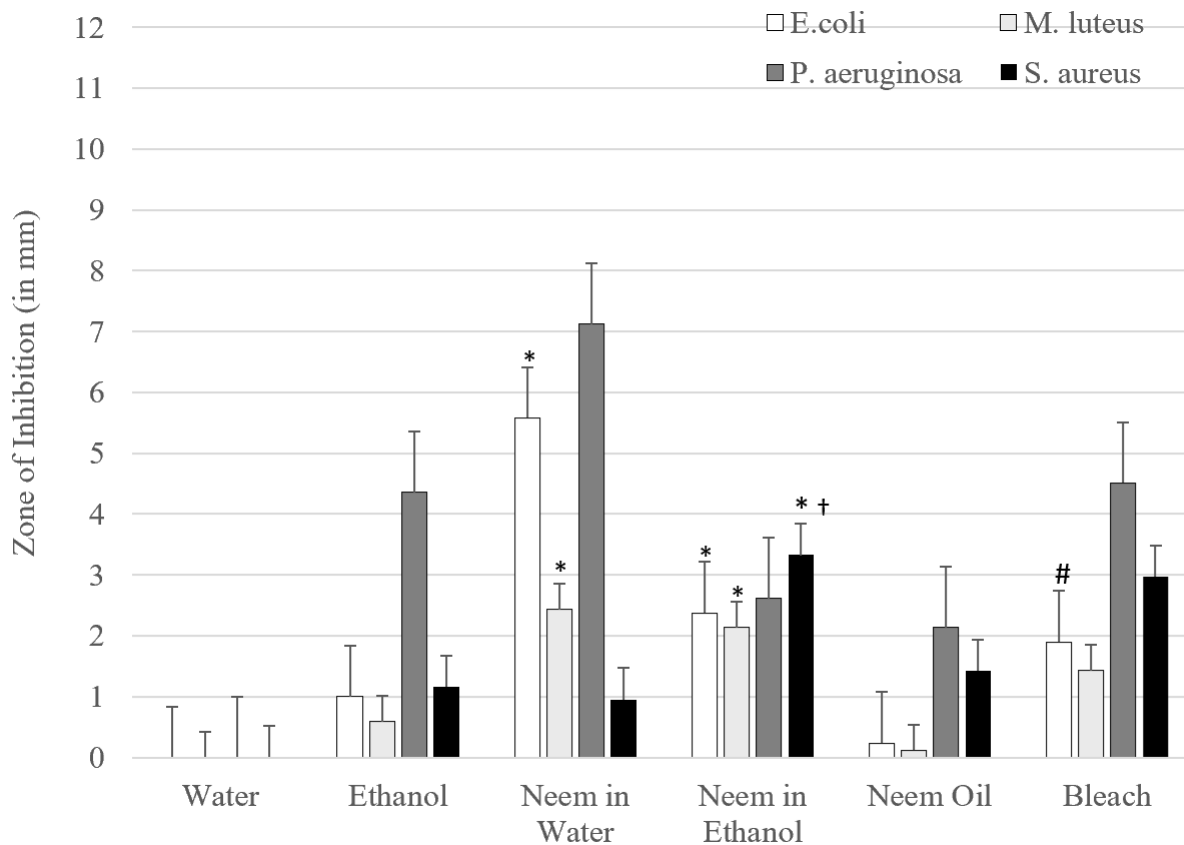


Figure 1. Inhibition of bacterial growth by Neem. Bars represent average radius for zone of inhibition for neem extracts, neem oil, and controls against select nosocomial organisms (n=8). * represents statistically significant differences ($p < 0.05$) between the zone of inhibition from the species highlighted compared to the zone of inhibition of the same species in 95% ethanol. † represents significant differences ($p < 0.05$) between the zone of inhibition from the species highlighted compared to the zone of inhibition of the same species in 10% bleach. #represents statistically significant differences ($p < 0.05$) that show that the highlighted control outperformed neem oil.

We visually observed via the opacity of solutions and reported the minimum inhibitory concentration (MIC) in **Table 1**. In general, neem powder in distilled water tended to have the most opacity and have the darkest, murkiest color for all test tubes because of the growth of the bacteria. This was determined based on visual comparison of the solutions before and after growth. *E. coli* and *M. luteus* were the least opaque of each test tube out of neem powder in distilled water and neem oil, respectively, while *P. aeruginosa* was the most opaque of each test tube overall.

Antimicrobial agents with low activity against an organism usually give a high MIC, while those that are highly effective give low MIC values. **Table 1** summarizes the MICs of neem powder in distilled water and neem oil for *E. coli*, *M. luteus*, *P. aeruginosa*, *S. aureus*, and *S. cerevisiae*. Data show that *E. coli* were the least susceptible bacteria. *S. aureus* and *S. cerevisiae* were the most susceptible, and neem oil produced the lowest MIC.

MIC values for *P. aeruginosa*, *S. aureus*, and *S. cerevisiae* were 0.1 g/mL for neem extract in water. *M. luteus* had a higher MIC of 0.6 g/mL, while no MIC was determined for *E. coli* due to limited resources. Neem oil produced similar MIC values for *M. luteus*, *S. aureus*, and *S. cerevisiae*, all at 0.1 g/

mL. Neem oil also produced MICs of 0.4 g/mL for *E. coli* and *P. aeruginosa*.

DISCUSSION

Our experiments indicate that neem powder in distilled water, neem powder in 95% ethanol, and neem oil were effective in killing *S. aureus*, *E. coli*, *P. aeruginosa*, and *M. luteus*. We also concluded that neem powder in distilled water was more effective in inhibiting the microorganisms listed above than 95% ethanol, distilled water, 10% bleach, and neem oil. Lastly, we concluded from the minimum inhibitory concentration experiment that neem oil produced a lower inhibitory concentration compared to neem powder in distilled water. Collectively, these conclusions support the hypothesis that various neem extracts, when applied to the common nosocomial organisms *E. coli*, *S. aureus*, *P. aeruginosa*, *S. cerevisiae*, and *M. luteus*, would inhibit the growth of these microorganisms.

We speculate that neem powder in distilled water showed higher inhibitory activity because the antibacterial and antifungal components were readily soluble in the aqueous solution. In addition, the solution could diffuse easily through the solid agar plate to produce the larger zones of inhibition.

Microorganism	MIC of neem powder in distilled water (n=4)	MIC of neem oil (n=4)
<i>E. coli</i>	Exceeded 0.6 g/mL	0.4 g/mL
<i>M. luteus</i>	0.6 g/mL	0.1 g/mL
<i>P. aeruginosa</i>	0.1 g/mL	0.4 g/mL
<i>S. aureus</i>	0.1 g/mL	0.1 g/mL
<i>S. cerevisiae</i>	0.1 g/mL	0.1 g/mL

Table 1. Minimum Inhibitory Concentrations (MICs) of neem powder in distilled water and neem oil against select nosocomial organisms.

On the other hand, neem oil, being highly lipophilic, had limited diffusivity in solid agar plates and hence produced relatively smaller zones of inhibition. This finding also explains neem oil's effectiveness in the minimum inhibitory concentration experiments, where neem oil was mixed well in liquid nutrient broth. This helped produce comparable MICs to those of neem powder in distilled water.

Because of limited resources, MIC for *E. coli* in neem powder in distilled water was not determined was due to limited resources, as higher concentrations could not be tested. Other limitations of this experiment include contamination of *S. cerevisiae* during the agar-well diffusion experiment, not having enough test tubes and nutrient broth to measure the minimum inhibitory concentration for *E. coli*, inability to accurately measure zone of inhibition due to the streaking method, and inability to accurately measure turbidity for minimum inhibitory concentration. These problems, if addressed, could statistically change the outcome of the experiment. Because the *S. cerevisiae* culture had experienced contamination, the results were erroneous and have not been reported. The addition of this data would have strengthened the support for the conclusions. Lack of a sufficient number of test tubes and nutrient broth to test higher concentrations of *E. coli* in the minimum inhibitory concentration experiment did not allow for the obtaining of the exact MIC value and of the data to support the hypothesis for this organism. Accuracy in the measurements of streaking of zone of inhibition and the turbidity for minimum inhibitory concentration are crucial to substantiate the findings and reinforce the conclusions. The streaking method is slightly weaker in comparison to the pouring technique because microorganisms do not grow uniformly and do not distribute in the plate evenly. Visual assessment of turbidity is a subjective method in comparison to an objective method of measuring turbidity using techniques such as spectroscopy. These problems can be fixed by creating more sterile conditions to stop contamination, using more test tubes to measure the minimum inhibitory concentration, using a pouring technique for the zone of inhibition for uniform distribution of the microorganisms, and using spectroscopy to determine the

minimum inhibitory concentration. Specifically, more sterile conditions could be achieved by cleaning the workplace before working, sterilizing the inoculating loop and straws for longer periods of time, and working closer to a lit Bunsen burner.

The nosocomial bacteria and fungi are known to survive and remain infectious under varieties of environmental conditions, including pH and temperature fluctuations (4, 5, 6, 7, 8). Hence, future experiments should include evaluating the effect of temperature on neem extract activity against the microorganisms, the effect of pH on neem extract activity, the inclusion of other nosocomial organisms that would be extracted from hospitals, and the addition of an antibiotic as a positive control in the experiment. By studying more variables in the experiment, such as temperature and pH, the best use of neem extract to inhibit certain nosocomial organisms will be narrowed down and scientific knowledge about the therapeutic benefits of neem will be enhanced. By using more species of bacteria and fungi, effectiveness of neem can be studied more accurately, and the data can be used to determine better treatment options, specifically for hospital-like conditions. Also, adding a commonly-used antibiotic by hospitals that kill nosocomial organisms to the experiment would allow for better comparison of results against neem and the antibiotic.

MATERIALS AND METHODS

All experimental work was performed in a biosafety level 2 microbiology laboratory at Kennesaw State University. Neem oil and neem powder, manufactured respectively by Mary Tylor Naturals LLC and Metiista LLC, were purchased and stored in plastic bags in shade to prevent contamination and degradation. The following reagents were prepared: 1) A 10% solution of neem in distilled water was made with 10 grams of neem powder dissolved in 100 mL of distilled water, and, 2) A 10% solution of neem in 95% ethanol was made with 10 grams of neem powder dissolved in 100 mL of 95% ethanol. Distilled water was used as a negative control, expected to have no effect on organisms, and a 10% bleach solution and 95% ethanol served as positive controls, expected to inhibit growth of microorganisms.

The following pathogen strains obtained from the American Type Culture Collection and were used in this study: *Saccharomyces cerevisiae* (S288C), *Micrococcus luteus* (NCTC2665), *Staphylococcus aureus* (MRSA), *Escherichia coli* K12, and *Pseudomonas aeruginosa* (PA01). Samples were refrigerated at 4 degrees Celsius. Under sterile conditions, one colony of each microorganism was scooped using a loop and inoculated into 40 mL of nutrient broth (Standard I Nutrient Broth obtained from HiMedia Labs) (13). Eight inoculations were done for each microorganism, from which sterile inoculation loops were used to transfer small amounts of the cultures into test tubes containing nutrient broth for each microorganism. The microorganisms were taken from the parental microorganism strain's petri plate.

Similarly, petri plates were prepared and streaked to create a lawn with uniform growth (14). The test tubes placed in an orbital shaker and petri plates were incubated for 24 hours at 37°C.

To analyze antibacterial activity, an agar well diffusion method was followed. After incubation and growth of the microorganisms, 6 holes (4 mm in diameter) were punched aseptically on each petri plate using a sterile plastic straw. On each plate, 100 µL of each test material or control was pipetted into a well, which was labeled with different colored tape on the bottom of the plate for identification. The petri plates were left on a flat bench to dry for one hour and were then incubated for 18 hours at 37°C. Thereafter, the petri plates were analyzed for the radius of the zone of inhibition around each well of each solution using a ruler. There were 8 replicates for each strain.

To calculate the minimum inhibitory concentration (MIC), 1, 2, 4, and 6 mL of 10% neem powder in water and neem oil were pipetted into a test tube for each microorganism. The test tubes were then incubated at 37°C and inserted back into the orbital shaker for another 18 hours. The test tubes were analyzed for MIC by observing for absence of visible microbial growth against natural light and noting that concentration of the solution. The MIC for each set of 4 test tubes for each microorganism was recorded in a data table.

Statistical analyses were performed using Microsoft Excel version 16.16.7. For antimicrobial effectiveness, the mean and standard error of 8 data points for each organism was calculated and the zone of inhibition data were analyzed using the Student's t-test, defining statistical significance at a *p*-value of < 0.05. All comparisons were made against 10% bleach and 95% ethanol, the positive controls. Statistical analysis (*p* ≤ 0.05) was performed to show differences between the sizes of the zone of inhibition in positive control - 95% ethanol and neem powder in distilled water, neem powder in 95% ethanol, and neem oil, which are indicated with an * in **Figure 1**. In addition, the same analysis was also conducted between positive control - 10% bleach and neem powder in distilled water, neem powder in 95% ethanol, and neem oil, which are indicated with a † in **Figure 1**. # indicates that the control outperformed neem oil. Apart from the significant data listed in the **Table 1**, all other comparisons showed no differences in statistical significance.

Received: January 3rd, 2018

Accepted: August 7, 2019

Published: January 27, 2020

REFERENCES

1. Ogbuwu, I.P., *et al.* "The Growing Importance of Neem (*Azadirachta Indica* A. Juss) in Agriculture, Industry, Medicine and Environment: A Review." *Research Journal of Medicinal Plant*, vol. 5, no. 3, 2011, pp. 230–245., doi:10.3923/rjmp.2011.230.245.
2. Mondali, N.K., *et al.* "Antifungal Activities and Chemical Characterization of Neem Leaf Extracts on the Growth of Some Selected Fungal Species in Vitro Culture Medium." *Journal of Applied Sciences and Environmental Management*, vol. 13, no. 1, Mar. 2009, pp. 49–53.
3. Stubblefield, H. "Hospital-Acquired Infection: Definition and Patient Education." Healthline, Healthline Media, 6 June 2017, www.healthline.com/health/hospital-acquired-nosocomial-infections.
4. "E. coli General Information." *Centers for Disease Control and Prevention*, Centers for Disease Control and Prevention, 1 Dec. 2014, www.cdc.gov/ecoli/general/index.html.
5. "Staphylococcus aureus in Healthcare Settings." Centers for Disease Control and Prevention, Centers for Disease Control and Prevention, 17 Jan. 2011, www.cdc.gov/hai/organisms/staph.html.
6. "Pseudomonas aeruginosa in Healthcare Settings." Centers for Disease Control and Prevention, Centers for Disease Control and Prevention, 13 Nov. 2019, www.cdc.gov/hai/organisms/pseudomonas.html.
7. Smith, D. L. "Brewer's Yeast as a Cause of Infection." *Clinical Infectious Diseases*, vol. 22, no. 1, 1996, pp. 201–201., doi:10.1093/clinids/22.1.201.
8. Seifert, H., *et al.* "Micrococcus luteus Endocarditis: Case Report and Review of the Literature." *Zentralblatt Für Bakteriologie*, vol. 282, no. 4, 1995, pp. 431–435., doi:10.1016/s0934-8840(11)80715-2.
9. "Chemistry of Neem." *Neem Foundation*, 7 July 2017, www.neemfoundation.org/about-neem/chemistry-of-neem/.
10. Sharma, P., *et al.* "Review of Neem: Thousand problems and one solution." *International Research Journal of Pharmacy*, vol. 2, no. 12, 2011, pp. 97-102.
11. Sultana, S., *et al.* "Antibacterial effect of Aqueous Neem (*Azadirachta indica*) leaf extract, crude neem leaf paste, and Ceftriaxone against *Staphylococcus aureus*, *Escherichia coli* and *Pseudomonas aeruginosa*." *Malaysian Journal of Medical and Biological Journal*, vol. 2, no. 2, 2015, pp. 89-100., doi:10.18034/mjmb.
12. Mahmoud, D. A., *et al.* "Antifungal Activity of Different Neem Leaf Extracts and the Niminol Against Some Important Human Pathogens." *Brazilian Journal of Microbiology*, vol. 42, no. 3, 2011, pp. 1007-1016., doi: 10.1590/S1517-838220110003000021
13. HiMedia Laboratories. (2015). *Standard Nutrient Broth No. 1: Technical Data*. Mumbai, India: HiMedia Laboratories.
14. "Kirby Bauer Antibiotic Method." Student Health Center Manuals, shs-manual.ucsc.edu/policy/kirby-bauer-antibiotic-sensitivity.

Copyright: © 2019 Shah, Ereddia, Shah and Reese. All JEI articles are distributed under the attribution non-commercial, no derivative license (<http://creativecommons.org/licenses/by-nc-nd/3.0/>). This means that anyone is free to share, copy and distribute an unaltered article for non-commercial purposes provided the original author and source is credited.

Threshold frequency of a bubble is positively correlated to the density of the surrounding fluid

Alexander Han¹, Eric Samson¹.

¹ Korea International School, Jeju Campus, Republic of Korea

SUMMARY

When a fluid is oscillated vertically, under certain parameters, bubbles may move downwards instead of rising. Prior publications defined the threshold frequency as the frequency at which bubbles oscillate in a stationary state. Beyond the threshold frequency, however, bubbles move downwards. This paper investigated the hypothesis that the threshold frequency will increase as the density of the oscillating fluid increases. The parameters in this study were restricted to the frequency of the oscillating fluid and the density of the liquid. As the fluid density increased, the threshold frequency was measured to be higher. Our data analysis concluded that the threshold frequency is positively correlated to the density of the surrounding fluid.

INTRODUCTION

Bubble dynamics have a wide range of potential applications from aerospace to medicine. Although their motions are generally predictable, abnormal effects often occur under vertical oscillations, such as those commonly found in transportation mechanics including fuel tanks of rockets. At frequencies higher than the threshold oscillation frequency, bubbles will sink towards the bottom of the container (1). These sinking bubbles may interfere with the mechanics and likely impose problems (2). To address this issue, we conducted a thorough analysis to determine the existence of a threshold frequency that is integral in deciding the motion of the bubble. We conducted this experiment to test our hypothesis that the increase in fluid density would also increase the threshold frequency of the bubble as the buoyancy force and added mass of the surrounding fluid would decrease (Figure 1). The results also indicated that the position of the bubble was a major factor influencing the dynamics of the bubble.

In this analysis, the bubble volume pulsations caused by Laplace pressure are taken into account. The Laplace pressure and the volume pulsations are dependent on the external and internal pressure of the bubble, which are caused by fluid oscillations (3). Since these bubble pulsations are considered to be isothermal, the following condition is applied:

$$P_t V_b = P_o V_o \quad (\text{Equation 1}),$$

$$P_t = P_o + \rho x (g + A\omega^2 \sin \omega t) \quad (\text{Equation 2}),$$

P_o : external pressure (1.013×10^5 Pa), V_o : volume of bubble near surface, V_b : current volume of bubble, P_t : current fluid pressure exerted on bubble, g : gravitational acceleration constant

The following equation can be written as:

$$V_b = \frac{V_o}{1 + \frac{\rho x}{P_o} (g + A\omega^2 \sin \omega t)} \quad (\text{Equation 3}),$$

This indicates to the notion that the volume of the bubble is dependent on its depth, and oscillation.

During the course of a motion through a fluid, an object experiences a force exerted opposite to its relative movement. This is known as drag force and is given as follows (4):

$$F(\dot{x}) = 4\rho R^2 \Psi(Re) \dot{x}^2 \quad (\text{Equation 4}),$$

R : radius of the bubble, $\Psi(Re)$: coefficient of resistance.

Archimedes' Principle states that the upward force on the submerged bubble is identical to the weight of the fluid displaced by the same bubble. This is attributed to the pressure difference in the upper and lower portion of the object. The bottom end will experience higher pressure and will accelerate the object upwards. This phenomenon is expressed as follows:

$$F_B = -\rho V_b g \quad (\text{Equation 5}),$$

ρ : density of fluid, V_b : bubble volume.

When an object moves through the liquid, it uses energy to not only move its own mass but its surrounding fluid as well. This additional work done by the object can be interpreted as added mass. The volume of the added mass can be derived as (5):

$$I = \frac{2}{3} \pi R^3 \quad (\text{Equation 6}),$$

I : volume of added mass, R : radius of the bubble

Calculate mass with ρ , the density of the liquid:

$$m_{add} = \frac{2}{3} \pi \rho R^3 \quad (\text{Equation 7}),$$

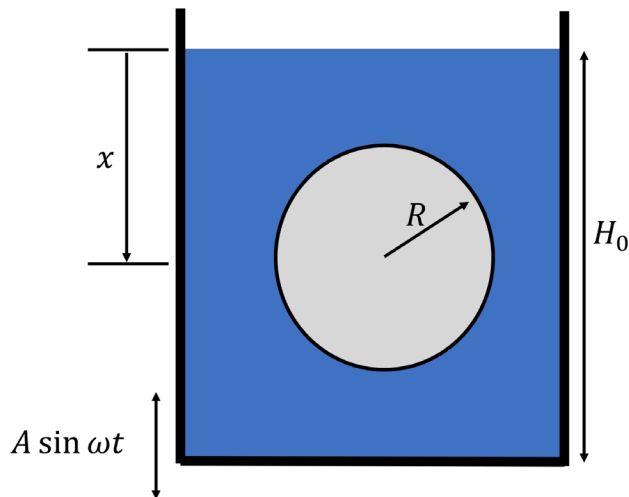


Figure 1. Electron microscopy images of different separators.

Equation [6] indicates that the mass of the added liquid is half of the displaced liquid. There are additional variations of attached mass that consider distinct conditions including when bubbles are positioned near plane wall or free surface. These other variations, however, can be ignored in our experimental model as the ratio between the depth of bubble x and radius of bubble R exceeds the value of 8 (6). The $F=ma$ form of Newton's Second Law would not be appropriate for this situation as the mass is not constant. Since the added mass changes with the bubble size, a different variation of Newton's Second Law must be employed, in which attached mass variations are taken into account (7).

$$F = (m + m_{add})\ddot{x} + \dot{m}_{add}\dot{x} \quad (\text{Equation 8}),$$

Considering all the forces, the following is achieved:

$$(m + m_{add})\ddot{x} + \dot{m}_{add}\dot{x} = -F(\dot{x}) - (\rho V_b - m)(g + A\omega^2 \sin \omega t) \quad (\text{Equation 9}).$$

In summary, equation [9] demonstrates that the "sinking bubble" phenomenon occurs when the added mass-induced forces exceed the buoyancy and drag forces.

RESULTS

In order to determine the threshold frequencies for the three fluids, their motions were first recorded on a 240 fps high definition camera and later computed into graphical representations in video analysis. The motions of 5 bubbles were followed for each frequency. To achieve greater accuracy, we controlled the bubble radius and initial depth of the bubble.

The threshold frequency ω_0 in 99% ethanol (C_2H_5OH) is

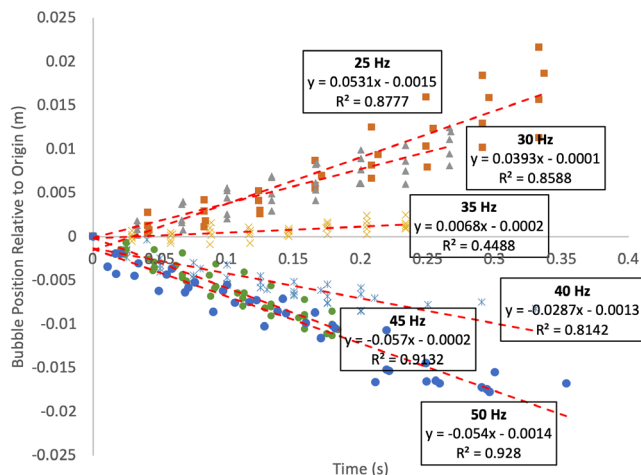


Figure 2. 99% C₂H₅OH Bubble Position vs Time from 25 Hz to 35 Hz at an interval of 5 Hz.

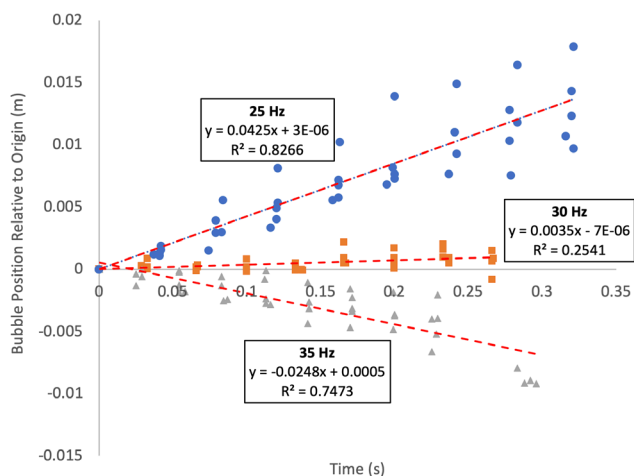


Figure 3. H₂O Bubble Position vs Time from 25 Hz to 35 Hz at an interval of 5 Hz.

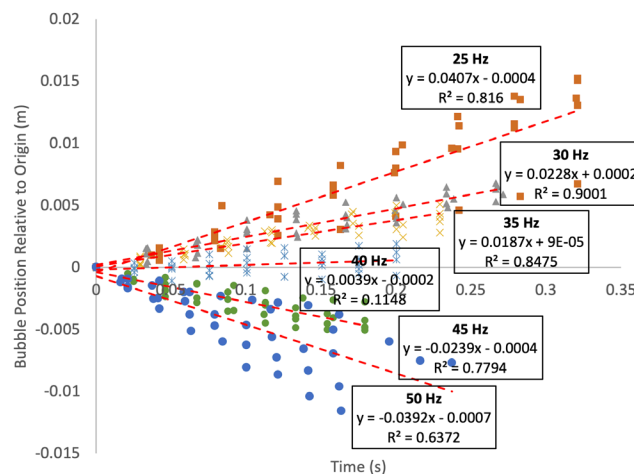


Figure 4. 50% C₃H₈O₃ Bubble Position vs Time from 25 Hz to 50 Hz at an interval of 5 Hz.

35 Hz was also observed at 40 Hz, 45 Hz, 50 Hz, 55 Hz, and 60 Hz. The only minor difference is the angle of the negative slope, which becomes increasingly negative as the frequency of the oscillation increases from 35 to 60 Hz (Figure 2).

In water (H₂O), the threshold frequency ω_0 is 35 Hz (Figure 3). The velocity of the “sinking bubble” was observed to be correlated to the frequency of the oscillation. Parallel to our findings in ethanol, as the oscillating frequency increases from 35 Hz to 50 Hz, the slope becomes increasingly negative. Moreover, there is a larger slope differential from 30 Hz to 35 Hz and 35 Hz to 40 Hz compared to other frequencies.

The threshold frequency ω_0 is 40 Hz in a solution of 50% glycerol (C₃H₈O₃) and 50% water (H₂O) (Figure 4). As the frequency increased beyond 50 Hz, the separation between the two liquids (C₂H₅OH and H₂O) became more prominent. This can be attributed to the distinct density and mass of the two liquids. Furthermore, in frequencies higher than 50 Hz, the small dimensions of bubbles prohibited an accurate analysis of their motions.

DISCUSSION

The threshold frequencies determined in this study are not exact values, but rather experimentally calculated values (Table 1). The threshold frequency was defined as the frequency at which fewer than five bubbles displayed non-stationary motion. Nevertheless, the data indicates that the threshold frequency is correlated with the density of the fluid. As the density of the fluid increased, the threshold frequency increased. The rationale behind this correlation between fluid density and threshold frequency can be attributed to the decreased added mass and buoyancy force.

Equation [4] highlights that the buoyancy force, the force responsible for the rising motion of the bubble, is dependent on the density of the fluid. It can be concluded that a decrease in fluid density will decrease the magnitude of buoyancy force and thus allow the sinking phenomenon to occur at a lower frequency. However, it is valid that Equation [2] suggests otherwise. Equation [2] emphasizes that the density of the fluid influences the volume of the bubble. Considering all other variables are kept constant and only the density of the fluid is increased, the bubble is likely to undergo more distinct changes. In short, increase in fluid density will further decrease the volume of the bubble and decrease the magnitude of buoyancy force. Equation [2] and [4] suggest two contrasting relationships between fluid density and buoyancy force. However, when the values themselves are taken into account, it is evident that the value for fluid density is far larger than the bubble volume. To conclude, decrease in fluid density decreases the magnitude of buoyancy force.

The added mass of the surrounding fluid is dependent on fluid density, as indicated by Equation [6]. The equation ascertains that decrease in fluid density will result in decreased added mass. As the added mass is an integral factor in determining the motion of the bubble, we can indicate that the decrease in added mass will increase the impact of

Fluid Type	Fluid Density	Threshold Frequency ω_0
99% C ₂ H ₅ OH	789 kg/m ³	30Hz
H ₂ O	997 kg/m ³	35Hz
50% C ₃ H ₈ O ₃	1139 kg/m ³	40Hz

Table 1. Threshold Frequencies of Three Fluids with Varying Density

oscillations. The fundamental equation ($F=ma$) indicates that when a constant force is applied the mass of the object will directly determine its acceleration. Applying this notion to the motion of the bubble, when the added mass decreases, the acceleration of the bubble will increase. Increased acceleration results in decreased threshold frequency as there is less force needed to be applied for the bubble to sink. In accordance with our hypothesis, the data indicated that a decrease in fluid density lowers the threshold frequency, as it decreases added mass and increases the acceleration of the bubble.

Human error was minimized through our experimental design which considered a minimum of five trials for each frequency. It is true, however, that parameters including fluid density, driving frequency, fluid properties, and bubble size have a significant role in achieving the “sinking bubble” phenomenon. With this in consideration, this experiment explored the correlation between density and driving frequency alone by reducing the significance of other variables. The bubble radius was controlled between certain boundaries to promote consistency in exerted forces and added mass. Moreover, we attempted to control fluid viscosity and other fluid properties of the C₃H₈O₃ solution through significant dilutions.

MATERIALS AND METHODS

The following experimental setup was used to generate bubbles at controlled oscillation frequencies for all tests (Figure 5). A 50 ml cylindrical container containing 45 ml fluid (either 99% C₂H₅OH, H₂O, or 50% C₃H₈O₃) was placed on the center of the cone of a 30 watt subwoofer run by a DC regulated power supply (Protek PL-3003S). A balance was used to ensure that the container was positioned consistently. A 240 fps camera recorded the data, and a tripod was utilized to ensure that the video footage was not susceptible to any oscillations.

The experimental amplitude was fixed at 0.005 m by an amplifier (Sound Stream U.S.A Handover Hi-Fi Stereo 2 CHANNEL SS-100). The oscillating frequency was varied by a computer application (Tone Generator) at an interval of 5 Hz, ranging from 25 Hz to 50 Hz. For every interval, a 240 fps video was recorded. The durations of the videos were one minute from the start of the oscillation. The container was then replaced with another containing a different fluid. The amplitude was determined through video analysis (Logger Pro 3.15).

The variable H_0 was fixed to the origin point where the motion of the bubble was first recorded. The radius of the bubbles were consistently between 1 mm and 1.2 mm, as larger or smaller bubbles were excluded from the analysis.

This allowed the relevant parameters including buoyancy force, drag force, and added mass to be relatively constant.

Due to the limitations of the video and software, the motion of the bubble could not be continuously analyzed through the tracker application. Therefore, during the data analysis, the lowest point of each cycle was plotted. For instance, when the container oscillates once in 4 frames, the bubble was plotted every four frames when one oscillating period was completed. This allowed a conclusive observation of the general motion of the bubble. The depth of the bubble was restricted to the following parameter: $0.043 < x < 0.063$.

This depth range was large due to trial to trial variations. For each frequency, five bubbles were analyzed to ensure the accuracy of the general motion. Thus, a total of 90 bubbles were analyzed (6 frequencies each for 3 fluids).

Although bubble dynamics are generally predictable, we identified that abnormal motions occur in certain conditions of oscillation. The threshold frequency marks the lowest frequency at which this anomaly can be observed. We further established that a correlation exists between the threshold frequency and the fluid density. Our examination of such anomaly in bubble dynamics carries seminal significance as motions of bubbles have wide range of applications in fields such as aerospace and medicine.

Received: May 18, 2019

Accepted: January 17, 2020

Published: January 16, 2020

REFERENCES

1. Jameson, G.J. & Davidson, J.F.. (1966). The motion of a bubble in a vertically oscillating liquid: theory for an inviscid liquid, and experimental results. *Chemical Engineering Science*. 21. 29–34. 10.1016/0009-2509(66)80004-0.
2. F. T. Dodge and D. D. Kana. "Bubble behavior in liquids contained in vertically vibrated tanks." *Journal of Spacecraft and Rockets*, Vol. 3, No. 5 (1966), pp. 760-763.
3. Blekhman, I.I., *et al.* "Motion of Gas Bubbles and Rigid Particles in Vibrating Fluid-Filled Volumes." *Procedia IUTAM*, vol. 8, 2013, pp. 43–50, 10.1016/j.piutam.2013.04.007.
4. Wymer, J., *et al.* "Sinking Bubbles in an Oscillating Liquid." Math.Arizona.Edu.
5. Sorokin, V. S., *et al.* "Motion of a Gas Bubble in Fluid under Vibration." *Nonlinear Dynamics*, vol. 67, no. 1, 2011, pp. 147–158.
6. Web.mit.edu. Retrieved 3 February 2019, from http://web.mit.edu/2.016/www/handouts/Added_Mass_Derivation_050916.pdf
7. Zoueshtiagh, Farzam & Caps, H & Legendre, M & Vandewalle, Nicolas & Petitjeans, Philippe & Kurowski, Pascal. (2006). Air bubbles under vertical vibrations. *The European physical journal. E, Soft matter*. 20. 317-25. 10.1140/epje/i2005-10131-6.

Copyright: © 2020 Han and Samson. All JEI articles are distributed under the attribution non-commercial, no derivative license (<http://creativecommons.org/licenses/by-nc-nd/3.0/>). This means that anyone is free to share, copy and distribute an unaltered article for non-commercial purposes provided the original author and source is credited.

The Effects of Various Plastic Pollutants on the Growth of the Wisconsin Fast Plant

Nathan Sobotka, Karissa Baker

Saint Paul Academy and Summit School, St. Paul, MN
contact: kbaker@spa.edu

SUMMARY

Plastic pollutants are known to cause problems in ocean basins; however, the effects of plastic pollutants on terrestrial life are relatively unknown. We performed this experiment to determine the effects of various plastic pollutants on the growth of *Brassica rapa*. Five plastic treatment groups, including compostable, biodegradable, and recyclable plastics, and one control group were prepared. At the end of the experiment the number of germinations, flowers, biomass, height, soil macronutrients nitrogen, phosphorus, and pH were measured. In the first trial, the height of the mushroom plastic variants was significantly shorter than the height of the polystyrene variants. The plants in the mushroom plastic had significantly lower biomass in both trials than all of the other variants including the control, other than HDPE milk jugs. There was no significant difference for flowering, germination, nitrogen, or pH in the soil. However, there was a significantly large amount of phosphates in the soil of the NaturBag compost bags. The significant decreases in height and biomass of the plants grown in the mushroom plastic show that they are impeding the growth, likely by physically blocking access to space and therefore nutrients. The increase in the NaturBag bags phosphorus levels indicates that the NaturBag is breaking down and releasing a large amount of phosphorus.

INTRODUCTION

Since the 1950s, 8.3 billion metric tons of plastics have been mass-produced. Only 30% of those plastics are still currently in use, with nearly 80% of all plastics ending up in landfills or ocean basins at the end of their lifespan (1). Only 9% of plastics are recycled, with 8% only being recycled once, ending up in landfills after they are discarded for the second time (1). Once in landfills, plastics can release toxins into the environment (2). Single-use packaging is the biggest conventional use of plastics, and most are not recycled when discarded. Recently, efforts have been made to produce more biodegradable plastics that will break down into smaller plastic polymers known as microplastics, and compostable plastics, which can be fully broken down into base elements (2). Both biodegradable and compostable plastics are thought to be more environmentally friendly than recyclable plastics, with compostable plastics having the least environmental impact (2).

This experiment used five different types of plastics and

Brassica rapa as a model organism. *Brassica rapa*, known as the Wisconsin Fast Plant, was genetically engineered at the University of Wisconsin to have a rapid growth time of about 22 days, not including the time to produce seeds. They have been extensively researched and have ideal growing conditions that are well established (3). The plastics used in this study are some of the most common types of plastic, primarily plastics used for packaging (2). This includes recyclable polystyrene packing peanuts, high-density polyethylene (HDPE) milk jugs, biodegradable PET #1 water bottles, compostable NaturBag garbage bags, and EcoVation mushroom plastic packaging material. The recyclable plastics are known to last thousands of years before degrading, while biodegradable plastics may also last the same amount of time, however, they break down into much smaller polymers. Compostable plastics degrade in a range of weeks to months. These plastics, as well as a control group with no plastic, will be used to test the health of the Wisconsin Fast Plant in an environment containing these plastic variants. Additionally, a second control group with plants in ceramic pots will be used to grow the Wisconsin Fast Plants in an environment devoid of plastic, including the plastic seedling containers.

Marine-based plastic contamination has been studied due to the large plastic waste buildups in ocean basins (1). However, plastic buildups occur not only in oceans and lakes, but also throughout land ecosystems, and the effects of plastic on terrestrial plant and animal health are relatively unknown (1). Therefore, we designed this experiment as a starting point in researching the effects of plastic pollutants on terrestrial plant health. This research addresses the question, what is the effect of various plastic pollutants on the growth of the Wisconsin Fast Plant through multiple hypotheses. First, we hypothesize that if the plastic is recyclable then it will harm the plant health due to the toxins that can be released as the plastic breaks down in the soil (2). Second, we hypothesize that if the plastic is biodegradable, then there will be no effects on the plant health because no toxins or organic nutrients will be released, and microplastics will not be formed over the relatively short timeline of this experiment (1). Finally, we hypothesize that the compostable plastics will have a positive effect on plant health because of the helpful nutrients released, such as nitrogen (4, 5). This experiment aims to test this question and the hypotheses that accompany it, as well as determine what type of plastic is best, comparatively, for the plastics in terrestrial environments.

RESULTS

Given Immediate Plastic Exposure

In trial one, the seeds were planted in the soil at the same time as the plastics, and then grown for 22 days within controlled conditions. There were 36 plants per group. We recorded data for germination, the number of flowers, height, biomass, as well as nitrogen, phosphorus, and pH in the soil. We performed ANOVAs and t-tests to determine whether or not there were significant changes between treatment groups for germination, number of flowers, height, and biomass. We also recorded changes in nitrogen, phosphorus, and pH in the soil.

The mushroom plastic was well ahead of the rest of the plastics during its growth stages, ending up roughly 5-8 days ahead of the typical growth time (Figure 1). The mushroom plastic variants reached the stage of life where they were able to seed and drop all of their flowers, while all other treatment groups were still in the flowering stages of the life cycle.



Figure 1: Experimental setup. Left column is compost bags, the middle column is ice mountain water bottles, and the right column is mushroom plastic. Three days after planting, buds in the mushroom plastic are widely seen, with one or two sprinkled throughout the compost bags and ice mountain water bottles.

While we were not able to determine whether or not the number of flowers remaining on the plants was statistically significant, the amounts of flowers were proportional to the number of germinations, with the very slight exception of the mushroom plastic. This means that roughly the same number of flowers were being produced per plant, and the differences were insignificant. While the mushroom plastic did not have as many flowers on the plants compared to the peanuts, which had the same germination, this was to be expected, seeing as the plants had started to drop their flowers at the end of the growth period. Additionally, there was no significant difference in germination rate between any groups (Figure 2). Any differences in germination rates were due to chance, and were not attributed to the various treatments.

Germination Rates per Plastic Variant

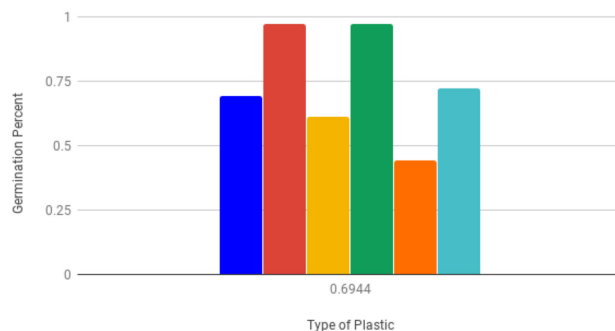


Figure 2: Germination rates per plastic variant. Germinations for each soil type were obtained using a chi-square test comparing germination rates to the control group ($p=0.9978$). This suggests the differences in germination between treatment groups were due to chance.

There were significant changes in both mean height and biomass in trial one. The heights across all treatment groups were not significant; however, the difference in height between the polystyrene packing peanuts and the mushroom plastic was statistically significant (Figure 3, t-test $p=0.0466$). All other combinations were insignificant. The mean plant height for the polystyrene condition was 5.8 cm, while the mean height for mushroom plastic was 4.9 cm. Although NaturBag compost bags had a mean height of 4.5 cm, these plants did not have enough germinations, resulting in a larger margin of error and no significant difference compared to any of the other plastics. The difference in mean biomass between mushroom plastic and every other treatment group, except for HDPE, was significant (Figure 4, ANOVA and individual t-tests). The mean biomass of the mushroom plastic was 0.057g. Additionally, HDPE had significantly less biomass than PET #1, with a mean biomass of 0.062g compared to 0.084g, respectively (Figure 4, t-test $p=0.0315$). The mushroom plastic had significantly less biomass compared to the control, which means that the mushroom plastic significantly harmed the biomass of the Wisconsin Fast Plant.

Effects of Plastic Variant on Plant Height

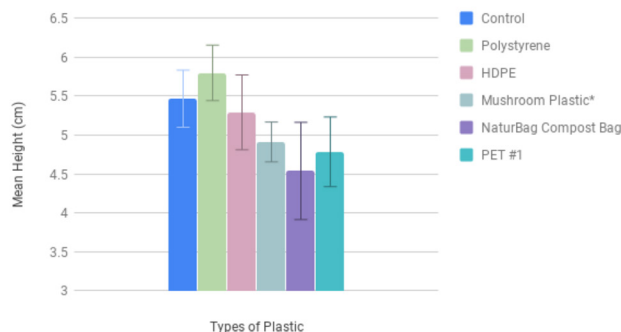


Figure 3: The average height depending on the plastic variants in the soil in trial one. The ANOVA is insignificant, $p=0.2211$, but the t-test between polystyrene and mushroom plastic shows mushroom plastic is significantly shorter $p=0.0466$. The error bars are the standard error of the mean height in trial 1 (ANOVA).

The changes in nitrogen or pH were not significant for any of the treatments (Table 1). However, for the phosphorus tests, all treatments, including the control, had 5ppm except for NaturBag, which had 25ppm. This significant change indicates that NaturBag compost bags are causing some significant difference in the soil phosphates.

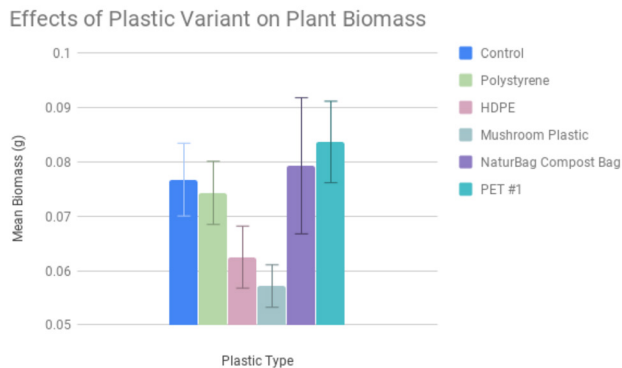


Figure 4: The average biomass depending on plastic variants in the soil in trial 1 (ANOVA $P=0.0315$). The following t-tests between mushroom plastic were significant for all other treatments other than HDPE ($P<0.05$). HDPE compared to PET#1 was also significant (t-test, $P=0.0315$). The error bars are the standard error of the mean biomass in trial 1.

	Nitrogen (ppm)	Phosphorus (ppm)	pH
Before	5ppm	5ppm	6.5
After	Control: 10ppm Polystyrene: 5ppm HDPE: 10ppm Mushroom: 5ppm NaturBag: 10ppm PET#1: 5ppm	Control: 5ppm Polystyrene: 5ppm HDPE: 5ppm Mushroom: 5ppm NaturBag: 25ppm PET#1: 5ppm	Control: 6 Polystyrene: 6 HDPE: 6 Mushroom: 6 NaturBag: 6 PET#1: 6

Table 1: The results of soil test kits in trial 1. Each trial was repeated once per box, or three times per plastic type. The most notable difference is a 25ppm phosphorus in the NaturBag soil, compared to 5ppm in all other soils.

Pre-Incubation of the Plastics

In trial two, we implanted the plastics in the soil 18 days ahead of the seeds with the assumption that they would degrade more and therefore have more noticeable effects on the plants. Once again, there were 36 plants per group. The changes in the number of flowers per plant, depending on the plastic in the soil, were insignificant for both the first second trial. The germination rates were not affected by the plastics in the soil for either trial one or two. Any variation in the germination rates was due to chance.

Once again, there were significant changes in the mean heights and biomass'. The heights across all plastics were decreased compared to the first trial (Figure 3, Figure 5). The mean heights were 1.26cm and 1.63cm for the polystyrene and mushroom plastics, respectively. They were both significantly shorter than all other plastics variants ($p<0.05$). The mean mass of the mushroom plastic was much lighter than other plastic groups, at 0.0126g (Figure 6, $p<0.05$). This trial corroborates the first trial in that the mushroom plastic impeded the growth and biomass of the Wisconsin Fast Plant.

We did not observe significant changes in nitrogen or pH for any of the treatments (Table 2). However, for the phosphorus tests, all treatments, including the control, had 12.5ppm except for NaturBag, which had 37.5-50ppm. This is a significant change, meaning NaturBag compost bags are causing some significant difference in the soil phosphate.

The biomass of Wisconsin Fast Plants was significantly decreased by the presence of mushroom plastic in the soil, and the phosphorus content in the soil was significantly increased in the presence of NaturBag compost bags.

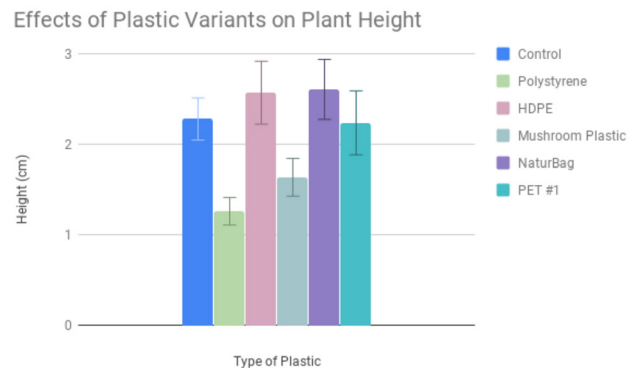


Figure 5: The average height depending on the plastic variants in the soil in trial 2. The heights between the various plastic groups were significant in trial two (ANOVA $p=0.00175$). The polystyrene packing peanuts and the mushroom plastic are both significantly shorter than all other plastics (t-tests $p<0.05$), but not each other. The error bars are the standard error of the mean height in trial 2.

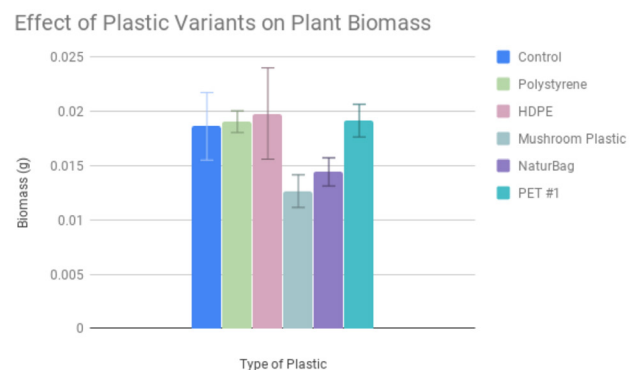


Figure 6: The average biomass depending on plastic variants in the soil in trial 2. The ANOVA of biomass in trial two between all of the groups was insignificant ($P=0.249$). However, t-tests between the mushroom plastic and all other groups other than HDPE showed significant differences ($p<0.05$). The error bars are the standard error of the mean biomass in trial 2.

DISCUSSION

The biomass of Wisconsin Fast Plants was significantly lower in the presence of mushroom plastic in the soil. The mushroom plastic is significantly lighter than all plastics and the control except the HDPE milk jugs (Figure 4, $p=0.0315$). These results were also corroborated in trial two, indicating that this trend was truly due to the plastics. One possible reason for this is that the loss of the flowers in only

the mushroom plastic group caused the loss of biomass. Additionally, the mushroom plastic plants also were shorter than the control and other groups. Another possible reason for the lack of biomass for the mushroom plastic group is that the mushroom plastic broke down, resulting in it taking up more volume. By increasing the volume of the plastic in the relatively small area, the mushroom plastic could have been impeding growth more than the benefits were helping the growth (6). By having something hard within the soil, the ability for the roots to grow and intake the required nutrients becomes more difficult (6). Additionally, the packing peanuts rose to the top of the soil when watered, therefore removing them from the soil and out of the path of the roots. A future experiment regarding these two plastics would be to grow them in much larger containers and compare the results between the different size containers.

	Nitrogen (ppm)	Phosphorus (ppm)	pH
Before	5ppm	5ppm	6.5
After	Control: 5ppm Polystyrene: 10ppm HDPE: 5ppm Mushroom: 5ppm NaturBag: 5ppm PET#1: 5ppm	Control: 12.5ppm Polystyrene: 12.5ppm HDPE: inconclusive. Test was too green to determine on the color chart, which included only ranges of blue. Mushroom: 12.5ppm NaturBag: 37.5-50ppm PET#1: 12.5ppm	Control: 6 Polystyrene: 6 HDPE: 6 Mushroom: 6 NaturBag: 6 PET#1: 6

Table 2: The results of soil test kits in trial 2. Each trial was repeated once per box, or three times per plastic type. The most notable difference is 37.5-50ppm phosphorus in the NaturBag soil, compared to 12.5ppm in all other soils.

The differences in flowering and germination were due to chance, rather than the plastics in the soil ($p=0.9978$ for trial one, $p>0.99$ for trial two). While the significance for the flowering was not able to be determined in trial one, the proportions of flowers to germinations were nearly the same (**Figures 2 & 3**). In trial two, there was no effect of the plastic on flowering ($p=0.278$). Given that the number of flowers is reduced by stress put on a plant, an equal proportion of flowers help to indicate the conditions are putting an equal amount of stress on each different treatment group (7). The largest change between the germination rate and flowers was the mushroom plastic. However, this change was seen to be farther in its life cycle. The plants have the capability to seed between 22 and 40 days, with most being around 30 days (3). This puts the mushroom plastic at about 5-8 days ahead of the typical growth expectancy, while the others were around the 21-22-day mark as expected. One possible reason for this is that if a plant is stressed it may attempt to flower and reproduce more quickly and focus energy on reproduction rather than growth. Again, growing the plants in larger containers may eliminate the space issues.

In trial one, an ANOVA showed that there was no significance in mean height across all of the six different treatment groups, however, a t-test showed a significant difference in height between polystyrene and mushroom plastic, with mean heights of 5.8 and 4.9 cm, respectively

($p=0.0466$). The difference between polystyrene and mushroom plastic is the only significant difference between all of the treatment groups, and it indicates that it is likely the difference between the heights was due to the plastic in the soil. However, in trial two, the results were drastically different ($p=0.00175$). The mushroom plastic was once again the smallest. However, the polystyrene was very short as well. Similar to the changes in biomass, it is possible this change was due to the mushroom plastic impeding the growth of the Wisconsin Fast Plant by getting in the way of the roots (6). However, because the polystyrene floated, there must be some other reason that the packing peanuts were harming the height of the plants in trial two. It is important to note that while the packing peanuts and the mushroom plastic may have been significantly different from each other in trial one, there were no significant changes in height compared to the control group, indicating that neither one deviated significantly from growth with no additional plastics. Additionally, the results from trial two are opposite of trial ones, and therefore another trial should be run to see which is more accurate.

There were no significant changes in the nitrogen or pH in the soils of all of the treatment groups for either trial one or two. A couple of possible reasons for this are that the plastics may not have had enough time to release any nutrients or H^+ ions into the soil, or that the changes were not detectable with the equipment used. Another possibility is that if there were significant changes in a nutrient such as nitrogen, it could have been absorbed by the Wisconsin Fast Plants, and therefore not be detectable in the soil. A possible future experiment would be to measure the nitrogen in the plants after they were uprooted. While there were no significant differences between nitrogen or pH, NaturBag compost bags had a phosphorus level of 25ppm, while every other treatment group had 5ppm in trial one. A possible reason for this is that the NaturBag is composed of more phosphorus than any other plastics, and releases it when it degrades. Natural polymers, which are what the NaturBag compost bag is composed of, are known for fast degradation and could possibly have released more phosphates in the course of the trial (8). The second trial had similar results on a larger scale. The NaturBag had levels of between 37.5-50ppm, while the others had phosphorus levels around 12.5ppm. These higher levels of phosphorus are approaching a point where they may be dangerous if they get into a water supply, because the phosphates may cause algal blooms (9). The next step in these sets of experiments will be to isolate the NaturBags and test the water runoff under similar conditions as the previous trials. This will determine whether or not the degradation of the NaturBag has risk of being harmful to the environment even though it is a compostable plastic.

The differences in plastics in the soil of the Wisconsin Fast Plant resulted in many significant changes of mean biomass, with mushroom plastic and HDPE being significantly lighter than most of the other plants in both trials. The changes in the number of flowers and the germination rates were due to

chance. There was one significant change in mean height, which was between mushroom plastic and polystyrene, however, these changes were not significant compared to the control group and because of the differences in the two trials, it is unclear whether or not the polystyrene is affecting the height of the plants. Finally, the soil macronutrients saw a significant rise in phosphorus for the NaturBag compost bags, indicating something about the bags causes increased phosphorus in the soil. Future experiments could be attempting the same experiment in a larger growing container, to lower the likelihood of the plastics impeding growing space. While the plastics overall seemed to have very few negative impacts on growth, this does not imply that they do not have negative impacts on the health of the plants, with the color of leaves possibly indicating a less healthy plant. Additionally, there may be problems later in life that were not addressed. A possible future experiment to test the long term effects would be to carry the tests through multiple generations. Additionally, it would be important to test these effects with even smaller plastics, such as microplastics. Another important note is that while the plastics were not stuck in the soil, many of them did float when watered. In a real-world situation, this would mean the plastics would be carried into water supplies, and eventually out to oceans, where their negative impacts have been well documented and explored.

A third trial has been started which is focusing on the phosphorus from the NaturBag, and the possible effects that come through water runoff. It will use a spectrophotometer to more accurately measure the phosphorus content.

Between trials one and two, the significant changes in mean biomass and the amount of phosphorus in the soil showed the same trends, despite the incubation period. The mean biomass of the mushroom plastic was less than the others, indicating that something about the compostable mushroom plastic caused a decrease in growth. Similarly, the NaturBag released substantially more phosphorus in both trials, although the impacts of that phosphorus on the plants' growth were not noticeable.

MATERIALS AND METHODS

Standard Growth Conditions

The growing conditions for this experiment were closely controlled through the use of a Conviron growth chamber, which controls temperature, humidity, and light levels in an enclosed environment. Wisconsin Fast Plants were grown in 1" by 1" by 2.25" plastic planting containers, as well as a control group in a similar-sized ceramic pot. These pots were filled with 26.5 to 28.5 grams of untreated topsoil. The plants were watered three times a week, typically Monday, Wednesday, and Friday, with 10 mL of tap water per container. There were two Wisconsin Fast Plant seeds per container, which were planted about 1 cm under the soil. The plants were grown for 22 days in a Conviron growth chamber, which maintained a constant temperature of 22°C and a constant 24-hour light on the brightest available setting. The Conviron chamber

was also supposed to keep the relative humidity constant, however, the sensor did not work and the chamber was kept at around 35--55% humidity. These growing conditions were recommended by the University of Wisconsin (3).

Growth Conditions with Plastics

To test the effects of various plastic pollutants, the varying types of plastics were placed in the growing containers. There were 6 groups with 18 growing containers each or 36 seeds per group. The first group was a control group with no additional plastic. The second and third groups were the recyclable plastics: polystyrene packing peanuts and HDPE milk jugs. The fourth group was a semi-biodegradable plastic: the PET #1 Ice Mountain water bottles. The fifth and sixth groups were the compostable plastics: the mushroom plastic and the NaturBag compost bags. One additional group with the same amount of seeds was grown with no plastics in small clay pots. All plastics were cut into two 1 cm by 1 cm squares, with as close to 1 cm of depth as possible. The plastics were inserted about the same depth as the seed to maximize contact with the seed; however, many of the plastics came loose and rose to the top of the soil during watering. For the second trial, the soil and plastics were mixed and then kept damp, with the same conditions as the Conviron chamber, for 18 days. The seeds were then planted, and the trial was completed as before.

Metrics for Growth

The Wisconsin Fast Plants growth was measured by counting the flowers and germination rates, measuring the biomass at the end of the 22-day trial, measuring the final height, and measuring the soil nutrients before and after the trial. To measure the final height, the plants were measured on the twenty-second day from the base of the soil to the top of the tallest shoot in centimeters. To measure the biomass, the plants were uprooted, the soil was washed off; they were dried, and then massed in grams. To take measurements of the soil nutrients, nitrogen, and phosphorus, as well as the pH, LaMotte soil macronutrient test kits were used following the manufacturer's instructions. These tests were taken once from the soil before the test and then once per box, totaling three times from each plastic, from the soil after the test.

Statistical Analysis

To determine if there were statistically significant differences in biomass, plant height, flowering, germination, and soil macronutrient levels, ANOVAs, t-tests, and Chi-squares were run using Google sheets. Chi-squares were run using the actual number of germinations compared to the control group, but are represented in Figure 2 as percentages. Changes were considered significant at $p < 0.05$.

REFERENCES

Special thanks to Dr. Julie Grossman, an associate professor at the University of Minnesota. She specializes in organic

agriculture and soil nutrient cycling, and her advice has been invaluable over the course of my experiment. She was the one who suggested the idea behind my second trial, pre-incubating the plastics to allow the soil microbes to start degrading the plastics.

A link to her faculty page on the University's website: <https://horticulture.umn.edu/people/faculty/juliegrossman>

Received: September 18, 2018

Accepted: January 9, 2020

Published: January 28, 2020

REFERENCES

1. Geyer, Roland, et al. "Production, Use, and Fate of All Plastics Ever Made." *Science Advances*, vol. 3, no. 7, 2017, doi:10.1126/sciadv.1700782.
2. Song, J. H., et al. "Biodegradable and Compostable Alternatives to Conventional Plastics." *The Royal Society*, vol. 364, no. 1526, 2009. EBSCOhost, doi:10.1098/rstb.2008.0289.
3. "Wisconsin Fast Plants." University of Wisconsin, fastplants.org/.
4. Goldstein, Jerome. "Compost Research and Organic Agriculture." *Compost Science and Utilization*, vol. 11, no. 3, 2003, p. 187. EBSCOhost, doi:10.1080/1065657X.2003.10702125
5. Bayer, Eden. "Are Mushrooms the New Plastic." *TED conference*, July 2010. Speech.
6. Passioura, JB. "Soil Structure and Plant Growth." *Australian Journal of Soil Research*, 1991. EBSCOhost, vol. 29, no. 6, 1991, doi:10.1071/SR9910717.
7. Gellesch, Ellen, et al. "Grassland Experiments under Climatic Extremes: Reproductive Fitness versus Biomass." *Environmental & Experimental Botany*, vol. 144, 2017, pp. 68-75. EBSCOhost, doi:10.1016/j.envexpbot.2017.10.007.201
8. Itävaara, Merja, et al. "Biodegradation of Polylactide in Aerobic and Anaerobic Thermophilic Conditions." *Chemosphere*, vol. 46, no. 6, 2002, p. 879. EBSCOhost. doi: 10.1016/S0045-6535(01)00163-1
9. "Phosphorus and Excess Algal Growth." *Canada.ca*, 8 June 2017, www.ec.gc.ca/grandslacs-greatlakes/default.asp?lang=en&n=6201fd24-1.

Copyright: © 2020 Sobatka and Baker. All JEI articles are distributed under the attribution non-commercial, no derivative license (<http://creativecommons.org/licenses/by-nc-nd/3.0/>). This means that anyone is free to share, copy and distribute an unaltered article for non-commercial purposes provided the original author and source is credited.

Effects of Wi-Fi EMF on *Drosophila melanogaster*

Mary Anand and Herm Anand

Anand Homeschool, Pittsburgh, PA

SUMMARY

Wi-Fi is commonplace in developed countries, and the number of people exposed to it is increasing. The health effects of Wi-Fi electromagnetic fields (EMF) are not well-documented. This research study engineered an apparatus, a “Box Setup,” to expose fruit flies, *Drosophila melanogaster*, to three concentrations of Wi-Fi EMF and a control. Wi-Fi EMF exposure produced a statistically significant decrease in the number of total progeny adults, and number of pupae. There was no significant effect on the progeny male:female ratio, nor the adult:pupa ratio. Only the highest Wi-Fi EMF concentration (100%) decreased the number of progeny adults, number of progeny females, and number of pupae; whereas even a low EMF concentration (5%) decreased the number of progeny males. This suggests that male *D. melanogaster* are more sensitive to Wi-Fi EMF than female *D. melanogaster*. Further research is needed to identify what aspects of fruit fly biology are affected by Wi-Fi EMF exposure, and why males are more sensitive than females.

INTRODUCTION

Electromagnetic fields (EMF) consist of electric and magnetic waves that feed off each other and produce each other, producing a forward propagation of waves (2). The EMF produced by Wi-Fi routers is non-ionizing, *i.e.* it does not carry enough energy to remove electrons from atoms (1, 3, 4, 5). Wi-Fi is used to connect computers, smartphones, and other devices to the Internet or each other. In developed countries, many households and businesses use Wi-Fi EMF at all times, which means that many humans are under constant Wi-Fi EMF exposure. Also, there is less scientific literature investigating Wi-Fi EMF’s health effects than there is for cellphone EMF. Given Wi-Fi EMF’s widespread and growing usage, scientists must carefully evaluate whether Wi-Fi EMF has health effects on humans.

The purpose of this research project was to determine whether Wi-Fi electromagnetic fields affect the health of *Drosophila melanogaster*. *D. melanogaster* is a model organism for scientific research, as much of its biology and physiology mirrors that of other organisms, including humans (6). The focus of this study was to investigate the effects of Wi-Fi EMF, if any, on the *D. melanogaster* as a whole organism. If statistically significant results emerged at the organismal

level, targeted research might be conducted by the scientific community to determine the specific *D. melanogaster* physiology affected most by Wi-Fi EMF, which could translate to human physiology.

We hypothesized that Wi-Fi EMF Radiation would affect *D. melanogaster* as measured by changes in the number of progeny adults, the number of pupae, the number of progeny males, the number of progeny females, the progeny adult:pupa ratio, and the male:female ratio. Changes in these variables could be caused by a variety of effects, including effects on fecundity, development, or survival. The term “progeny adult” indicates an eclosed adult *D. melanogaster* that was an offspring of the male and female *D. melanogaster* pair introduced to the vial. A progeny adult was exposed to Wi-Fi EMF for its entire life cycle, and was the offspring of a *D. melanogaster* pair that had been exposed to Wi-Fi EMF for their entire life cycle. Different statistical comparisons separated progeny adults into “progeny males” and “progeny females” to investigate whether sex-selective effects occurred.

RESULTS

At the start of the experiment, no affordable and effective apparatus suitable for a home setting could be found to produce controlled concentrations of EMF for testing with *D. melanogaster*. Therefore, a testing chamber had to be engineered that was both affordable and provided effective EMF control inside the chamber while keeping the *D. melanogaster* healthy. The Box Setup (**Figure 1**) is the testing chamber engineered for this purpose. Four Box Setups (**Figure 1A**) were constructed, one for each of the three concentrations and the control. The Box Setups each had design features (**Figure 1B**) that successfully prevented exterior EMF from entering, provided a means of ensuring that all the Wi-Fi routers were functioning, were grounded Faraday cages (7, 8), maintained adequate humidity, had consistent air circulation, and were quiet. The temperature fluctuated between 22 and 25 degrees Celsius, which did not negatively affect the *D. melanogaster* (9).

Three concentrations of Wi-Fi EMF and a control were tested (**Table 1**). The different concentrations were produced by covering the Wi-Fi router antennae with carbon fabric EMF-absorbent sleeves of varying sizes. The concentrations tested were percentages of the full Wi-Fi EMF dose from a TP-LINK® Wi-Fi router, determined from EMF measurements taken in this study. Since the TP-LINK® Wi-Fi router is

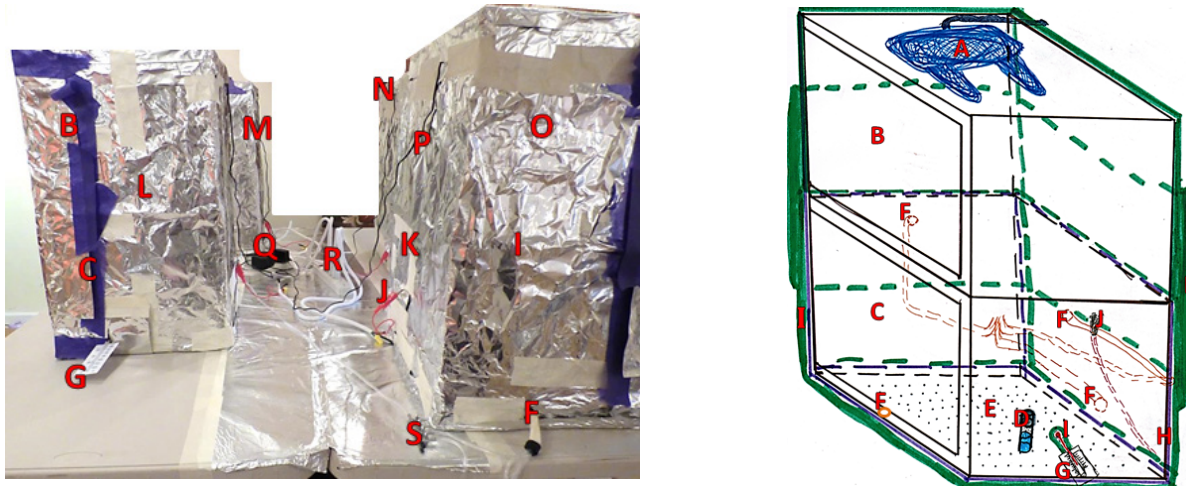


Figure 1. Box Setup Photo and Diagram. Not pictured are the carbon-impregnated fabric sleeves placed on the Wi-Fi router antennae to create different EMF concentrations. D. melanogaster were placed inside each Box Setup to receive EMF exposure of a specific concentration. Pictured are the (A) Wi-Fi router under the roof of the Wi-Fi Chamber, (B) Wi-Fi Chamber with a door flap for access inside, (C) *Drosophila melanogaster* Chamber with a door flap for access inside, (D) vial with a *D. melanogaster* male and female (each Box Setup had 15 vials); vial positioned in a grid square that has mean EMF measurements within the defined range for that EMF concentration, (E) Grid on floor of *D. melanogaster* Chamber used for EMF measurement and vial positioning, (F) Air tubes to provide air circulation in the *D. melanogaster* Chamber, two air tubes provided air input and two provided venting, the four tubes were gathered in a bundle to exit the shielding, (G) Thermometer with bulb covered in EMF-reflective shielding and inside *D. melanogaster* Chamber while the end protruded outside for easy temperature reading, (H) Carbon impregnated fabric for EMF-absorbent shielding surrounded the *D. melanogaster* Chamber, (I) aluminum foil EMF-reflective shielding surrounded the entire Box Setup, (J) Alligator clip for grounding system was attached to EMF-reflective shielding then plugged into the wall outlet's "Ground", (K) Piece of EMF-reflective shielding to cover the seam between the Wi-Fi Chamber and the *D. melanogaster* Chamber, (L) 100% EMF concentration Box Setup, (M) 5% EMF concentration Box Setup, (N) Control Box Setup, (O) 20% EMF Concentration Box Setup, (P) Power cord for Wi-Fi Router, (Q) Power strip for Wi-Fi Router's power supply, (R) Power strip for grounding system, (S) Air valve for air circulation system

intended for home use, the Wi-Fi EMF concentrations tested are likely levels that humans experience.

To analyze the data, ANOVA and t-test statistical tests were conducted and graphs were constructed. The graphs, which display the mean number of *D. melanogaster* for each Wi-Fi concentration, show a negative trend: as the Wi-Fi EMF concentration increases, the number of *D. melanogaster* decreases. This negative correlation can be observed for the comparisons involving the number of progeny adults, the number of pupae, the number of progeny males, and the number of progeny females. The trend does not appear for the male:female ratio or the adult:pupa ratio.

When collecting data, the *D. melanogaster* vials exposed to the 20% concentration were placed upright in the freezer causing the adult flies to freeze into the medium. Therefore, the data for the number of progeny males, number of progeny females, and male:female ratio could not be collected for this concentration. This disturbance compromised the accuracy of the data collected for the number of progeny adults and the number of pupae since these data could not be collected the same way as they were for the other concentrations. Though these data could not be assumed to be reliable under these conditions, the data collected for the 20% concentration did follow the negative trend observed for the other concentrations; namely, as the concentration of Wi-Fi EMF increases, the number of *D. melanogaster* decreases.

Further research is needed to confirm these results for the 20% concentration.

The hypothesis was that Wi-Fi EMF Radiation would affect *D. melanogaster* as measured by changes in the number of progeny adults, the number of pupae, the number of progeny males, the number of progeny females, the progeny adult:pupa ratio, and the male:female ratio

For the number of progeny adults, high levels of Wi-Fi EMF exposure (100% concentration) reduced the number of flies, but low levels (5% concentrations) did not. ANOVA comparison ($\alpha=0.05$) of the number of progeny adults across all EMF concentrations (0%, 5%, 100%) produced a statistically significant result; the *p*-value was less than

Wi-Fi Concentration	Range of EMF Exposure (mW/m ²)
0% (Control)	0
5%	5 – 9
20%	25 – 32
100%	125 – 147

Table 1. Wi-Fi EMF concentrations tested on *D. melanogaster*.

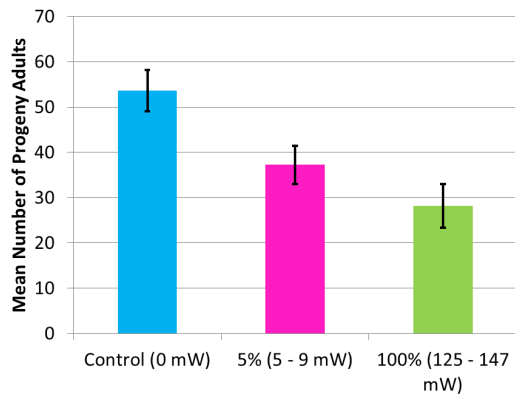


Figure 2. Effect of EMF on Number of *D. melanogaster* Adult Progeny. Bars represent mean number of progeny adults for each EMF concentration. Error bars represent one standard error above the mean and one standard error below the mean.

α ($p=0.0013$; **Figure 2**). Two-tailed t-test comparison ($\alpha=0.025$) of the 0% and 100% concentrations produced a statistically significant result since the p -value was less than α ($p=0.00076$), with a Hedge's g_s effect size of 1.4 and a 95% CI: [0.62, 2.3]. There was no significant difference between the 5% and 0% concentrations.

Another way that the effects of Wi-Fi were measured was by comparing male and female progeny adults. The results suggest that male flies are more sensitive to Wi-Fi EMF than female flies. Even at a low (5%) concentration, the number of progeny males was significantly fewer than the control. ANOVA comparison ($\alpha=0.05$) of the number of progeny males for concentrations 0%, 5%, and 100% produced a statistically significant result ($p=0.0036$; **Figure 3**). Two-tailed t-test comparison ($\alpha=0.025$) of the 0% and 5% concentrations yielded a p -value less than α ($p=0.0030$), with a Hedge's g_s effect size of 1.2 and 95% CI: [0.41, 2.0]. Two-tailed t-test comparison ($\alpha=0.025$) of the 100% and 0% concentrations produced a p -value less than the α ($p=0.0069$), with a Hedge's g_s effect size of 1.1 and 95% CI: [0.33, 1.9].

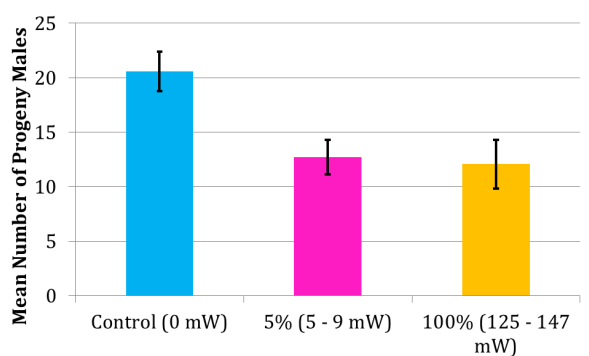


Figure 3. Effect of EMF on Number of Progeny Male Adults. Bars represent mean number of progeny male adults for each EMF concentration. Error bars represent one standard error above the mean and one standard error below the mean.

For progeny female adults, high levels of Wi-Fi EMF exposure (100% concentration) reduced the number of flies, while low levels (5% concentration) did not. ANOVA comparison ($\alpha=0.05$) of the number of progeny females for concentrations 0%, 5%, and 100% produced a statistically significant result ($p=0.0014$; **Figure 4**). Two-tail t-test comparison ($\alpha=0.025$) of the 100% and 0% concentrations also yielded a p -value less than α ($P=0.00053$), with a Hedge's g_s effect size of 1.4 and 95% CI: [0.64, 2.3]. There was no significant difference between the 5% and 0% concentrations.

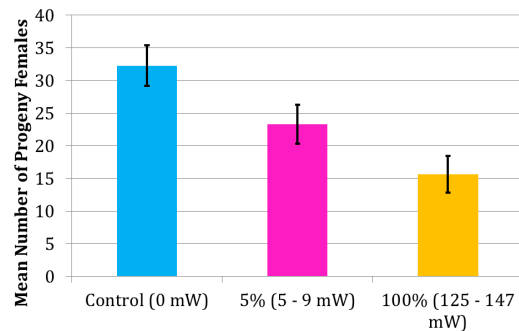


Figure 4. Effect of EMF on Number of Progeny Female Adults. Bars represent mean number of progeny female adults for each EMF concentration. Error bars represent one standard error above the mean and one standard error below the mean.

To investigate whether Wi-Fi EMF has developmental effects, the number of pupae was also analyzed. High levels of Wi-Fi EMF exposure (100% concentration) decreased the number of pupae, but lower levels (5% concentration) did not. ANOVA comparison ($\alpha=0.05$) of the number of pupae across all EMF concentrations (0%, 5%, 100%) produced a statistically significant result ($p=0.0035$; **Figure 5**). Two-tailed t-test comparison ($\alpha=0.025$) of the 0% and 100% concentrations yielded a p -value less than α ($p=0.0019$),

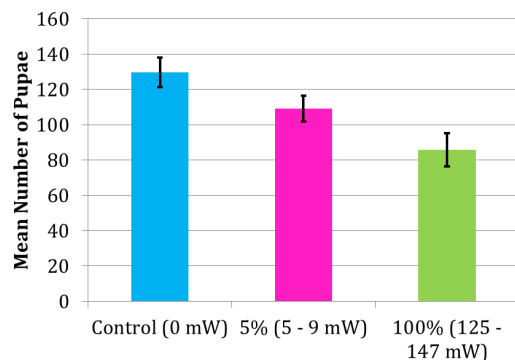


Figure 5. Effect of EMF on Number of Pupae. Bars represent mean number of pupae for each EMF concentration. Error bars represent one standard error above the mean and one standard error below the mean.

with a Hedge's g_s effect size of 1.3 and 95% CI: [0.50, 2.1]. There was no significant difference between the 5% and 0% concentrations.

Wi-Fi EMF's effect on the male:female ratio is unclear. A low (5%) concentration showed a marginally significant decrease, whereas the 100% concentration showed no significant difference. ANOVA comparison ($\alpha=0.05$) of concentrations 0%, 5%, and 100% produced a p -value less than the α , and was statistically significant ($p=0.038$; **Figure 6**). Two-tailed t-test comparison ($\alpha=0.025$) of the 5% and 0% concentrations ($p=0.089$) was marginally non-significant, since the p -value is close to the α . Two tail t-test comparison ($\alpha=0.025$) of the 100% and 0% concentrations ($p=0.23$) did not produce p -values below the α , and was not statistically significant. Visual observation of the chart did not show any obvious pattern in the male:female ratio as the EMF concentration increases. Further research is necessary to determine how Wi-Fi EMF exposure affects the progeny male:female ratio.

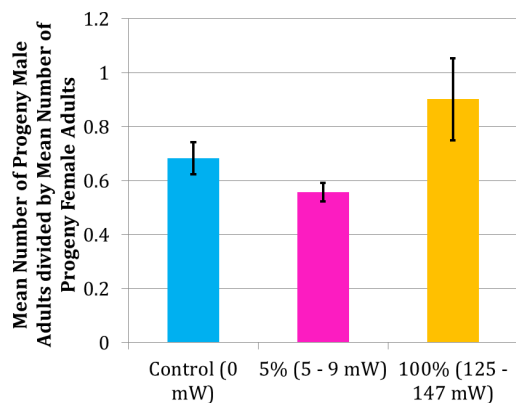


Figure 6. Effect of EMF on Male:Female Ratio of Adult Progeny. Bars represent mean male:female ratio for each EMF concentration. This is the data before the logarithmic transformation. Error bars represent one standard error above the mean and one standard error below the mean.

None of the statistical comparisons of the adult:pupa ratio emerged as statistically significant (**Figure 7**). This suggests that Wi-Fi EMF exposure does not affect the adult:pupa ratio of *D. melanogaster*.

DISCUSSION

The results of this study show that Wi-Fi EMF has a statistically significant effect on the number of total progeny adults, number of progeny males, number of progeny females and number of pupae. The progeny adult male:female ratio was not significant. There was no statistically significant effect for the progeny adult:pupa ratio. This suggests that when *D. melanogaster* are exposed to Wi-Fi EMF, the number of progeny adults, number of progeny male adults,

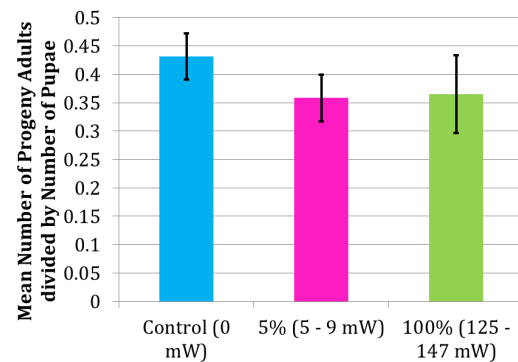


Figure 7. Effect of EMF on Adult:Pupa Ratio. Bars represent mean progeny adult:pupa ratio for each EMF concentration. This is the data before the logarithmic transformation. Error bars represent one standard error above the mean and one standard error below the mean.

number of progeny female adults, and number of pupae, are reduced. Results for the progeny adult male:female ratio are inconclusive. Meanwhile, the results suggest that the progeny adult:pupa ratio is unaffected. The results of this study support the hypothesis, since they suggest that Wi-Fi EMF affects *D. melanogaster*.

Since the t-tests performed were two-tailed, their statistical significance does not indicate whether the number of *D. melanogaster* increased or decreased. However, there was no reliable data collected for the 20% concentration and if this data is excluded from the charts, a clear negative trend is apparent. As the Wi-Fi EMF concentration increased, the number of flies decreased. This trend applies to the mean number of progeny adults, mean number of progeny male adults, mean number of progeny female adults, and mean number of pupae. This negative correlation does not seem to exist for the male:female ratio or the adult:pupa ratio.

Given this negative correlation, the results suggest that only a high concentration of EMF (100%) decreases the number of progeny adults, the number of progeny females, and the number of pupae, and that low (5%) EMF levels do not produce a statistically significant effect. It may be that these groups are only affected when Wi-Fi EMF surpasses a threshold concentration. In contrast, even a low EMF concentration (5%) produced a statistically significant decrease in the number of progeny males. This suggests that male *D. melanogaster* are more sensitive to EMF than female *D. melanogaster*. There was not a statistically significant difference in the progeny adult:pupa ratio for any EMF concentration, which suggests that EMF exposure does not impair eclosion of pupae. The results for the male:female ratio are inconclusive, since the ANOVA comparison produced a p -value less than the α , but the t-test comparisons to the control did not.

Further research is necessary to identify which specific aspects of *D. melanogaster* biology—such as

fecundity, hormone modulation, eating behavior, or larval development—are affected to cause the decrease in the number of *D. melanogaster*. Research into specific areas of *D. melanogaster* biology, and research using more complex organisms such as mice, could shed light on any effects of Wi-Fi EMF for humans. Another relevant question is whether Wi-Fi EMF has generational effects. This could be investigated by studying multiple generations of *D. melanogaster* and focusing on generational effects. Further research is needed to determine Wi-Fi EMF's effects on the male:female ratio. Future studies could employ a two-way ANOVA to better understand Wi-Fi EMF's effect on the male:female ratio.

The Box Setup apparatus could be improved by adding a parabolic reflector to the Wi-Fi Chamber of the Box Setup, which could produce more consistent EMF measurements across the grid on the floor of the *D. melanogaster* chamber of the Box Setup. The *D. melanogaster* chamber should also be lined with a more effective EMF-absorbent material than the carbon-impregnated fabric used in this experiment to improve EMF absorbance and mitigate standing waves. The *D. melanogaster* chamber could also be modified so that EMF concentrations on the grid floor can be measured while the door flap is closed and all the shielding is in place.

A published experimental setup designed to expose small animals, such as mice, to controlled concentrations of EMF experienced many of the same physics challenges encountered in this experiment, and this setup could be utilized for future research with Wi-Fi EMF (11).

The implications of this study extend beyond Wi-Fi usage. Non-ionizing Radiofrequency EMF, which is the type of EMF used for Wi-Fi, is also produced by cellphones, smart meters, and cellphone towers (1, 3, 4, 5). These technologies may exhibit similar biological effects as Wi-Fi.

An uncontrolled variable that may have occurred is slight warming of the *D. melanogaster* vials from the EMF; however, a warmer temperature would be expected to accelerate the *D. melanogaster* life cycle (9, 10) and subsequently increase the number of progeny, not decrease the number of progeny, as occurred with Wi-Fi EMF exposure in this experiment. If the Control (0% EMF concentration) *D. melanogaster* chamber was consistently warmer than the other three *D. melanogaster* chambers, this could explain its greater number of progeny. However, this was not the case. The *D. melanogaster* chambers with the higher EMF concentrations sometimes experienced slightly higher temperatures than the others, yet they had fewer progeny. Throughout the experiment, the four *D. melanogaster* chambers were kept at approximately 24 degrees Celsius. The control *D. melanogaster* chamber and the 5% EMF concentration *D. melanogaster* chamber sometimes measured 0.5 degrees Celsius less than the *D. melanogaster* chambers for the 100% and 20% EMF concentrations. This cooler temperature was probably because the 5% and control *D. melanogaster* chambers were positioned closer to an exterior wall and this experiment was conducted in winter. Throughout the experiment, the *D.*

melanogaster chambers were 22 to 25 degrees Celsius.

The *D. melanogaster* vials and foam plugs likely reflected or absorbed a small percentage of the Wi-Fi EMF. However, the nature of Wi-Fi EMF is such that it penetrates many types of materials so that it can provide Wi-Fi service throughout an entire home. The influence of the vials and foam plugs on the *D. melanogaster*'s EMF exposure is negligible for the purposes of this experiment. Furthermore, any effect the vials and foam plugs had on the Wi-Fi EMF exposure is a controlled variable, because all of the *D. melanogaster* were placed in the same type of vials with identical foam plugs.

Due to the wave nature of EMF, a change in the polarity or angle of the EMF meter, a change in the EMF shielding's position, or a three centimeter (cm) change in the position of the EMF meter caused the EMF measurement to change unpredictably. In addition, EMF measurements may have changed when the shielding was positioned over the door flap. This is a limitation of this study, but is consistent across all the Box Setups including the control.

METHODS

Summary of Procedure

Four Box Setup apparatuses were designed and constructed. Each apparatus consisted of two cardboard boxes on top of each other. The top box was the "Wi-Fi chamber," with a router inside, and the bottom box was the "*D. melanogaster* chamber," where the *D. melanogaster* vials were placed.

The Box Setup apparatus required intensive design and construction. First, a thermometer, air tubes, and a Wi-Fi router were installed in each Box Setup. The Box Setups were then covered with EMF shielding. EMF-reflective shielding used was Reynolds Wrap® Extra Heavy Duty aluminum foil, and EMF-absorbent shielding used was carbon-impregnated fabric. Sleeves of the carbon-impregnated fabric were placed on the Wi-Fi router antenna to attenuate the Wi-Fi EMF. Different-sized carbon fabric sleeves were used to make the different concentrations of Wi-Fi EMF Radiation. The control (0% concentration) was achieved by placing two layers of aluminum foil between the Wi-Fi chamber and the *D. melanogaster* chamber, blocking all measurable EMF. The air supply, grounding system, and electrical system were connected to each Box Setup. Grounding of the Box Setups was done based on a study in which the aluminum Faraday Cage did not successfully block EMF until it was grounded (8). A grid was marked on the floor of the *D. melanogaster* chamber and five EMF measurements were taken in each square of the grid. Microsoft Excel was used to calculate the mean of these five measurements. The squares of the grid which had mean EMF measurements which fell within the defined EMF ranges were chosen for *D. melanogaster* vial positioning.

Upon completion of a functional Box Setup for each

EMF concentration, the focus was shifted towards the *D. melanogaster*. Sixty vials were prepared with medium, distilled water, and yeast. *D. melanogaster* adults, which were 1-4 days old, were anesthetized and sexed. One male and one female *D. melanogaster* were placed in each vial. The vials were positioned in grid squares with mean EMF measurements within the defined Wi-Fi EMF ranges. There were 15 vials for each EMF concentration. After positioning the vials, the fronts of the *D. melanogaster* chambers were covered with shielding. (See **Figure 1**) The *D. melanogaster* were exposed to Wi-Fi EMF for 14 days. The *D. melanogaster* vials were then removed from the Box Setups and frozen. The data was collected and recorded for the number of progeny adults, number of progeny males, number of progeny females, number of pupae, male:female ratio, and adult:pupa ratio.

Choice of Shielding Materials

Aluminum was chosen as an EMF reflective material because at 1.5 GHz/s and 3.0 GHz/s, 99.0% of EMF is reflected by aluminum (12). The Wi-Fi EMF used in this experiment was 2.4 GHz, which falls within this range. Very little EMF travels through aluminum at Gigahertz frequencies (12). Extra Heavy Duty aluminum foil is chiefly aluminum (98.5%), and the remaining metals are mostly iron and silicon (13).

The Skin Effect principle (14, 15) was used to confirm that Extra Heavy Duty aluminum foil (thickness of 32 μm) is suitable for EMF reflective shielding.

Skin Effect Depth equation: $\delta = \sqrt{\rho / \pi f \mu}$

δ is the skin effect depth in m,

ρ is the resistivity of the conductor in $\Omega \times \text{m}$,

f is the frequency of the EMF wave in Hertz,

μ is the absolute magnetic permeability. This is the relative permeability of the conductor multiplied by $4\pi \times 10^{-7}$ H/m.

For aluminum, the skin depth is $\approx 1 \mu\text{m}$. So, after every 1 μm of aluminum thickness, EMF power density is decreased by $1/e$. After 32 μm , the thickness of Extra Heavy Duty aluminum foil, the power density is $(1/e)^{32}$, which is approximately 10^{-14} . Carbon is EMF absorbent in some forms (16, 17). A carbon-impregnated fabric, "Microwave Absorbing Sheet," was obtained as an EMF absorber for this experiment (18, 19). The Less EMF website, where the carbon fabric was purchased, advertised it as an effective EMF absorbent material, providing more than 25 decibels of attenuation at 2 GHz. Carbon fabric was selected instead of other available EMF attenuating fabrics made from silver and nickel because those fabrics have antimicrobial properties. Antimicrobial properties could adversely affect the *D. melanogaster* which rely on a variety of microbes to ferment their medium.

Steps were taken to avoid build-up of heat inside the Box Setup. In theory, EMF is converted to heat as the EMF-absorbent carbon fabric absorbs it. Cardboard boxes have a thermal conductivity of $0.21 \text{ Wm}^{-1}\text{K}^{-1}$, indicating that

cardboard is a poor thermal conductor, and therefore a good insulator (20). If the carbon fabric lined the inside of the cardboard box, then as it absorbed EMF, the cardboard would retain the heat. For this reason, the carbon fabric was layered on the exterior of the cardboard boxes, so that any heat produced by EMF absorption would be transferred to the environment, and not be trapped in the cardboard box. The EMF-reflective shielding, aluminum foil, was placed as the outermost layer, on top of the carbon fabric since its thermal conductivity is $210 \text{ Wm}^{-1}\text{K}^{-1}$, indicating that it is a good thermal conductor and heat is readily conducted out of it (20). So, any heat produced by the carbon fabric absorbing EMF would be easily transferred to the aluminum foil, and be transferred to the surrounding air. As expected, the temperature inside the Box Setups did not increase over time as it would if heat was trapped inside.

Construction of "Box Setup" Testing Apparatus

Each Box Setup consisted of two 46 by 32 by 35 cm cardboard boxes stacked on top of each other. Cardboard boxes were chosen as the structure for the testing chamber because of their shape, sturdiness, and availability. The upper box, the "Wi-Fi Chamber" contained the TP-LINK® Wi-Fi router (21), the source of the EMF. This Wi-Fi router was selected because it was one of the most highly rated routers available for home use at the time of the experiment. The lower box, the "*D. melanogaster* Chamber" held the *D. melanogaster* vials.

In addition to effective control of EMF within the testing chamber, other objectives for the Box Setup were determined. Control of EMF levels inside the chamber was maintained by the twofold strategy of blocking exterior EMF from entering and absorbing EMF reflections inside the chamber. Different concentrations of EMF were created by changing the size of sleeves of absorbing EMF material placed over the Wi-Fi router antennae. To maintain the *D. melanogaster* inside the closed testing chamber, an air circulation and humidity system were installed. Relative humidity was maintained at approximately 40%, a level high enough to avoid the drying of the medium and low enough to avoid mite infestation or bacterial contamination.

So that the Control vials would also be exposed to any heat that could have been produced by the router, the Wi-Fi chamber in the Control Box Setup also contained a Wi-Fi router that was producing Wi-Fi. The control (0% concentration) was achieved by placing two layers of aluminum foil between the Wi-Fi Chamber and the *D. melanogaster* chamber.

The flat floor of the *D. melanogaster* chamber ensured that all the *D. melanogaster* vials would rest on an even surface. This was pursued because EMF exposure can change when there is a difference in position of only a few millimeters. However, after observing the nature of EMF, the authors do not think that the flat floor feature made a measurable impact on EMF exposure. Nevertheless, the flat floor was a useful feature to make the grid squares easier to draw.

A layered shielding system was used so that openings in the shielding could be made without allowing measurable amounts of exterior EMF to enter the Box Setup through them. These openings were necessary for the thermometers and air tubes. The layering system involved alternating layers of EMF-reflective and EMF-absorbent shielding.

Rationale for Air Circulation

It was necessary that there be adequate air circulation to mitigate the carbon dioxide produced by the fermenting medium and *D. melanogaster*. An air tube and air valve system were designed and installed to provide 24/7 air circulation. The air valve system was used to distribute air equally among the four Box Setups. A Tetra Whisper® aquarium air pump designed for a 378.5 L fish tank was selected and positioned to minimize vibrations and noise as uncontrolled variables. To prevent the *D. melanogaster* medium from drying, the incoming air was humidified. The Vicks® Warm Mist humidifier was selected because it created vapor by heating water and therefore did not require an antibacterial filter. “Cool-air” humidifiers were avoided because they use antimicrobial agents to prevent bacterial contamination; exposure to antimicrobial agents would be an uncontrolled variable that could modify the fermentation of the *D. melanogaster*'s medium. Also, only distilled water was used in the humidifier to minimize potentially uncontrolled variables because of water solutes.

Construction of Wi-Fi Chamber

The “Wi-Fi Chamber” was identical for all the Box Setups. The flaps of the cardboard box which would normally form the floor were cut off. The flaps which form the top were taped with packing tape with the short flaps facing inwards, then the long flaps. Measurements were drawn using an aluminum T-square. A utility knife was used to cut openings. A door flap was cut in the front of the box to provide access to the interior. The left edge of the box served as the hinge for the door flap. The door flap was cut from the front of the box 23 cm from the left edge, 4 cm from the top edge, and 4 cm from the bottom edge. A 5 cm sturdy ribbon was stapled to the right edge of the door flap to be used for opening it. The Wi-Fi router was attached to the ceiling of the box using zip ties. Circular openings for the two zip ties were made by punching a sharp pencil through the ceiling of the box. The openings for the first zip tie were made 21.5 cm from the front edge, 15.5 cm from the left edge and 21.5 cm from the front edge, 1 cm from the left edge. The openings for the second zip tie were made 14 cm from the front edge, 15.5 cm from the left edge and 14 cm from the front edge, 1 cm from the left edge. The plastic zip ties were threaded through the openings made. The Wi-Fi router was positioned within 8.5 cm from the front and back edge, and 7.5 cm from the left edge. The zip ties were tightened until snug, and the position of the router was double checked. If necessary, adjustments were made, and the zip ties were tightened completely. Excess zip tie length was cut

off. A circular opening for the Wi-Fi router's power cord was made by punching a thick pen through the ceiling of the box 5 cm from the back edge, 13 cm from the left edge. The power cord was inserted through the opening and connected to the Wi-Fi router. The Wi-Fi router button was pressed to the “On” setting so that when power was connected, Wi-Fi EMF would begin automatically. The Wi-Fi Chamber was taped on top of the *D. melanogaster* Chamber using packing tape, making a Box Setup. The door flap was taped shut with painter's tape.

Construction of *D. melanogaster* Chamber

The “*D. melanogaster* Chamber” was identical for all four Box Setups. Using packing tape, the floor was taped with the longer cardboard flaps facing inwards, making a flat floor for the vials to rest on. Packing tape was used to seal all edges and seams of the box. Measurements were drawn using an aluminum T-square. A utility knife was used to cut openings. A door flap was cut in the front of the box to provide access to the interior of the *D. melanogaster* Chamber. The left edge of the box served as the hinge for the door flap. The door flap was cut from the front of the box 23 cm from the left edge, 4 cm from the top edge, and 4 cm from the bottom edge. A 5 cm sturdy ribbon was stapled to the right edge of the door flap to be used for opening it. Circular openings for air tubes for the air circulation system were made by punching a sharp pencil through the walls of the box. For the front and back of the box, openings were made 2 cm from the bottom edge and 23 cm from the left edge. For the right and left sides of the box, openings were made 18 cm from the left edge and 28 cm from the bottom edge. A rectangular 2.5-cm by 1-cm opening for the thermometer was made on the right side of the box 11 cm from the left edge and 4 cm from the bottom edge. Plastic aquarium airline air tubing was then cut for the air circulation system: two 90-cm pieces and two 50-cm pieces. The 90 cm pieces were labeled “O” for output, and the 50 cm pieces were labeled “I” for input. Two rotations of 2 cm wide masking tape were wrapped around the end of each air tube piece. The 50 cm air tubes were inserted through the circular openings made in the front and back of the box, and the 90 cm air tubes were inserted through the openings in the right and left sides of the box. The piece of masking tape wrapped around the end of each tube prevented the tubes from falling out of the openings. Wood glue was used to keep the air tubes in place. Pieces of masking tape were used to secure the air tubes along the outside walls of the box, so that they all came together at the back. The air tubes were gathered in a bundle, secured with a Velcro® strip, then secured with 4 cm wide masking tape, then secured with a Velcro® strip, then secured with 4 cm wide masking tape, then secured with a Velcro® strip.

Emitting Different Concentrations of Wi-Fi

EMF-absorbing carbon impregnated fabric shielding was placed on the Wi-Fi router antennae by rolling the fabric into hollow, cylindrical sleeves and sliding the sleeves onto each

antenna. The sleeves were secured in place with masking tape on the interior of the sleeves. The carbon fabric sleeves attenuated the Wi-Fi EMF, and different dimensions of carbon fabric were used to create the different EMF concentrations. Each Wi-Fi router antennae was 17.5 cm long. The 100% concentration Wi-Fi Chamber did not receive any carbon fabric sleeves on the Wi-Fi router antennae.

For the 20% concentration Wi-Fi Chamber, six pieces of carbon fabric were cut 4.5 cm long, 7 cm wide. These carbon fabric rectangles were then rolled into hollow cylindrical sleeves with a length of 4.5 cm. On each antennae, the sleeves were positioned: first a 1 cm space with no sleeve, 4.5 cm sleeve, 1 cm no sleeve, 4.5 cm sleeve, 1 cm no sleeve, 4.5 cm sleeve, 1 cm no sleeve.

For the 5% concentration Wi-Fi Chamber, six carbon fabric pieces were cut 5.5 cm long, 7 cm wide. These carbon fabric rectangles were then rolled into hollow cylindrical sleeves with a length of 5.5 cm. On each antennae, the sleeves were positioned: first a 0.25 cm space with no sleeve, 5.5 cm sleeve, 0.25 cm no sleeve, 5.5 cm sleeve, 0.25 cm no sleeve, 5.5 cm sleeve, 0.25 cm no sleeve.

The Control (0% Wi-Fi EMF concentration) did not receive any sleeves on the router antennae because the sleeves are not capable of completely blocking EMF. The router was kept "On" so that any heat it produced would be a controlled variable among all the Box Setups. The Control (0% concentration) was achieved by placing two layers of Extra Heavy Duty aluminum foil between the Wi-Fi Chamber and the *D. melanogaster* Chamber. The aluminum foil blocked the EMF from entering the *D. melanogaster* Chamber and reflected the EMF back into the Wi-Fi Chamber. The Skin Effect calculation confirmed that two layers of Extra Heavy Duty aluminum foil would attenuate virtually all of the Wi-Fi EMF. The only difference between the Control Box Setup and the Box Setups for the other concentrations was two layers of reflective shielding blocking the Wi-Fi before it reached the vials.

The Control (0% concentration) was confirmed by changing the EMF meter to its "Sound" setting, placing the EMF meter inside the *D. melanogaster* Chamber, closing the *D. melanogaster* Chamber, and listening for EMF readings. In "Sound" mode, the intensity of the EMF level is proportional to the intensity of the meter's buzzing. Silence indicates no measurable EMF. No measurable EMF was detected by the EMF meter in the Control (0% concentration) *D. melanogaster* Chamber when the router was "On"—it did not produce any sound. Measurements were drawn using an aluminum T-square and permanent marker. A utility knife was used to cut the shielding.

Applying Shielding to Wi-Fi Chamber

The reflective shielding was Reynolds Wrap® Extra Heavy Duty aluminum foil. This shielding was 45.7 cm wide off the roll. Three pieces of reflective shielding were cut (a) 118 cm long, 45.7 cm wide, (b) 66 cm long, 31 cm wide, and (c) 52 cm

long, 45.7 cm wide.

This shielding was applied to the Wi-Fi Chamber using masking tape. The shielding was applied in a specific order: first piece (a) on left side, back side, and right side of box; second piece (c) applied on top side; edges overlapping piece (a); third (b) applied to front side; edges tuck under (c) and (a).

Measurements were drawn on shielding using an aluminum T-square and permanent marker. A utility knife was used to cut shielding.

Applying Shielding to *D. melanogaster* Chamber

A 31- by 121.5-cm piece of EMF-absorbent shielding (carbon impregnated fabric) was wrapped around the *D. melanogaster* Chamber to cover the left side, back side, and right side and overlap slightly over the front of the Chamber.

Next, the shielding layering system for the air tube bundle was done. A 20 cm by 15 cm piece of EMF-reflective shielding was positioned on the left side of the Chamber so that it aligned with the left side's left edge and bottom edge. On top of this piece, a 33-cm by 15.5-cm piece of EMF-absorbent shielding was positioned so that it aligned with the left edge and bottom edge of the left side of the Chamber. An opening was cut in these pieces for the air tube bundle to feed through; the opening was 2.5 cm from the Chamber left side bottom edge and 9.5 cm from its left edge.

A 47-cm by 57-cm piece of EMF-absorbent shielding covered the bottom of the *D. melanogaster* Chamber. It had overlap over all four sides of the Chamber. A 92- by 45.7-cm piece of EMF-reflective shielding covered the right side and back of the Chamber; it had overlap over the bottom and left side of the Chamber. A 40- by 47.5-cm piece of EMF-reflective shielding covered the left side of the Chamber and overlapped onto its back. A 52- by 44.5-cm piece of EMF-reflective shielding covered the bottom of the *D. melanogaster* Chamber; it overlapped over all four sides of the Chamber.

For the control *D. melanogaster* Chamber only, two 52- by 44.5-cm pieces of EMF-reflective shielding covered the top of the Chamber, with overlap over all four sides of the Chamber. These blocked the EMF produced by the Wi-Fi router from reaching the *D. melanogaster* Chamber.

Where the shielding on the *D. melanogaster* Chamber met the shielding of the Wi-Fi Chamber, there was a small gap, where there was no shielding. A 45.7- by 120 cm piece of EMF-reflective shielding was used on the exterior of the Box Setup to cover this gap.

Next, the shielding layering system for the thermometer opening was conducted. A 16- by 18-cm piece of EMF-reflective shielding was centered over the place where the thermometer opening had been cut into the *D. melanogaster* Chamber cardboard box. The thermometer bulb, which was wrapped in a sleeve of EMF-reflective shielding, was inserted through the 16- by 18-cm piece of EMF-reflective shielding. Wrapping it in a sleeve did not affect the temperature readings, since aluminum foil is a good thermal conductor (20). A 14- by 17-cm piece of EMF-absorbent shielding was layered next. A

14- by 14-cm piece of EMF-absorbent shielding was the final layer for the thermometer's shielding layering system.

The last step was for shielding to be applied to the front of the *D. melanogaster* Chamber. A 57.5- by 30-cm piece of EMF-absorbent shielding covered the front side of the Chamber, and overlapped onto its left side. A 63- by 30- cm piece of EMF-reflective shielding covered the front side of the Chamber, and overlapped onto its left side. Finally, a 56- by 44-cm piece of EMF-reflective shielding covered the front side of the Chamber, and overlapped onto its left side.

All shielding was secured with masking tape, except the shielding used to cover the front of the *D. melanogaster* Chamber. That shielding was secured using Painter's tape so that it was easily removable, allowing the door flap to be opened to access the interior of the *D. melanogaster* Chamber.

Installation of Air Circulation System

The Box Setups were placed on two adjacent tables; the air circulation apparatus (humidifier, air pump, etc.) was placed underneath the tables. Plastic garbage bags were spread on the floor and a stool was covered with a garbage bag to stay dry. The aquarium air pump was placed on the stool and the humidifier was placed next to the stool. The aquarium air pump and humidifier were plugged into a GFCI outlet, which was used for safety in case of a water spill. Two pieces of Extra Heavy Duty aluminum foil (a) 75 cm long, 45.7 cm wide, (b) 34 cm long, 45.7 cm wide, were cut and shaped into a hood to direct water vapor from the humidifier towards the intake of the aquarium air pump. The aluminum foil hood was secured to the bottom of the table and stool using masking tape.

Air valves, which each had four openings, were used. Before starting the experiment, the air valves were all opened and closed to reduce their stiffness. Pieces of plastic aquarium airline air tube (a) 1 piece: 115 cm long, (b) 4 pieces: 102 cm long, (c) 1 piece: 42 cm long—were cut for use as connectors between air valves. Piece (a) connected the air pump to the main air valve which rested on the table. Piece (b) connected the main air valve to the individual air valves for each Box Setup. Piece (c) connected to one of the openings of the Control Box Setup's air valve. This airline tube was used to measure the humidity of the air that the *D. melanogaster* were being exposed to. All four openings of the main air valve were opened. They attached to a valve for each Box Setup, which split the air flow into two tubes before leading it into the *D. melanogaster* Chamber. For the Control Box Setup, a third air valve opening connected to Piece (c). This Piece (c) opening was kept closed except when measuring humidity. The aluminum hood was adjusted until the desired relative humidity was achieved, as measured with the Humidity Measuring Procedure. The humidifier was filled with distilled water.

Grounding System

A grounding system was installed in the Box Setups to make them grounded Faraday Cages. Four electrical cords with a plug at one end were obtained by cutting the cords off of power strips. The ground wire, which was covered in green insulation, was stripped at its end. This end was twisted around the exposed wire of an alligator clip. The joint was secured with a wire nut. The alligator clip was attached to the piece of aluminum foil which covered the small gap where the *D. melanogaster* chamber shielding met the Wi-Fi chamber shielding. The section of aluminum foil which the alligator clip clamped onto was folded to add thickness so that the alligator clip would not puncture it. Using a multimeter, the resistance between the aluminum shielding and grounding pin on the cord's plug was measured and recorded. The resistance was 0.1 Ω for all four Box Setups. The alligator clips were attached to cords, which were plugged into a power strip, which was then plugged into a wall outlet, providing a "Ground."

EMF Measurement in Grid Squares

To measure the EMF in every square of the grid on the floor of the Box Setups, first a simple holder was made for the EMF meter. This was necessary because higher-than-normal EMF measurements were observed when the device was hand-held; this could have been caused by human body conducting stray EMF in the environment. Two erasers were taped with masking tape at one end of the bottom of a plastic ruler. The EMF meter was taped to the plastic ruler at a right angle to the ruler, directly above the two erasers. This made a holder for the EMF meter which did not seem to conduct environmental stray EMF. The backlight of the EMF meter was kept "On," to make the measurements easy to read. EMF measurements were then taken in each grid square. This was repeated for each Box Setup except the Control. The Control (0% EMF concentration) Box Setup did not have a grid.

Holding the plastic ruler, the researcher positioned the EMF meter in a grid square. The EMF meter's position was parallel to the router antennae at all times so that they shared the same polarity. The researcher waited two seconds for the EMF measurements to settle, then recorded five EMF measurements on a prepared piece of graph paper which had a sketch of the grid squares on it. The decimals were truncated to the ones place.

Horizontal Position Effect on EMF Concentration

Due to the nature of EMF and the strong EMF-reflection properties of aluminum foil, EMF levels did not seem to have a discernable pattern based on location in the grid. For example, some of the highest EMF concentrations were measured at the edge of the floor, rather than the center. Therefore, to determine where to position the *D. melanogaster* vials, the grid system was developed. Each Box Setup had a grid drawn on its floor. Each grid square was 3 cm by 3 cm because this is approximately one third of the Wi-Fi EMF wavelength, which is 12.5 cm. This size was also chosen because it is approximately the space

required for one vial of *D. melanogaster*. Since this is about one third of the wavelength, EMF levels were expected to be relatively consistent throughout an individual square. Five EMF measurements were taken in each square of the grid and the mean of those measurements was calculated. *D. melanogaster* vials were placed in grid squares with EMF levels within the concentration ranges.

D. melanogaster Care

D. melanogaster Wild Type (+) were purchased from Ward's Science. They were kept in cellulose acetate propionate plastic vials and fed 4-24 Instant Drosophila Medium Blue, both from Carolina® Biological Supply Company. The *D. melanogaster* were cared for following the guidelines of the Carolina® Drosophila Manual (10). These original 16 culture vials, which were of indeterminate ages, were stored in a cool, dry location for 16 days while the Box Setups were engineered. Then, four culture vials were placed in each Box Setup for 14 days. It was assumed that each culture vial's average EMF exposure corresponded to each Box Setup's respective EMF concentration, even though the vials were not positioned in specific grid squares. During these 14 days, eggs were laid that developed into larvae and pupae, and would eventually develop into the adult *D. melanogaster* used as the parents in this experiment.

After 14 days, the Box Setups were opened and all the adult *D. melanogaster* present were removed using a vacuum cleaner, so that only eggs, larvae, and pupae remained. Then, the vials were returned to the Box Setups, and the pupae were allowed to eclose for four days, producing 1-4 days old adult *D. melanogaster* that had been exposed to the different Wi-Fi EMF concentrations for their entire lifetime. The Box Setups were opened and the vials removed so that the *D. melanogaster* adults could be anesthetized, sexed, and paired as the parent *D. melanogaster* whose progeny were studied in this investigation.

For each Box Setup, 15 vials, or 15 pairs of *D. melanogaster* were placed in the Box Setups for 14 days. Each pair of parent *D. melanogaster* laid eggs that developed into larvae, pupae, and progeny adults. These pupae and progeny adults were counted as data for the experiment. The progeny adults were 1-5 days old. Therefore, the progeny adults and pupae that were counted in this experiment were from the second generation of *D. melanogaster* to be exposed to Wi-Fi EMF for their entire life cycle. *D. melanogaster* age was calculated by assuming a life cycle of 10 days, since the temperature varied within a range of approximately 22 degrees Celsius and 25 degrees Celsius (15).

D. melanogaster Vial Preparation

All materials were collected and a plastic garbage bag was spread on a table to protect the work space. Plastic cups were labeled as "Everclear," "Distilled water," "Medium," and "Dump." A large funnel was labeled as "Medium," and a small funnel as "Distilled water." The work area and utensils were

sanitized by swabbing them with Everclear® (75.5% ethanol solution) and allowed to dry. Vials were labeled with their concentration (represented by letters A-D) and numbers 1-15. An example of a vial label would be "A1."

There were a total of 60 vials. 15 mL of dry 4-24 Instant Drosophila Medium Blue was added to all the vials. Then, 15 mL of room temperature distilled water was added to all the vials. Between 5-8 grains of Dry Active Yeast were added to each vial. Using a 2-mL plastic pipette, an additional 2-mL of distilled water was added to each vial, which was then immediately covered with a foam plug to minimize evaporation.

Anesthetization and Sexing of *D. melanogaster*

All materials were collected and a plastic garbage bag was spread on a table to protect the work space. The work area and utensils were sanitized by swabbing them with Everclear®. Everything was allowed to dry.

The *D. melanogaster* were anesthetized using FlyNap® (22) via the anesthetization procedure described in the Carolina® Drosophila Manual (10). *D. melanogaster* were transferred from their culture vial to an empty vial prior to anesthetization. They were emptied onto a white paper immediately after anesthetization.

The anesthetized *D. melanogaster* were sexed to identify male/female pairs for the experimental vials. A camel hair brush was used to gently manipulate the anesthetized *D. melanogaster*. 10-15 anesthetized *D. melanogaster* were transferred onto the dissecting microscope's plate. At 10X magnification, the *D. melanogaster* were sexed based on diagrams found in the Carolina® Drosophila Manual (10). The anesthetized *D. melanogaster* were sorted into the following groups: unsorted *D. melanogaster* to the back, males to the left, females to the right, and discards to the front. Discarded *D. melanogaster* were either (a) pale indicating recent eclosure so they probably would not survive anesthetization, (b) injured, or (c) of indistinguishable sex. The discarded *D. melanogaster* were placed into an oil morgue. The camel hair brush was used to drop a male and female *D. melanogaster* in each experimental vial, then the foam plug was replaced on the vial.

Measuring Temperature, Humidity, Watt Consumption

It was important to have a way to make sure that all the Wi-Fi routers were functioning, even when they were not visible because they were inside the Box Setups. This was necessary because if a Wi-Fi router turned off unexpectedly, the *D. melanogaster* inside would not be exposed to Wi-Fi EMF. To address this, the power adapters for all the routers were plugged into a single power strip which was connected to a Watt meter plugged into the wall outlet. The Watt readings were recorded twice a day to ensure that power consumption did not change. When all the routers were on and producing Wi-Fi, Watt usage was 5.5-5.6 W.

Approximately every 12 hours, the Humidity Measuring

Procedure was conducted (see below). While waiting the 5 minutes for the relative humidity measurement, the temperature of each Box Setup was recorded from the thermometers in each *D. melanogaster* chamber. Adjustments to the environment were made as necessary to keep the temperature within the desired range of 22-25 degrees Celsius. To increase the temperature, the furnace air vent which heats the room where the experiment was conducted was opened or the space heater temperature was increased. To decrease the temperature, the opposite was done. The height of the distilled water in the humidifier tank was measured and recorded to monitor water consumption. The humidifier was refilled with distilled water. Finally, the Watt consumption was recorded.

It was essential that adequate humidity be maintained since dry air could cause dry medium, which could starve the *D. melanogaster*. Furthermore, when medium is dry, larvae pupate directly onto it instead of on the walls of the vial, making them difficult to observe and record accurately. The relative humidity of the air pumped into the Box Setups was maintained at approximately 40%. The relative humidity inside the *D. melanogaster* Chamber could not be measured since the Box Setups were kept sealed during the experiment.

The humidity was measured approximately every 12 hours. To do this, the air valve connected to air tube Piece (c), which was connected to the Control Box Setup, was opened. The main air valve openings for Box Setups 2, 3, and 4 were closed. This way, all the air was being pumped through Piece (c). The end of Piece (c) was placed into a graduated cylinder lying on its side, and the hygrometer was placed into the graduated cylinder with its sensor facing the end of Piece (c). After 5 minutes, the relative humidity measurement was recorded. The air valves were then returned to normal.

Statistical Analysis

Rigorous statistical tests, including control of the familywise error rate, were used to minimize the probability of the results solely occurring by chance. Statistical Analysis was conducted using Microsoft Excel's ® Analysis ToolPak ®. Data was eliminated for vials where the *D. melanogaster* did not survive anesthetization and there were no progeny adults. Statistical test data was rounded to two significant figures.

The statistical tests and comparisons conducted on the data were planned before the data was collected, to avoid bias (23). Statistical tests used were single factor ANOVA and two-sample t-test Assuming Unequal Variances. The ANOVA null hypothesis was that there was not a statistically significant difference among the groups tested. The t-test null hypothesis was that there was not a statistically significant difference between two concentrations. Null hypotheses were rejected if the *p*-value was less than the alpha value for the ANOVA and the alpha for one of the t-tests. Alpha represents the Type I Error.

For the t-tests, the two-tail *p*-value was used instead of the one-tail *p*-value, to investigate whether a change exists

when *D. melanogaster* are exposed to Wi-Fi EMF. A change could be either an increase or a decrease. The hypothesis was that Wi-Fi EMF exposure would cause a change in the variables tested, and did not specify directionality of change, i.e. whether the change would be an increase or a decrease. For the male:female ratio and the adult:pupa ratio, statistical tests were conducted after a logarithmic transformation on the data, since ratios may not have a normal distribution (24). The male:female ratio and the adult:pupa ratio are ratios, so the Cohen's *d_s* effect size, Hedge's *g_s* effect size, and 95% confidence interval could not be calculated for this data.

The Bonferroni correction was used to control the familywise error rate for the t-tests by dividing the 0.05 alpha by the number of t-tests (25). The Cohen's *d_s* effect size was calculated using Equation 1 from an article by Lakens (26). Since Cohen's *d_s* can be biased in samples with a count of less than 20 individuals, the Hedge's *g_s*, or corrected effect size, was calculated and used to report effect size (26). Cohen's *d_s* effect size was only used to calculate the 95% confidence interval (CI) (27).

REFERENCES

1. Behari *et al.* Bioinitiative 2012:A Rationale for Biologically-based Public Exposure Standards for Electromagnetic Fields (ELF and RF). Rep. Ed. Sage Cindy and Carpenter O. David. Bioinitiative Report, 2012.
2. Resnick, Robert, David Halliday, and Jearl Walker. *Fundamentals of Physics*. p. 890, 8th ed. Vol. 2. Hoboken, NJ: John Wiley and Sons, 2008.
3. "Cell Phones and Cancer Risk." National Cancer Institute. National Cancer Institute at the National Institutes of Health, 24 June 2013. Web. 10 Sept. 2015.
4. Electromagnetic Fields (300 HZ TO 300 GHZ). Rep. no. 137. World Health Organization, 1993. International Programme on Chemical Safety. World Health Organization.
5. Health and Electromagnetic Fields. Rep. European Commission - Research-Directorate General - European Communities, 2005.
6. Beckingham *et al.* "*Drosophila melanogaster*--the Model Organism of Choice for the Complex Biology of Multi-cellular Organisms." *Gravitational and Space Biology Bulletin: Publication of the American Society for Gravitational and Space Biology* 18.2 (2005): pp 17-29.
7. Murphy, Tom. "Faraday Cages and Microwaves, Lecture 14." UC San Diego Department of Physics. Regents of the University of California, 18 May 2006.
8. Engels *et al.* "Anthropogenic Electromagnetic Noise Disrupts Magnetic Compass Orientation in a Migratory Bird." *Nature* 509.7500 (2014): pp. 353-56.
9. Economos *et al.* "Developmental Temperature and Life Span in *Drosophila melanogaster*. II. Oscillating Temperature." *Gerontology* 32.1 (1986): pp 28-36.
10. Flagg, Raymond O., Ph.D. Carolina © *Drosophila* Manual.

- N.p.: Carolina © Biological Supply, 2005.
11. Guy, Arthur W., Jack Wallace, and John A. McDougall. "Circularly Polarized 2450-MHz Waveguide System for Chronic Exposure of Small Animals to Microwaves." *Radio Science* 14.6S (1979): pp. 63-74.
 12. Cuddihy, William F., and Lloyd H. Shreve. "Microwave Reflectivity of Deposited Aluminum Films for Passive Relay Communications." NASA Technical Reports Server. NASA Scientific and Technical Information Program, 27 Jan. 2004.
 13. "Heavy Duty Aluminum Foil, Product FAQs." Reynolds Kitchens. Reynolds Consumer Products LLC, 2015.
 14. "Calculator for Skin Effect Depth." Chemandy Electronics. Chemandy Electronics Ltd, 17 June 2015.
 15. Popović, Branko. "Chapter 20: The Skin Effect." *Introductory Electromagnetics*. By Zoya Popović. N.p.: Prentice Hall, 2000. 382-92.
 16. Castro Folgueras, Luiza De, Evandro Luis Nohara *et al.* "Dielectric Microwave Absorbing Material Processed by Impregnation of Carbon Fiber Fabric with Polyaniline." *Materials Research* 10.1 (2007): pp. 95-99.
 17. Neo, C. P., and V. K. Varadan. "Optimization of Carbon Fiber Composite for Microwave Absorber." *IEEE Transactions on Electromagnetic Capability* 46.1 (2004): 102-06. *IEEE*.
 18. "Laminated Microwave Absorbing Sheet:RF Shielding with Minimal Reflection." LessEMF.com. Less EMF Inc., 2015.
 19. "Microwave Absorbing Sheet." LessEMF.com. Less EMF Inc., 2015. Web. 28 Aug. 2015.
 20. "Physics Resources Database, Thermal Properties Thermal Conductivities, K." The University of Sydney, Australia School of Physics. Ian Cooper, School of Physics, University of Sydney, Australia, 17 Feb. 1999.
 21. "TP-LINK ® User Guide: TL-WR841N, TL-WR841ND, 300Mbps Wireless N Router." TP-LINK ®. TP-LINK ® Technologies Co., Ltd., 2012.
 22. "Material Safety Data Sheet: FlyNap." Carolina ®. Carolina ® Biological Supply Company, 18 July 2012.
 23. Ruxton, Graeme D., and Guy Beauchamp. "Time for Some a Priori Thinking about Post Hoc Testing." *Behavioral Ecology* 19.3 (2008): pp. 690-93.
 24. McDonald, John. "Data Transformations." *Handbook of Biological Statistics*, 3rd ed., Sparky House Publishing, Baltimore, MD, 2014.
 25. Sokal, Robert R., and F. James Rohlf. "Single-Classification Analysis of Variance." *Introduction to Biostatistics*, 2nd ed., Dover Publications, Inc., Mineola, NY, 2009, pp. 173-179.
 26. Lakens, Daniël. "Calculating and Reporting Effect Sizes to Facilitate Cumulative Science: a Practical Primer for t-Tests and ANOVAs." *Frontiers in Psychology*, vol. 4, 26 Nov. 2013, pp. 1-12.
 27. Lee, Dyong Kyu. "Alternatives to P Value: Confidence Interval and Effect Size." *Korean Journal of Anesthesiology*,

vol. 69, no. 6, Dec. 2016, pp. 555-562.

Received: December 29, 2015

Accepted: October 18, 2018

Published: January 29, 2020

Copyright: © 2020 Anand and Anand. All JEI articles are distributed under the attribution non-commercial, no derivative license (<http://creativecommons.org/licenses/by-nc-nd/3.0/>). This means that anyone is free to share, copy and distribute an unaltered article for non-commercial purposes provided the original author and source is credited.

Sponsorship



Editor's Circle

\$10,000+



Patron

\$5,000+



PORTFOLIOS
WITH PURPOSE®

Institutional Supporters



HARVARD
UNIVERSITY



HARVARD
MEDICAL SCHOOL



Tufts
UNIVERSITY

Charitable Contributions

We need your help to provide mentorship to young scientists everywhere.

JEI is supported by an entirely volunteer staff, and over 90% of our funds go towards providing educational experiences for students. Our costs include manuscript management fees, web hosting, creation of STEM education resources for teachers, and local outreach programs at our affiliate universities. We provide these services to students and teachers entirely free of any cost, and rely on generous benefactors to support our programs.

A donation of \$30 will sponsor one student's scientific mentorship, peer review and publication, a six month scientific experience that in one student's words, 're-energized my curiosity towards science', and 'gave me confidence that I could take an idea I had and turn it into something that I could put out into the world'. **If you would like to donate to JEI, please visit <https://emerginginvestigators.org/support>, or contact us at questions@emerginginvestigators.org.** Thank you for supporting the next generation of scientists!

'Journal of Emerging Investigators, Inc. is a Section 501(c)(3) public charity organization (EIN: 45-2206379). Your donation to JEI is tax-deductible.'



emerginginvestigators.org